Symposium on Emerging Fields in Mechanism and Machine Science

1st IFToMM Young Faculty Group Symposium on Emerging Fields in Mechanism and Machine Science

19 – 21. November 2024

Organization

Organizing Committee
Francisco Geu Flores (Germany)
Sajjad Keshtkar (Japan)
Claudio Villegas (Chile)

Technical Committee
Cristina Castejón (Spain)
Pau Català (Spain)
Onur Denizhan (Turkey)
Saioa Herrero (Spain)
Andrés Kecskeméthy (Germany)
Qizhi Meng (China)
Jiang Ming (Japan)

Moderation
Francisco Geu Flores (Germany)

Symposium on Emerging Fields in Mechanism and Machine Science

Imprint

1st IFToMM Young Faculty Group Symposium on Emerging Fields in Mechanism and Machine Science: 19 - 21. November 2024, Online Symposium

2024

DOI: 10.17185/duepublico/82370

Issuing body:
University of Duisburg-Essen
University Library, DuEPublico
Universitätsstraße 9-11
45141 Essen
Germany
https://duepublico2.uni-due.de

© 2024 the authors. The rights/licenses stated in the individual symposium contributions apply.

Preface

The International Federation for the Promotion of Mechanism and Machine Science (IFToMM) is one of the largest international scientific communities dedicated to the field of mechanism and machine science and its applications. Since its foundation in 1965, it has been devoted to the mission of bringing people from all nationalities and systems together to exchange science and technology and strengthen their international bonds.

IFToMM's Young Faculty Group is a cross-disciplinary group founded in 2024 to pursue IFToMM's mission from within the working core of academia. It regularly summons young researchers and lecturers from all over the world not only to discuss the technological challenges of the present and the future, but also to share experiences in academia and support each other in the harsh endeavor of making a career in the academic world.

The IFToMM Young Faculty Group Symposium on Emerging Fields in Mechanism and Machine Science (IFToMM YFG-MMS 2024) was launched this year as a cornerstone of the Young Faculty Group activities. The first IFToMM YFG-MMS was held online from the 19th to the 21st of November 2024 and gathered more than 30 participants from 14 different countries and 6 continents. A total of 27 contributions from the fields of robotics, mechatronics, multibody dynamics, transportation machinery, vibrations, biomechanics, as well as education were selected for presentation after peer review by two independent reviewers. This book contains the final versions of all the selected abstracts.

We would like to thank IFToMM and, in particular, Andrés Kecskeméthy, President of IFToMM, Burkhard Corves, Chair of the MO Germany, Victor Petuya, Chair of the MO Spain, and Guisseppe Carbone, Chair of the TC Mechatronics and Robotics, for their valuable support. We would also like to thank the open-access institutional repository of the University of Duisburg-Essen, DuEPublico, and, in particular, Elisabeth Wünnerke for their friendly and professional assistance in the publication process.

We hope that the IFToMM YFG-MMS 2024 was just the beginning of a long-lasting series of many more young faculty meetings to come.

Francisco Geu Flores
Sajjad Ketshkar
Claudio Villegas

Program

1. Day, Tuesday 19.11.2024	
12:00 - 12:05	**Claudio Villegas**, Chair of the IFToMM Young Faculty Group Welcome words
12:05 - 12:15	**Andrés Kecskeméthy**, President of IFToMM Opening speech
12:15 - 12:20	**Francisco Geu Flores** Zoom warm-up
12:20 - 12:35	**Mathias Hüsing**, Deputy Director of the IGMR RWTH Aachen Keynote lecture: IIDEA-Project – Inclusion and Integration on the first labor market using collaborative robotics
12:35 - 12:50	**Michele Conconi** and Nicola Sancisi Impact of a Novel, MRI Based Approach for Ligament Personalization in Knee Modeling
12:50 - 13:05	**Fernando Viadero-Monasterio**, Miguel Meléndez Useros, Manuel Jiménez-Salas, Beatriz Lopez Boada and Maria Jesus Lopez Boada Current Trends in Automated Driving Systems
13:05 - 13:20	**Ruijie Tang**, Qizhi Meng, Xin-Jun Liu and Jinsong Wang Structure Design of Polyhedral Grippers with Deployable Faces for Capturing Non-cooperative Targets
13:20 - 13:35	**Sajjad Keshtkar** and Hirohisa Kojima Advances in Deployable Mechanisms in Space
13:35 - 13:50	**Discussion in break-out rooms**
13:50 - 14:05	**María del Pilar Dávila-Verduzco**, Santiago Ramírez-Durán, Beatriz Alejandra Hernández García, Ivo Neftali Ayala-Garcia and Alejandro González Estimation of Lower Limb Muscle Strength through the Daniels Scale
14:05 - 14:20	**Onur Denizhan** and Meng-Sang Chew Application of Two Tension Springs in the Four-Bar Engine Hood Linkage Mechanism
14:20 - 14:35	**Sebastian Röttgermann**, David Albrecht, Martin de Fries and Marcus Irmer Methodical Approach and Analysis of Highly Realistic Virtual Worlds as a Test Environment for the Evaluation of Disturbance Detection and Work Quality Monitoring Algorithms in the Agricultural Domain
14:35 - 14:50	**Mingkun Wu** and Burkhard Corves Optimal Input Shaper Tuning Using Constrained Bayesian Optimization in Industrial Robot Systems
14:50 - 15:05	**Thorsten Bartel** On methods to motivate students to self-organized learning and to enable them to acquire "future skills"
15:05 - 15:20	**Discussion in break-out rooms**
15:20 - 15:25	**Francisco Geu Flores** Closing words

2. Day, Wednesday 20.11.2024	
12:00 - 12:05	**Francisco Geu Flores** Opening words
12:05 - 12:20	**Burkhard Corves**, Chair of the IFToMM MO Germany Keynote lecture: IFToMM D-A-CH as an example for a regional workshop for doctoral candidates in the IFToMM domains
12:20 - 12:35	**Mariana Rodrigues da Silva**, Filipe Marques, Sérgio B. Gonçalves, Miguel Tavares da Silva and Paulo Flores Computational and Experimental Analysis of Crutch-Assisted Gait: Findings from a Case Study
12:35 - 12:50	**Cagri Yilmaz** Performance comparisons of different numerical methods for obtaining out-of-plane deflections of a resonant AFM micro-cantilever under acoustic emissions
12:50 - 13:05	**Pau Català**, David Caballero, Carles Domenech-Mestres and Alba Perez Gracia Mobile Robotic Platform Architecture Adaptable to Several Agricultural Applications
13:05 - 13:20	**Juan Pablo Mora Garota**, Carlos Francisco Rodriguez and Burkhard Corves Optimizing Energy Consumption of a Parallel Robot with Elastic Elements via Equilibrium Position Adjustment
13:20 - 13:35	**Discussion in break-out rooms**
13:35 - 13:50	Benet Fité Abril, Carlos Pagès Sanchis and **Míriam Febrer-Nafría** Towards the development of a simulation framework to assess and enhance crutch-assisted gait
13:50 - 14:05	**Filipe Marques** and Mariana Rodrigues da Silva Contact modeling between torus surfaces and plane using compliant force models
14:05 - 14:20	**Michał Olinski** Mobile robot for agriculture support in uneven terrain
14:20 - 14:35	**Ünal Dana** and Levent Çetin Dynamics of Towing for Trailer Path Tracking
14:35 - 14:50	**Mertcan Koçak** and Erkin Gezgin Development of a Graphical User Interface for Personalized Transfemoral Prosthesis Design
14:50 - 15:05	**Discussion in break-out rooms**
15:05 - 15:10	**Francisco Geu Flores** Closing words

3. Day, Thursday 21.11.2024	
12:00 - 12:05	**Francisco Geu Flores** Opening words
12:05 - 12:20	**Pau Català** What Moves Us? - Results of the IFToMM YFG Survey
12:20 - 12:35	Jian Zheng, Qizhi Meng and **Ming Jiang** Intent Detection Method and Assistive Device Development for Supporting Sit-to-Stand
12:35 - 12:50	**Claudio Villegas**, Diego Carrasco and Fabian Pierart Nonlinear-stiffness mechanism inspired in nature for wave energy conversion: A quick performance evaluation of its linear stiffness zone
12:50 - 13:05	**Tuğrul Uslu** and Erkin Gezgin An Optimization Approach for Array Geometry in Hall Effect Sensor Based Microrobot Tracking
13:05 - 13:20	**Joaquim Minguella-Canela** and Jordi Romeu Garbí Collaborative Learning Environments for Research-based Teaching of Mechanical Engineering
13:20 - 13:35	**Discussion in break-out rooms**
13:35 - 13:50	José Alejandro Ríos-Hincapié, Oscar Porras-Ramirez, **María Guadalupe Contreras-Calderón** and Arturo Nicole Gómez-Nava Pronosupination Device to assist Pronation and Supination Movements of the Forearm Rehabilitation with Virtual Interface
13:50 - 14:05	**Mohammed Khadem**, Dmitry Malyshev and Giuseppe Carbone Proposed Design of New Drones for Specific Applications in Field Cultural Heritage
14:05 - 14:20	**Daniel Lavayen-Farfán** and Enrique Pujada-Gamarra Origami inspired engineering: Challenges and opportunities in portable and foldable mechanisms in solar-power generation
14:20 - 14:35	**Zeki Ilhan** Nonlinear Robust Control Design for a Planar Robot Arm
14:35 - 14:50	**Tao Ma** and Burkhard Corves DMP-Based Cartesian Trajectory Learning from Multiple Demonstrations
14:50 - 15:05	**Discussion in break-out rooms**
15:05 - 15:15	**Claudio Villegas**, Chair of the IFToMM Young Faculty Group Closing speech

List of Abstracts

Conconi, Michele; Sancisi, Nicola ..... p. 8
Impact of a Novel, MRI Based Approach for Ligament Personalization in Knee Modeling
DOI: 10.17185/duepublico/82671

Viadero-Monasterio, Fernando; Meléndez-Useros, Miguel; Jiménez-Salas, Manuel; López-Boada, Beatriz; López-Boada, María Jesús ..... p. 10
Current Trends in Automated Driving Systems
DOI: 10.17185/duepublico/82624

Tang, Ruijie; Meng, Qizhi; Liu, Xin-Jun; Wang, Jinsong ..... p. 12
Structure Design of Polyhedral Grippers with Deployable Faces for Capturing Non-cooperative Targets
DOI: 10.17185/duepublico/82585

Keshtkar, Sajjad; Kojima, Hirohisa ..... p. 14
Advances in Deployable Mechanisms in Space
DOI: 10.17185/duepublico/82663

Dávila-Verduzco, María del Pilar; Ramírez-Durán, Santiago; Hernández García, Beatriz Alejandra; Ayala-García, Ivo Neftalí; González, Alejandro ..... p. 16
Estimation of Lower Limb Muscle Strength through the Daniels Scale
DOI: 10.17185/duepublico/82603

Denizhan, Onur; Chew, Meng-Sang ..... p. 18
Application of Two Tension Springs in the Four-Bar Engine Hood Linkage Mechanism
DOI: 10.17185/duepublico/82608

Röttgermann, Sebastian; Albrecht, David; de Fries, Martin Maximilian; Irmer, Marcus ..... p. 20
Methodical Approach of Highly Realistic Virtual Test Environments for the Evaluation of Monitoring Algorithms in the Agricultural Domain
DOI: 10.17185/duepublico/82631

Wu, Mingkun; Corves, Burkhard ..... p. 22
Optimal Input Shaper Tuning Using Constrained Bayesian Optimization in Industrial Robot Systems
DOI: 10.17185/duepublico/82614

Bartel, Thorsten ..... p. 24
On methods to motivate students to self-organized learning and to enable them to acquire "future skills"
DOI: 10.17185/duepublico/82628

Rodrigues da Silva, Mariana; Marques, Filipe; Gonçalves, Sérgio B.; Tavares da Silva, Miguel; Flores, Paulo ..... p. 26
Computational and Experimental Analysis of Crutch-Assisted Gait: Findings from a Case Study
DOI: 10.17185/duepublico/82584

Yilmaz, Cagri ..... p. 28
Performance comparisons of different numerical methods for obtaining out-of-plane deflections of a resonant AFM micro-cantilever under acoustic emissions
DOI: 10.17185/duepublico/82605

Català, Pau; Caballero, David; Domenech-Mestres, Carles; Perez Gracia, Alba ..... p. 31
Mobile Robotic Platform Architecture Adaptable to Several Agricultural Applications
DOI: 10.17185/duepublico/82604

Mora, Juan Pablo; Rodríguez, Carlos F.; Corves, Burkhard ..... p. 33
Optimizing Energy Consumption of a Parallel Robot with Elastic Elements via Equilibrium Position Adjustment
DOI: 10.17185/duepublico/82626

Fité Abril, Benet; Pagès Sanchis, Carlos; Febrer-Nafría, Míriam ..... p. 35
Towards the development of a simulation framework to assess and enhance crutch-assisted gait
DOI: 10.17185/duepublico/82613

Marques, Filipe; Rodrigues da Silva, Mariana ..... p. 37
Contact modeling between torus surfaces and plane using compliant force models
DOI: 10.17185/duepublico/82625

Olinski, Michal ..... p. 39
Mobile robot for agriculture support in uneven terrain – design and simulation
DOI: 10.17185/duepublico/82638

Dana, Ünal; Çetin, Levent ..... p. 41
Dynamics of Towing for Trailer Path Tracking
DOI: 10.17185/duepublico/82592

Koçak, Mertcan; Gezgin, Erkin ..... p. 43
Development of a Graphical User Interface for Personalized Transfemoral Prosthesis Design
DOI: 10.17185/duepublico/82619

Zhen, Jian; Meng, Qizhi; Jiang, Ming ..... p. 45
Intent Detection Method and Assistive Device Development for Supporting Sit-to-Stand
DOI: 10.17185/duepublico/82601

Villegas, Claudio; Carrasco, Diego; Pierart, Fabián ..... p. 47
Nonlinear-Stiffness Mechanism Inspired in Nature for Wave Energy Conversion: A Quick Performance Evaluation of its Linear-Stiffness Zone
DOI: 10.17185/duepublico/82701

Uslu, Tugrul; Gezgin, Erkin ..... p. 49
An Optimization Approach for Array Geometry in Hall Effect Sensor Based Microrobot Tracking
DOI: 10.17185/duepublico/82623

Minguella-Canela, Joaquim; Romeu Garbí, Jordi ..... p. 51
Collaborative Learning Environments for Research-based Teaching of Mechanical Engineering
DOI: 10.17185/duepublico/82606

Ríos-Hincapie, J. A.; Contreras-Calderón, M. G.; Porras-Ramirez, O.; Gomez-Nava, A. ..... p. 53
Pronosupination Device to assist Pronation and Supination Movements of the Forearm Rehabilitation with Virtual Interface
DOI: 10.17185/duepublico/82645

Khadem, Mohammed; Malyshev, Dmitry; Carbone, Giuseppe ..... p. 56
Proposed Design of New Drones for Specific Applications in Field Cultural Heritage
DOI: 10.17185/duepublico/82582

Lavayen-Farfán, Daniel; Pujada-Gamarra, Enrique ..... p. 58
Origami inspired engineering: Challenges and opportunities in portable and foldable mechanisms in solar-power generation
DOI: 10.17185/duepublico/82639

Ilhan, Zeki Okan..... p. 60
Nonlinear Robust Control Design for a Planar Robot Arm
DOI: 10.17185/duepublico/82623

Ma, Tao; Corves, Burkhard..... p. 62
DMP-Based Cartesian Trajectory Learning from Multiple Demonstrations
DOI: 10.17185/duepublico/82615

Impact of a Novel, MRI Based Approach for Ligament Personalization in Knee Modeling

Michele Conconi[1], Nicola Sancisi[1]

[1]Department of Industrial Engineering, University of Bologna, Italy {michele.conconi@unibo.it, nicola.sancisi@unibo.it}

ABSTRACT

1 Introduction

Several approaches are possible when modeling the knee joint's response to load [1-3]. A common crucial point is how to personalize the model, adapting its parameters so that the model prediction optimally matches the behavior of a specific subject. The model sensitivity may vary considerably depending on the approach [1]. In general, the correct identification of ligament origin, insertion, and resting length have a strong impact on the model response [1,4]. A standard procedure for optimizing ligament properties involves utilizing experimental data, where joint kinematics have been measured under various external loads.[1]. This approach is indeed very effective; however, it generally requires complex and invasive experimental measurements, which reduce its application in standard clinical scenarios, where typically only medical images are available. In this work, we want to present a novel process that uses kinematic prediction of individual joint models based on magnetic resonance images (MRI) to identify the ligament parameters. The results of this method will be compared with those achievable using data directly obtained from MRI, i.e., without an individual model.

2 Methods

We investigated six fresh-frozen lower-limb specimens (one female, five men; age: 67.3±17.2 years; weight: 69.4±13.2 Kg; height: 168.3±8.5 cm). A surgeon declared the legs free from anatomical defects and removed the forefoot and all soft tissues except those at the joint, leaving the knee capsule and ligaments intact. A stereophotogrammetric system (Vicon Motion Systems, Ltd., Oxford, UK) was used to measure the tibia and femur relative motion, employing two trackers directly fixed to the bones, thus introducing no soft-tissue artifacts. The specimen was mounted on a test rig for in vitro analysis of the knee joint motion [5]: the femur was connected to the rig and use to control the knee flexion, while the tibia was free to move according to its passive motion, i.e. without external forces acting on it. Computed tomography (CT) scans and MRI of each knee were acquired. Articular surfaces and ligament insertions were then manually segmented using the free open-source software Medical Imaging Interaction Toolkit. In particular, the origin and insertion areas of the main ligaments of the knee (ACL, PCL, MCL deep and superior bundles, LCL, ALL) were identified, together with their centroid. Anatomical reference systems were defined according to a standardized convention [6], and relative femoro-tibial orientation was expressed according to a YXZ Euler angle sequence [7], while the relative translations were represented as the coordinates of the femur origin in the tibia reference system. For each knee, two deformable multibody models were defined. Both include articular contact modeled with a variation of the mattress of springs and built on cartilage morphology; seven single-fiber ligaments with bilinear elastic characteristic, where the stiffness of ligament and contact was taken from the literature [8], and no viscous effect was introduced. The two models differ only by the location of the ligament insertions and resting length. In particular, one model (MRI-M) simply takes the centroid of the insertion area as identified in the MRI, and the resting length as the linear distance between ligament origin and insertion as measured in the scanning pose. The second model (KIN-M) is instead built on a prediction of knee motion based on the maximization of joint congruence [9] and the reciprocity among joint constraints and helical axis of motion [10]. From the predicted motion, the most isometric fiber of each ligament is identified, providing optimized insertions and resting length. The two models were then compared by computing the passive motion as the envelope of equilibrium position over the flexion range. Mean absolute rotational (MARE) and translational (MATE) errors were computed for each model with respect to the experimental measure.

Table 1: Mean absolute rotational (MARE) and translational (MATE) errors for the two models (MRI-M and KIN-M), computed for each subject and average on the population.

	Subject 1		**Subject 2**		**Subject 3**		**Subject 4**		**Subject 5**		**Subject 6**		**Average**	
	MRI-M	KIN-M	MRI-M	KIN-M	MRI-M	KIN-M	MRI-M	KIN-M	MRI-M	KIN-M	MRI-M	KIN-M	MRI-M	KIN-M
MARE [°]	6.2±1.9	1.8±2.2	12.5±3.2	2.3±0.8	6.7±3.6	4.7±2.9	11.9±6.6	1.5±0.9	7.5±1.2	1.4±1.1	3.2±0.7	1.4±0.7	**8.0±2.8**	**2.2±1.4**
MATE [mm]	4.2±1.1	1.9±0.5	4.7±1.8	3.6±1.0	3.6±2.0	2.6±0.8	6.3±2.8	3.8±1.4	4.6±2.0	2.6±1.2	9.0±2.6	4.1±2.2	**5.4±2.0**	**3.1±1.2**

© 2024 The authors. This work may be used under a Creative Commons Attribution 4.0 License (CC BY 4.0)

DOI: 10.17185/duepublico/82671

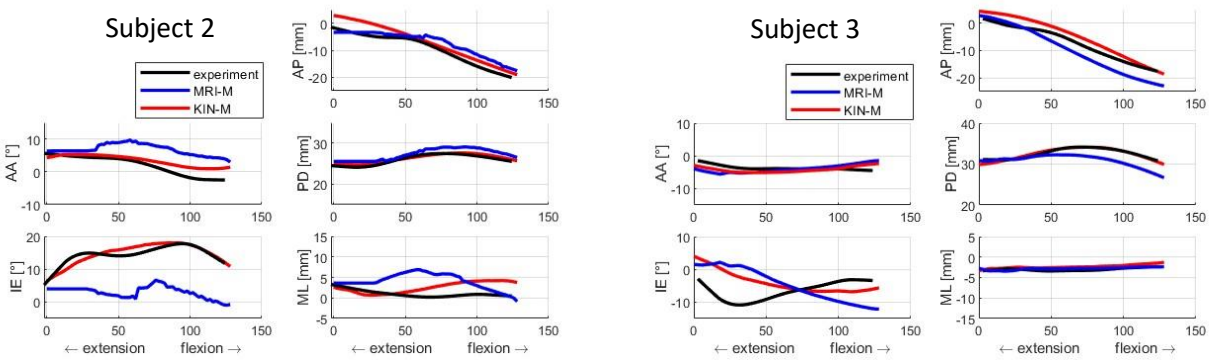

Figure 1: Femoro-tibia kinematics computed with the two models for two subjects: AA is abduction/adduction, IE internal/external rotation, AP anterior/posterior, PD proximal/distal, and ML medial/lateral translations.

3 Results

In Table 1, the MARE and the MATE for each subject are reported for both models. KIN-M always provides a better estimation of knee pose with respect to MRI-M. Interestingly, the discrepancy between the two models is not constant and varies considerably among the subjects. In particular, while MARE never exceeds 4.7° for KIN-M, it may reach up to 12.5° for MRI-M. The resulting passive kinematics reconstructed with the two models are compared to experimental data in Figure 1 for two subjects.

4 Conclusions

The proposed methods for the personalization of ligament properties provide a tool for the personalization of knee joint models based solely on information from MRI, thus making them non-invasive and compatible with clinical practice. The predictions of KIN-M show very good agreement with experimental data, supporting the validity of the approach. Interestingly, MRI-M shows alternate results, in some cases resulting equivalent to KIN-M, while in others, it provides considerable discrepancy with respect to the experimental motion. These results stress the importance of a solid and validated procedure for the definition and personalization of joint models.

References

[1] Andreassen, T. E., et al., "Deciphering the “art” in modeling and simulation of the knee joint: assessing model calibration workflows and outcomes", *Journal of Biomechanical Engineering*, vol. 145, pp- 1-12, 2023.

[2] Leardini, A., et al., “Kinematic models of lower limb joints for musculo-skeletal modelling and optimization in gait analysis”, *Journal of biomechanics*, vol. 62, pp. 77-86, 2017.

[3] Cooper, R. J., et al., “Finite element models of the tibiofemoral joint: A review of validation approaches and modelling challenges”, *Medical engineering & physics*, vol. 74, pp. 1-12, 2019.

[4] Farshidfar, S. S., et al., “The effect of modelling parameters in the development and validation of knee joint models on ligament mechanics: a systematic review”, *PLoS One*, vol. 17, pp. e0262684, 2022.

[5] Forlani, M., et al., “A new test rig for static and dynamic evaluation of knee motion based on a cable-driven parallel manipulator loading system”, *Meccanica*, vol. 51, pp. 1571-1581, 2016.

[6] Tashman, S. and Anderst,W. “In-vivo measurement of dynamic joint motion using high speed biplane radiography and CT: Application to canine ACL deficiency”, *J. Biomech. Eng,* vol. 125, pp. 238–245, 2003.

[7] E. S. Grood and W. J. Suntay, "A Joint Coordinate System for the Clinical Description of Three-Dimensional Motions: Application to the Knee," *J Biomech Eng*, vol. 135, pp.136-144, 1983.

[8] Sintini, I., Sancisi, N., and Parenti-Castelli, V., “Comparison between anatomical and approximate surfaces in a 3D kinetostatic model of the knee for the study of the unloaded and loaded joint motion” *Meccanica*, vol. 53, pp. 7-20, 2018.

[9] Conconi, M., Sancisi, N., and Parenti-Castelli, V., “Prediction of individual knee kinematics from an MRI representation of the articular surfaces”, *IEEE Transactions on Biomedical Engineering*, vol. 68, pp. 1084-1092, 2020.

[10] Conconi, M., Sancisi, N., and Parenti-Castelli, V., “The geometrical arrangement of knee constraints that makes natural motion possible: Theoretical and experimental analysis”, *Journal of Biomechanical Engineering*, vol. 141, pp. 051001, 2019.

Current Trends in Automated Driving Systems

Fernando Viadero-Monasterio, Miguel Meléndez-Useros, Manuel Jiménez-Salas, Beatriz López-Boada, María Jesús López-Boada

Department of Mechanical Engineering, University Carlos III de Madrid, Avda. de la Universidad, 30, 28911, Leganés, Madrid, Spain {fviadero@ing.uc3m.es}

ABSTRACT

1 Introduction

Automated driving systems (ADS) represent a transformative advancement in transportation technology, with the potential to significantly alter the landscape of mobility [1]. These systems, also known as autonomous vehicles or self-driving cars, utilize sophisticated sensors, artificial intelligence, and vehicle connectivity to operate without human intervention [2]. The primary benefits of ADS include improved safety, enhanced traffic efficiency, and expanded accessibility [3]. One of the most notable advantages is the potential to reduce traffic accidents, as human error is a leading cause of road incidents. With faster response times and advanced environmental sensing capabilities, ADS can more effectively detect and mitigate potential hazards, thereby reducing the risk of collisions.

Despite the potential advantages, the large-scale implementation of ADS faces significant challenges [4]. Ensuring the safety and reliability of these systems in complex, unpredictable scenarios (such as adverse weather conditions and interactions with both pedestrians and human-driven vehicles), remains a key concern. The development of robust algorithms, alongside comprehensive testing, is critical to ensuring the safe integration of ADS into real-world driving environments [5].

This paper aims to provide an overview of the current objectives within the field of driving automation systems, focusing on key challenges such as intelligent vehicle suspensions, vehicle platooning, path tracking and fault-tolerant vehicle control.

2 Intelligent vehicle suspension

Vehicle Suspension Systems (VSSs) are a fundamental component of vehicle dynamics, as they are highly related to road holding, ride comfort and safety. Given the inherent limitations of passive suspensions in achieving an optimal balance between road holding and ride comfort, significant research efforts have been directed towards the development of active and semi-active suspension systems over the past few decades [6, 7].

The implementation of these systems continues to encounter significant challenges, including the occurrence of faults in physical components and issues such as actuator chattering [8]. To address these problems, event-triggering mechanisms can be developed to enhance system reliability and performance [9]. Furthermore, actuators do not exert force instantaneously, making it essential to account for delays during the control design process [10].

3 Vehicle platoon

Vehicle platooning presents a promising approach to enhancing traffic flow in autonomous vehicle systems [3]. This method organizes highway traffic into groups of closely spaced vehicles, which adapt their acceleration according to the state of the vehicle platoon, measured by in-vehicle sensors such as radar/lidar, and received via vehicle-to-vehicle (V2V) communication. The benefits of this transportation model include shorter travel times, reduced environmental impact, improved fuel efficiency, and the ability to mitigate traffic congestion.

Despite these advantages, the technology remains underdeveloped due to several technical problems that complicate its real-world implementation. These challenges include the heterogeneity of vehicles, external disturbances like wind, road slope and rolling resistance, which affect the longitudinal dynamics of the vehicle, and communication issues such as delays and interruptions, among other factors [4].

4 Path tracking

Path tracking refers to the ability of an autonomous vehicle to follow a predetermined or dynamically generated trajectory with high precision [1]. Path tracking is a critical component of autonomous driving, as it ensures that the vehicle remains on the desired path while maintaining control over steering, speed, and orientation. Accurate path tracking is essential for safe navigation, particularly in complex environments such as urban roads or highways with obstacles, tight turns, and varying road conditions. It directly impacts the vehicle's ability to avoid collisions, minimize travel time, and maintain overall stability, making it a fundamental aspect of autonomous vehicle control systems.

Path tracking continues to present considerable challenges, including the inability to measure essential parameters of the vehicle in real time, such as the sideslip angle [11, 12]. Furthermore, the inherently nonlinear and sometimes unpredictable nature of vehicle

©2024 The authors. This work may be used under a Creative Commons Attribution - NonCommercial - NoDerivatives 4.0 License (CC BY-NC-ND 4.0)

DOI: 10.17185/duepublico/82624

dynamics requires the utilization of sophisticated control methodologies to guarantee system stability under all circumstances [2]. Many researchers have simplified the problem by assuming parameters such as cornering stiffness to be constant, which does not accurately reflect the true dynamic behavior of the vehicle.

5 Conclusion

This manuscript has provided an overview of the principal trends in automated driving systems and has offered recommendations for future research directions. The objective is to facilitate the progress of novice researchers in the field, offering direction as they explore potential research gaps and contribute to the advancement of the technique.

Acknowledgments

The work was supported in part by the grant [PID2022-136468OB-I00] funded by MCIN/AEI/ 10.13039/501100011033 and by "ERDF A way of making Europe".

References

[1] F. Viadero-Monasterio, A.-T. Nguyen, J. Lauber, M. J. L. Boada, and B. L. Boada, "Event-triggered robust path tracking control considering roll stability under network-induced delays for autonomous vehicles," *IEEE Transactions on Intelligent Transportation Systems*, vol. 24, no. 12, pp. 14 743–14 756, 2023.

[2] A.-T. Nguyen, J. Rath, T.-M. Guerra, R. Palhares, and H. Zhang, "Robust set-invariance based fuzzy output tracking control for vehicle autonomous driving under uncertain lateral forces and steering constraints," *IEEE Transactions on Intelligent Transportation Systems*, vol. 22, no. 9, pp. 5849–5860, 2021.

[3] F. Viadero-Monasterio, M. Meléndez-Useros, M. Jiménez-Salas, and B. L. Boada, "Robust adaptive heterogeneous vehicle platoon control based on disturbances estimation and compensation," *IEEE Access*, vol. 12, pp. 96 924–96 935, 2024.

[4] F. Viadero-Monasterio, M. Meléndez-Useros, M. Jiménez-Salas, B. L. Boada, and M. J. L. Boada, "What are the most influential factors in a vehicle platoon?" in *2024 IEEE International Conference on Evolving and Adaptive Intelligent Systems (EAIS)*, 2024, pp. 1–7.

[5] Z. Ju, H. Zhang, X. Li, X. Chen, J. Han, and M. Yang, "A survey on attack detection and resilience for connected and automated vehicles: From vehicle dynamics and control perspective," *IEEE Transactions on Intelligent Vehicles*, vol. 7, no. 4, pp. 815–837, 2022.

[6] F. Viadero-Monasterio, B. Boada, M. Boada, and V. Díaz, "H∞ dynamic output feedback control for a networked control active suspension system under actuator faults," *Mechanical Systems and Signal Processing*, vol. 162, p. 108050, 2022.

[7] F. Viadero-Monasterio, M. Meléndez-Useros, M. Jiménez-Salas, and B. L. Boada, "Robust static output feedback control of a semi-active vehicle suspension based on magnetorheological dampers," *Applied Sciences*, vol. 14, no. 22, 2024.

[8] M. Meléndez-Useros, M. Jiménez-Salas, F. Viadero-Monasterio, and M. J. López-Boada, "Novel methodology for integrated actuator and sensors fault detection and estimation in an active suspension system," *IEEE Transactions on Reliability*, pp. 1–14, 2024.

[9] F. Viadero-Monasterio, B. L. Boada, H. Zhang, and M. J. L. Boada, "Integral-based event triggering actuator fault-tolerant control for an active suspension system under a networked communication scheme," *IEEE Transactions on Vehicular Technology*, vol. 72, no. 11, pp. 13 848–13 860, 2023.

[10] F. Viadero-Monasterio, M. Jimenez-Salas, M. Meléndez-Useros, B. L. Boada, and M. J. L. Boada, "Event-triggered fault-tolerant control for vehicle rollover avoidance based on an active suspension with robustness against disturbances and communication delays," in *IFToMM World Congress on Mechanism and Machine Science*. Springer, 2023, pp. 795–805.

[11] F. Viadero-Monasterio, J. García, M. Meléndez-Useros, M. Jiménez-Salas, B. L. Boada, and M. J. López Boada, "Simultaneous estimation of vehicle sideslip and roll angles using an event-triggered-based iot architecture," *Machines*, vol. 12, no. 1, p. 53, 2024.

[12] B. L. Boada, F. Viadero-Monasterio, H. Zhang, and M. J. L. Boada, "Simultaneous estimation of vehicle sideslip and roll angles using an integral-based event-triggered h_∞ observer considering intravehicle communications," *IEEE Transactions on Vehicular Technology*, vol. 72, no. 4, pp. 4411–4425, 2023.

Structure Design of Polyhedral Grippers with Deployable Faces for Capturing Non-cooperative Targets

Ruijie Tang[1, 2], Qizhi Meng[1, 2, 3*], Xin-Jun Liu[1, 2*], and Jinsong Wang[1]

[1] The State Key Laboratory of Tribology in Advanced Equipment, Department of Mechanical Engineering (DME), Tsinghua University, Beijing 100084, China {trj22@malis.tsinghua.edu.cn, qizhi.meng@foxmail.com, xinjunliu@mail.tsinghua.edu.cn, wangjs@mail.tsinghua.edu.cn}
[2] Beijing Key Lab of Precision/Ultra-precision Manufacturing Equipment and Control, Tsinghua University, Beijing 100084, China
[3] Department of Mechanical Engineering, Tokyo Institute of Technology, Tokyo, 1528550, Japan

ABSTRACT

1 Introduction

Recently, with the growth of inactive satellites and debris, the orbit has become increasingly crowded, which creates risk and uncertainty for the conduction of space missions. For the sustainable utilization of orbit resources, various schemes and devices are proposed to capture non-cooperative targets through force interaction or form enclosure [1, 2]. Among relevant devices, polyhedral grippers [3, 4], able to transform between an unfolded diagram and the enclosed polyhedron, can realize target capture by form enclosure during the shape transformation. Due to the reduction of contact, polyhedral grippers have priority in concise control strategy, low damage to the targets, and avoidance of generating extra fragments. However, to capture larger targets, polyhedral grippers are required to form larger enclosed spaces, while the size enlargement brings storage difficulty. Developing polyhedral grippers with deployable functions may solve this contradiction between the large size requirement and limited launching space. In this paper, polyhedral grippers with deployable faces are proposed for enhanced capturing capacity, which have two degrees of freedom for deployment and capturing. The size of the polyhedral grippers can be adjusted through the synchronous fold or deployment of each deployable face. Therefore, the proposed grippers can be folded for storage, then conduct face deployment in orbit, and finally capture non-cooperative targets through the enclosure motion. This extended abstract provides a brief introduction to the proposed polyhedral grippers with deployable faces.

2 Structure design

2.1 Description of the design flow

For the easy conduction of the gripper design, a design flow is proposed to construct different polyhedral grippers with similar basic modules. These modules, containing three deployable polygon faces connected with revolute joints and constraint branch chains, can realize face deployment and shape transformation. By sharing two deployable faces, two basic modules can be expanded to a larger mechanism. Finally, a polyhedral gripper able to conduct size adjustment and enclosure motion can be achieved through module expansion.

2.2 Deployable polygon faces

To enhance the space utilization of the grippers in the launching vehicles, each face of the polyhedral grippers is expected to have the deployment function. Therefore, various deployable polygon faces are proposed for the gripper design. These deployable polygon faces are inspired by the Sarrus linkage. As an example, the mechanism design of a deployable square face is presented in Fig. 1. With the relative translational motion between the center node and the center frame, the face can transform from the folded state to the deployed state.

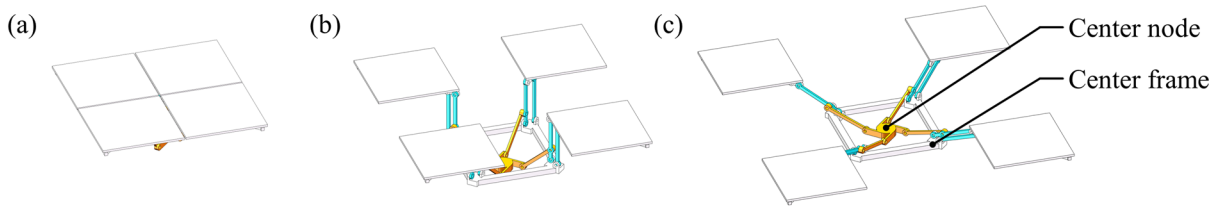

Figure 1: The proposed deployable square faces: (a) the folded state, (b) the intermediate state, and (c) the deployed state.

2.3 Gripper construction through the design flow

The basic module containing three deployable polygon faces is the key component of the proposed polyhedral grippers with deployable faces. To construct the polyhedral gripper, type synthesis of the basic modules is first conducted with the Grassmann line geometry and line graphs. A synthesized basic module containing three deployable square faces is presented in Fig. 2 as an

© 2024 The authors. All rights reserved.
DOI: 10.17185/duepublico/82585

example. The three deployable faces of the basic modules can realize deployment and synchronous motion.

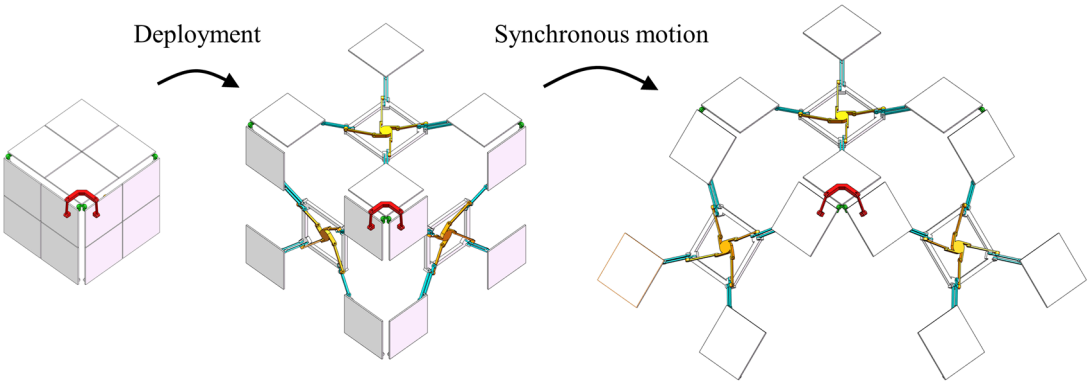

Figure 2: The function schematic of a synthesized basic module containing three deployable square faces.

According to the proposed design flow of the polyhedral gripper, two basic modules can be expanded to a larger mechanism by sharing two deployable faces, and the expected polyhedral gripper can be achieved through module expansion. Based on the basic module containing three deployable square faces in Fig. 2, a cube gripper with deployable faces is designed, which can conduct size adjustment and enclosure motion as presented in Fig. 3.

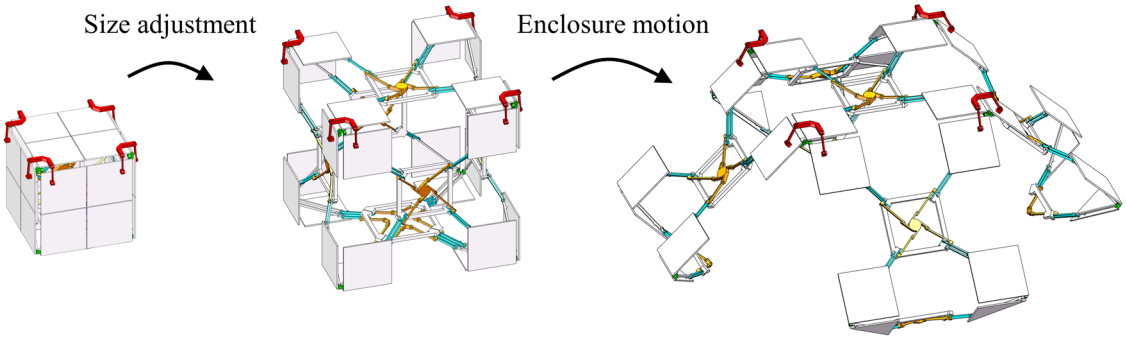

Figure 3: The function schematic of a cube gripper with deployable faces.

3 Conclusion

In this paper, polyhedral grippers with deployable faces are proposed to achieve the enhanced capacity of capturing non-cooperative targets by adopting deployable polygon faces. Through the in-orbit deployment of each deployable face, the proposed polyhedral grippers can be efficiently storage within the launching vehicles, and are competent for capturing larger objects. Based on different polyhedrons, various polyhedral grippers with deployable faces can be constructed by following the proposed design flow, and have the potential for satisfying different capturing requirements. These polyhedral grippers may serve as candidates for diverse spatial capturing missions, and provide references for the structure designs of deployable mechanisms with multiple degrees of freedom.

Acknowledgments

This work is supported by the National Natural Science Foundation of China (Grant No. 52105026).

References

[1] Mingming Wang, Jianjun Luo, Jianping Yuan, and Ulrich Walter. (2018). “An integrated control scheme for space robot after capturing non-cooperative target”, Acta Astronautica, 147: 350-363. https://doi.org/10.1016/j.actaastro.2018.04.016

[2] Guotao Li, and Peng Xu. (2020) “Design and Analysis of a Deployable Grasping Mechanism for Capturing Non-cooperative Space Targets”, Aerospace Science and Technology, 106: 106230. https://doi.org/10.1016/j.ast.2020.106230

[3] Yang Zhang, Hailin Huang, Tao Mei, and Bing Li. (2022). “Type Synthesis of Single-loop Deployable Mechanisms Based on Improved Atlas Method for Single-DOF Grasping Manipulators”, Mechanism and Machine Theory, 169: 104656. https://doi.org/10.1016/j.mechmachtheory.2021.104656

[4] Ruijie Tang, Qizhi Meng, Fugui Xie, Xin-Jun Liu, and Jinsong Wang. (2024). “Structural Designs of Novel Deployable Polyhedral Grippers for Noncontact Capturing Missions”, Journal of Mechanical Design, 146(4): 043302. https://doi.org/10.1115/1.4063968

Advances in Deployable Mechanisms in Space

Sajjad Keshtkar[1], Hirohisa Kojima[1]

[1]Department of Aeronautics and Astronautics, Tokyo Metropolitan University, 6-6 Asahigaoka, Tokyo 191-0065, Japan, {s.keshtkar@tmu.ac.jp}

ABSTRACT

1 Introduction

Deployable mechanisms are a critical part of space exploration, which enable large structures such as antennas, solar panels, and habitats to be stowed and stored in the cylindrical shape of the rocket during launch and then deployed in space. Recent advances in this field, which include materials, design, and actuation technologies, have shown improvements in reliability, stability, and precision. In this abstract, we review some of the latest developments in this system, which are used in satellites, highlighting new designs, materials, and mechanisms, as well as the challenges involved in the extreme conditions of space [1].

As long as the complexity and size of the satellite increase, the need for reliable, optimal, and lightweight deployable mechanisms is growing with it. The primary use of these mechanisms is to allow large structures, like antennas, panels, and other instruments, to be packed into the rocket during the launch and then to be deployed in orbit or on other planets or asteroids. The main challenge in this field involves designing mechanisms that have a balance between high stiffness and low mass while being reliable during the high-stress part of the launch and the harsh environment of space. In this abstract, we overview some recent advances in deployable mechanisms, highlighting their innovation and current and future applications in space.

2 Materials and Design

Thanks to advancements in materials, the possibility of developing lightweight and durable materials has also advanced. Examples of these materials include shape memory alloys (SMAs), carbon fiber composites, and bistable structures. These advanced materials, especially those designed for outer space conditions, provide high durability, improved mass-to-resistance ratio, and mechanical efficiency, critical factors for deployable mechanisms.

The possibility is that the SMAs will return to their pre-deformed or designed shape when subjected to certain stimulators for controlled unfolding or expansion [2]. Carbon fiber composites, with their high strength-to-weight ratio, have been exploited in structural elements, allowing for larger and more complex deployable structures [3].

Bistable structures for space shift into two or several stable conditions without continuous actuation to obtain a high-efficiency system for both stowed and deployed configurations. These designs offer high reliability and reduce space energy consumption [4]. In addition to materials, new designs, such as origami-inspired and tensegrity systems, are also being developed. These designs can achieve large deployable areas with minimal mass [5].

3 Actuation Techniques

Novelle actuation mechanisms, such as piezoelectric actuators, also improved the control of deployment. These actuators can generate motion in response to small electrical signals, offering fine control over small displacements [6]. SMAs can also be used as actuators which can offer a high force-to-weight ratio where thermal gradients are prevalent. Sensor fusion and integration for the deployment process is an important real-time adjustment method that has been used recently to monitor the deployment sequences, reducing the risk of failure. Apart from classical robust controls, emerging AI and machine learning techniques are also proposed for image processing during deployment.

4 Applications in Space Missions

Deployable mechanisms have been a common technique since the early stages of the space era. The most significant and expensive deployable site is the James Webb Space Telescope (JWST). In this satellite, several consecutive stages of deployment are achieved during various weeks, which include a large deployable sunshield made of five layers of Kapton antennas and the receiver. Similarly, small satellites, like CubeSats, often utilize deployable solar arrays and antennas to extend their functionality [7].

Emerging applications of deployable mechanisms include the development of structures and materials used to enable humans to inhabit other planets or new space stations. These could include inflatable modules that provide living quarters for astronauts, which should be lightweight and capable of withstanding the harsh conditions of space [8]. Another application is large space space-based solar power stations and antennas, which require large arrays of modules. The solar station, for instance, is meant to have several kilometers in diameter in orbit, capture solar energy, and convert it into electricity for use on Earth. High-precision deployment and orientation are key factors to ensure the functionality and efficiency of the system.

©2024 The authors. All rights reserved.
DOI: 10.17185/duepublico/82663

5 Challenges and Future Directions

Despite the significant progress, several fields of deployable mechanism systems remain challenged. One of these challenges is ensuring the shock absorption and vibration tests during the launch, which can cause major damage to any movable structure. Another active area of research is the design for the vacuum of space, where mechanical components are in the condition of extreme temperatures, radiation, and the absence of atmospheric pressure. These conditions can cause materials to behave unpredictably, potentially leading to failure during the deployment process. To address this, we need to develop more reliable lock mechanisms during launch and more robust materials that can withstand harsh conditions while maintaining their mechanical properties.

Another challenge is developing highly autonomous control and fault-tolerant systems that can detect possible faults in real time and respond to potential failures. Some of the failures these mechanisms should be capable of identifying include mechanical jamming, fatigue, or even actuator failures. There should also be some sort of adjustment policies, providing more flexibility during deployment to prevent mission failure. Research in this area can also include developing advanced sensor networks and sensor fusion techniques, as well as vision/AI-based control systems that can monitor the status of deployable mechanisms in real time.

Other potential future directions in this field include the development of self-healing and self-repairing structures, especially with the increasing risk of space debris. The long-term exploitation of long-duration and highly valuable missions where maintenance is not possible is one such scenario. Another possible area of research could be the development of deployment structures for capturing debris in small spaces.

6 Conclusion

Deployable mechanisms are one of the most essential parts of satellites for the current stage and future of space exploration. Advances in materials and designs, smart actuation techniques, and control strategies are making these systems more efficient and reliable for the deployment of larger and more complex space structures. As research in the field of space exploration with the need for larger and more precise satellites progresses, deployable mechanisms will also need to be developed accordingly, facilitating these new missions and structures. From new space telescopes, solar arrays, and solar stations and antennas to habituating on other planets, deployable mechanisms will play a critical role in the future of space technology. They will require a further interdisciplinary approach and research.

References

[1] R. L. Eadie, M. J. Johnson, and T. K. Davis, “Deployable space structures for large-scale applications,” *Journal of Spacecraft and Rockets*, vol. 55, no. 3, pp. 789–799, 2021.

[2] T. D. Dao, N. S. Ha, N. S. Goo, and W. R. Yu, “Design, fabrication, and bending test of shape memory polymer composite hinges for space deployable structures,” *Journal of Intelligent Material Systems and Structures*, vol. 29, no. 8, pp. 1560–1574, 2018.

[3] X. Ma, N. An, Q. Cong, J. B. Bai, M. Wu, Y. Xu, and Q. Jia, “Design, modeling, and manufacturing of high strain composites for space deployable structures,”

[4] T. Liu, J. Bai, and N. Fantuzzi, “Analytical model for predicting folding stable state of bistable deployable composite boom,” *Chinese Journal of Aeronautics*, vol. 37, no. 8, pp. 460–469, 2024.

[5] C. Wang, H. Guo, R. Liu, and Z. Deng, “A programmable origami-inspired space deployable structure with curved surfaces,” *Engineering Structures*, vol. 256, p. 113934,

[6] B. Wang, et al., “Space deployable mechanics: A review of structures and smart driving,” *Materials & Design*, p. 112557, 2023.

[7] K. A. Parrish and C. Starr, “Launching and Deploying the James Webb Space Telescope,” in *Proc. 73rd International Astronautical Congress*, no. IAC-22-B6.3.1, 2022.

[8] A. Lak and M. Asefi, “A new deployable pantographic lunar habitat,” *Acta Astronautica*, vol. 192, pp. 351–367, 2022.

Estimation of Lower Limb Muscle Strength through the Daniels Scale

María del Pilar Dávila-Verduzco[1], Santiago Ramírez-Durán[1], Beatriz Alejandra Hernández García[2], Ivo Neftalí Ayala-García[1], Alejandro González[1]

[1]Tecnologico de Monterrey, Epigmenio Gonzalez 500, Fracc, San Pablo, 76130 Santiago de Queretaro, Qro., Mexico {A01708943@tec.mx, A01704805@tec.mx, ivo.ayala@tec.mx, agonzalezda@tec.mx}
[2] Centro de Rehabilitacion Integral de Queretaro, DIF Estatal, Queretaro, Mexico. {dralehernandez@gmail.com}

ABSTRACT

1 Introduction

In the healthcare field, particularly in rehabilitation, the Daniels Scale is a commonly used technique to assess muscle strength. Developed by Daniels and Worthingham, this scale classifies muscle strength on a scale from 0 to 5, where each level represents the muscle's ability to move a limb against resistance, as detailed in Table 1. Usa et al. developed a formula to predict maximum muscle strength in young adults, middle-aged, and elderly individuals, based on the theoretical grade 3 strength value of the Scale. They found a linear correlation between this value and maximum strength in young adults, although accuracy decreased in older individuals, particularly in knee flexion [1]. Yepes et al. also combined the Daniels Scale with surface electromyography (sEMG) signals and machine learning algorithms to classify muscle strength in hand grip exercises. Their approach achieved a 68% accuracy across subjects and 71% within subjects, although factors like temperature affected the accuracy of the results [2]. Other applications include the work of Cotri-Melecez et al., where they developed a computer-assisted system to automate the prescription of rehabilitation therapies in patients with ankle fractures. They used the Daniels Scale to assess muscle strength and classify patients, allowing them to determine the type of exercises needed, such as isometric or isotonic. The system, validated with clinical records, achieved an accuracy of 97.4%, proving to be a reliable tool for optimizing clinical decision-making in rehabilitation [3]. Similarly, Hinojosa-Rodríguez et al. investigated the long-term effects of Katona therapy in children with moderate to severe perinatal brain injury, using the Daniels Scale to measure muscle strength. The results showed that 67% of the children treated with early intervention achieved motor performance comparable to a healthy group, highlighting the importance of early intervention in mitigating motor disabilities [4].

This project is based on the previous work of Avellaneda Arroyo et al. [5], who continued the project by Medina Anzaldo, I.B. et al., developing a knee brace equipped with EMG, artificial vision, and a mechatronic system to evaluate the range of motion and muscle strength of the knee. Unlike the traditional Daniels Scale, which is based on qualitative evaluations, this system aims to provide a quantitative measurement of muscle function [6].

The aim of this project is to redesign and optimize the original prototype, introducing improvements in hardware and software, as well as refining the method of muscle strength quantification, thus offering a more efficient and precise tool for healthcare professionals. In the evaluation of Daniels Scale levels, a specific protocol is implemented through lower limb extension exercises to determine each level. The table below shows the Daniels Scale levels for assessing muscle strength, along with the methods used to measure each level.

Table 1: Daniels Scale and its Evaluation Methods

Daniels Scale Level	*Description*	*Proposed Evaluation Method [5]*
Level 0	Total absence of muscle contraction.	EMG signals are used to deny or confirm muscle contraction.
Level 1	Minimal contraction without joint movement.	
Level 2	Active movement without the influence of gravity.	The subject's limb moves in the absence of gravity.
Level 3	Complete active movement against gravity, without additional resistance.	The subject performs full movement against gravity without applying external resistance.
Level 4	Full movement against light or moderate external resistance.	A resistance test is performed with a light torque applied.
Level 5	Total muscle strength, able to resist maximum force.	A resistance test is performed with a large torque applied.

The project's hypothesis is that, by using the torque generated by an actuator, in this case, the AK80-6 motor, it is possible to simulate the resistance corresponding to levels 4 and 5, allowing the accurate determination of the patient's level on the Daniels Scale. Additionally, the force (F) exerted by the patient can be calculated using the formula.

©2024 The authors. This work may be used under a Creative Commons Attribution 4.0 License (CC BY 4.0)
DOI: 10.17185/duepublico/82603

$$\boldsymbol{F} = \frac{\boldsymbol{T}}{\boldsymbol{r}}, \tag{1}$$

where T is the torque and r is the distance where the resistance is applied (20 cm, equivalent to mid-calf).

2 Design

As shown in Figure 1a, the knee brace will be placed on the lower limb. The aluminum design, adapted to perform the measurement function, will be attached to the knee brace for accurate measurement as shown in Figure 1b.

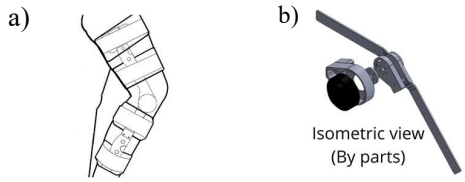

Figure 1: a) Knee Brace; b) Proposed devise redesign

The proposed model is an instrumented knee brace that integrates an AK80-6 motor, using parts manufactured from 6061 aluminum. The link placed over the thigh supports and secures the motor in a stable position, while the rotor connects to the calf link, which is the mobile part of the system, through an aluminum coupling and an adapter specifically designed for this function. Additionally, the axis of rotation of the knee joint is aligned with the axis of the motor's rotor, limiting the movement solely to flexion and extension of the joint.

3 Expected Results

The system is expected to help the medical practitioner to evaluate muscle function using the Daniels Scale, as detailed in Table 1. Additionally, the system should display the force associated with each level of the scale, providing accurate quantitative data. These results will be visualized through a digital interface, where each subject's data can be stored, facilitating medical follow-up and the evaluation of their continuous progress throughout the treatment.

References

[1] Usa, H., Matsumura, M., Ichikawa, K., & Takei, H. (2017). A Maximum Muscle Strength Prediction Formula Using Theoretical Grade 3 Muscle Strength Value in Daniels et al.'s Manual Muscle Test, in Consideration of Age: An Investigation of Hip and Knee Joint Flexion and Extension. Rehabilitation Research And Practice, 2017, 1-9. https://doi.org/10.1155/2017/3985283

[2] Yepes, J. C., Saldarriaga, A. J., Montoya-Leal, V., Orozco-Duque, A., Perez, V. Z., & Betancur, M. J. (2018). Classification Of Muscular Strength During Palmar Grasp Exercises Using Surface EMG Signals. International Seminar Of Biomedical Engineering (SIB). https://doi.org/10.1109/sib.2018.8467748

[3] Cotri-Melecez, B., Quiroz-Compean, G., Torres-Treviño, L., Rodriguez-Liñan, A., Raygoza, I. Q., & Fraire, O. S. (2024). Making Medical Prescription Automatic: The Case of Prescribing Therapies in Ankle Fracture Rehabilitation by Means of a Computer-Aided System. IEEE Access, 12, 97171-97183. https://doi.org/10.1109/access.2024.3426476

[4] Hinojosa-Rodríguez, M., De Leo- Jiménez, J. O., Colín, M. E. J., Moreira, E. G., Bautista, C. S. F., & Harmony, T. (2020). Long-term therapeutic effects of Katona therapy in moderate-to-severe perinatal brain damage. Neuroscience Letters, 738, 135345. https://doi.org/10.1016/j.neulet.2020.135345

[5] Avellaneda Arroyo, A., Medina Anzaldo, I. B., José A., & Vittoria, R. (2020). Estimación del rango de movilidad asociado a una potencia muscular. Unpublished work.

[6] Medina Anzaldo, I. B. , Sanroman Santana, L. Alejandra , Vittoria R., Islas, M. C., Ayala-Garcia, I. N., Gonzalez A. Measuring Range of Motion and Knee Torque with a Brace. 2024 IEEE 37th International Symposium on Computer-Based Medical Systems (CBMS), Guadalajara, Mexico, 2024, pp. 33-36, doi: 10.1109/CBMS61543.2024.00014.

Application of Two Tension Springs in the Four-Bar Engine Hood Linkage Mechanism

Onur Denizhan[1], Meng-Sang Chew[2]

[1]Department of Mechanical Engineering, Batman University, Batman, 72000, Türkiye, {onur.denizhan@batman.edu.tr}
[2]Department of Mechanical Engineering and Mechanics, Lehigh University, Bethlehem, PA, 18015, USA, {mc0p@lehigh.edu}

ABSTRACT

1 Introduction

The concept of designing mechanisms with various considerations, such as developing a four-bar linkage for kinematic and dynamic analysis, is not new. The typical process begins with determining the dimensions of the linkages, followed by optimization for various factors, including dynamic and kinematic considerations [1, 2]. Research commonly adheres to a two-step process: first, the synthesis of the mechanism, and then the modification of its components based on specific considerations. This traditional research framework has been the bases for numerous studies in mechanism design [3-7].

Previous studies have introduced four-bar automotive engine hood linkage mechanism loaded with tension and torsion springs, employing a conventional research methodology [8, 9]. Subsequently, a novel one-step procedure integrating kinetic synthesis with static balancing was developed [10, 11, 12]. This study investigates a two-tension-spring-loaded four-bar hood linkage mechanism using the previously established one-step procedure approach. The primary objective of this study is to demonstrate the design of an optimal two-tension-spring-loaded four-bar linkage mechanism for static balancing in the presence of friction. Additionally, this research serves as a further application of the one-step mechanism design procedure. The results of this study include optimization outcomes that are compared with previously reported results.

2 Problem Statement and Results

This study introduces the kinematic synthesis and optimization of a four-bar automotive engine hood linkage mechanism equipped with two attached tension springs. The configuration of the mechanism is illustrated in Fig. 1, where tension spring 1 and tension spring 2 are connected to links [AC] and [ED], respectively. Link [AC] serves as the driver link, and it is important to note that the rotation directions of both links [AC] and [ED] are the same during the hood motion.

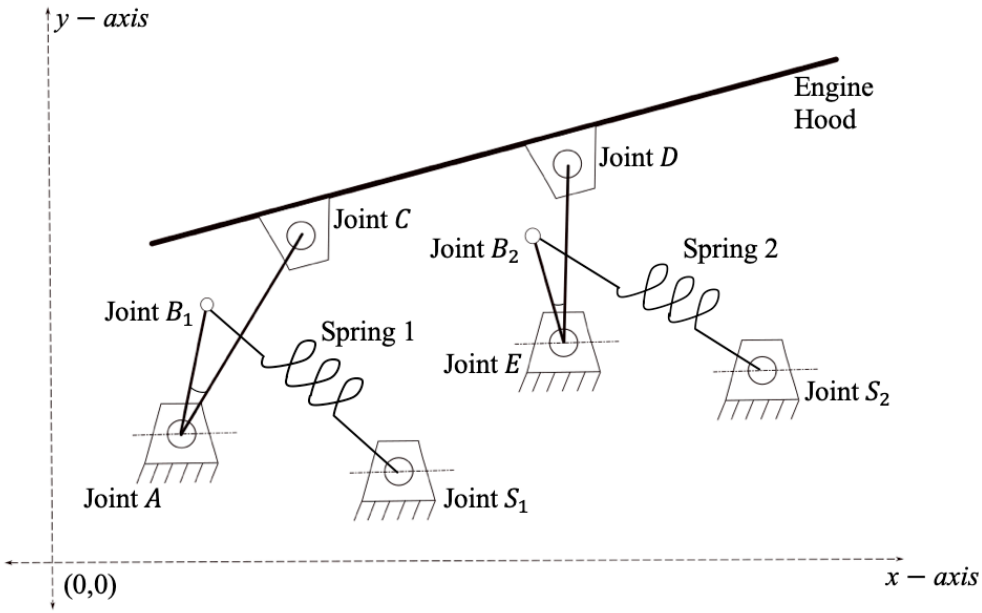

Figure 1: Two tension springs attached four-bar linkage mechanism

In this investigation, only the hood specifications are initially known: weight, length and the positions when fully-opened and fully-closed. The linkages and springs are assumed to be massless, with friction considered only at Joints *A, C, D* and *E.* To minimize the

©2024 The authors. This work may be used under a Creative Commons Attribution 4.0 License (CC BY 4.0)
DOI: 10.17185/duepublico/82608

number of design variables, tension springs 1 and 2 are selected to be identical. The introduced four-bar mechanism comprises eleven design variables, which include the spring constant, the angles of B_1AC ($\angle(B_1AC)$) and B_2ED ($\angle(B_2ED)$), x and y coordinates of Joints S_1 and S_2, the zero-spring lengths of springs 1 and 2, and the lengths of link [AB_1] and link [EB_2]. Furthermore, the two-position kinematic synthesis provides six free choices [2], of which five are designated as design variables. Additionally, the friction torques at the joints are treated as a design variable, assumed to be uniform across the joints. Consequently, the optimization process involves a total of seventeen design variables, with the objective of minimizing the applied force – or the balancing force at peak points – required to open or close the engine hood. The optimization results obtained are compared with previously reported results for the same four-bar hood linkage mechanism.

Acknowledgments

Authors wish to express their gratitude to the Ministry of National Education of the Republic of Türkiye which indirectly made this work possible.

References

[1] E. Soylemez, *Mechanisms,* 5th ed. ODTU Yayinlari, 2018. ISBN-13: 9786052456958.

[2] R. Norton, *Design of Machinery*, 6th ed. McGraw Hill, 2019. ISBN: 9781260113310.

[3] O. Denizhan, "A three-link gravity-balanced mechanism for operating room assistance", *Comptes rendus de l'Acade´mie bulgare des Sciences,* vol. 76, issue 10, pp. 1572-1580, 2023. doi: 10.7546/CRABS.2023.10.11

[4] O. Denizhan, "Dynamic modeling of the spring attached two-link planar manipulator", *International Journal of Computational and Experimental Science and Engineering,* vol. 9, issue 2, pp. 133-140, 2023. doi: 10.22399/ijcesen.1307444

[5] A. Zeiaee, R. Soltani-Zarrin, R. Langari, R. Tafreshi, "Kinematic design optimization of an eight degree-of-freedom upper-limb exoskeleton", *Robotica*, vol. 37, issue 12, pp. 2073-2086, 2019. doi:10.1017/S0263574719001085

[6] F. Freudenstein and MS. Chew, "Optimization of crank-and-rocker linkages with size and transmission constraints", ASME. *J. Mech. Des*., vol. 101, issue 1, pp. 51–57. January 1979. doi: 10.1115/1.3454024

[7] F. Freudenstein, "Designing linkages with optimum force transmission", *Product Engineering*, pp. 45-47, January 1978.

[8] O. Denizhan, "Three-position four-bar linkage mechanism synthesis, static balancing and optimization of automotive engine hood" Master's thesis, Lehigh University, Bethlehem, USA, 2015.

[9] O. Denizhan and MS. Chew, "Optimum design of a spring-loaded linkage mechanism in the presence of friction for static balancing", *Journal of Engineering Design and Analysis*, vol. 2, issue 1, pp. 5-11, 2019. doi: 10.24321/2582.5607.201901

[10] O. Denizhan, "Incorporation of kinematic analysis, synthesis and optimization into static balancing" Doctoral dissertation, Lehigh University, Bethlehem, USA, 2021.

[11] O. Denizhan and MS. Chew, "Optimum synthesis and design of a hood linkage for static balancing in one-step", *Tehnički vjesnik*, vol. 30, issue 3, pp. 855-862, 2023. doi: 10.17559/TV-20221122144345

[12] O. Denizhan and MS. Chew, "Integrated optimum design of a torsion spring-compensated automotive engine hood linkage mechanism", *International Journal of Scientific Research in Science, Engineering and Technology (IJSRSET*), vol. 10, issue 5, pp. 89-99, 2023. doi: 10.32628/IJSRSET2310524

Methodical Approach of Highly Realistic Virtual Test Environments for the Evaluation of Monitoring Algorithms in the Agricultural Domain

Sebastian Röttgermann[1], David Albrecht[1], Martin Maximilian de Fries[2,3], Marcus Irmer[2,3]

[1]LEMKEN GmbH & Co. KG, Advance Development, Weseler Straße 5, 46519 Alpen, Germany, {s.roettgermann@lemken.com}
[2]TH Köln – University of Applied Sciences, Betzdorfer Straße 2, 50679 Cologne, Germany
[3]Uppsala University, Ångströmlaboratoriet, 752 37 Uppsala, Sweden {marcus.irmer@th-koeln.de, martin.defries@th-koeln.de}

ABSTRACT

Agricultural implements for soil preparation, mechanical weeding, sowing, and other field operations are increasingly incorporating advanced intelligence. In pursuit of full autonomization, it is imperative that these implements possess the capability to autonomously detect incipient faults, without reliance on operator or supervisory intervention, and to mitigate them at an early stage. For both current and future generations of agricultural machinery, rapid identification of disturbance inputs or anomalies and the capacity for proactive corrective actions are critical. Moreover, current agricultural systems necessitate that farmers manually parameterize implements based on specific operational requirements and continuously monitor work quality. Future machine generations (as an example, see Fig. 1) will need to prioritize advanced process intelligence, with a focus on autonomous process monitoring and real-time assessment of work quality.

Our current research focuses on disturbance input detection (or anomaly detection) [2, 3] and performance monitoring [4] for agricultural implements. Specifically, we are developing vision-based systems for detecting blockages and tool damage, such as in cultivators, as well as vision-based performance monitoring for implements like cultivators and mechanical weeders. In the context of disturbance variable detection, it is critical to automatically identify both continuous tool wear and unexpected damage during operation. Examples include tool breakage or failure due to collisions with subsurface obstacles. Additionally, excessive accumulation of soil or plant material on the implement presents another significant disturbance variable in soil tillage processes.

Beyond the detection of disturbance variables, there is an urgent demand for a highly automated approach to evaluate the quality of work across various stages of agricultural field cultivation. Currently, this evaluation is performed manually by the operator, who uses the assessment to adjust machine settings. However, in fully autonomous systems, the machine must be capable of responding to sensor-derived data in real-time, adjusting its operational parameters accordingly to maintain optimal performance.

Figure 1: Combined Powers machine [1] – combination of a smart implement with an autonomous towing vehicle (image source: LEMKEN GmbH & Co. KG)

The mentioned system comprises a camera, a control unit, and software incorporating an image processing algorithm capable of detecting cultivator tines within captured images and assessing their wear condition visually. The camera is mounted on the frontmost beam of the cultivator's steel frame, oriented against the direction of travel with a slight downward tilt to focus on the mounted tines. In the event of tine wear or damage, the operator is notified via the assistance system. In fully autonomous configurations, the monitoring system assumes responsibility for wear detection, thereby eliminating the need for operator intervention.

The development and validation of the image processing algorithm necessitate a substantial volume of image data. This data is predominantly derived from video sequences recorded during field trials of the system at the testing site.

©2024 The authors. All rights reserved.
DOI: 10.17185/duepublico/82631

While generating images in real field conditions (see Fig. 2 (a) and Fig. 2 (b)) is a common practice, it has several limitations. One major drawback is the difficulty in ensuring reproducibility of test scenarios, as the environmental conditions during real-world tests – such as weather, lighting, or the path taken – cannot be consistently replicated. In agriculture, this challenge is further compounded by the seasonal variability of vegetation at the test site. Moreover, real-world test drives require extensive preparation, execution, and post-processing, which are both time-consuming and labor-intensive.

These challenges have prompted the exploration of using high-resolution virtual environments as a substitute for real test drives, as in the present case. Simulation environments offer significant advantages, including reduced time and personnel requirements, leading to cost savings and an accelerated development process. However, to effectively use virtually generated images for evaluating software performance, these images must be highly accurate reconstructions of the original recordings captured by the real camera system. This research presents a methodology for generating such image reconstructions in virtual test environments (see Fig. 2 (c) and Fig. 2 (d)) as well as it gives some preliminary results on the performance of the detection algorithms which have been fed with artificial created images.

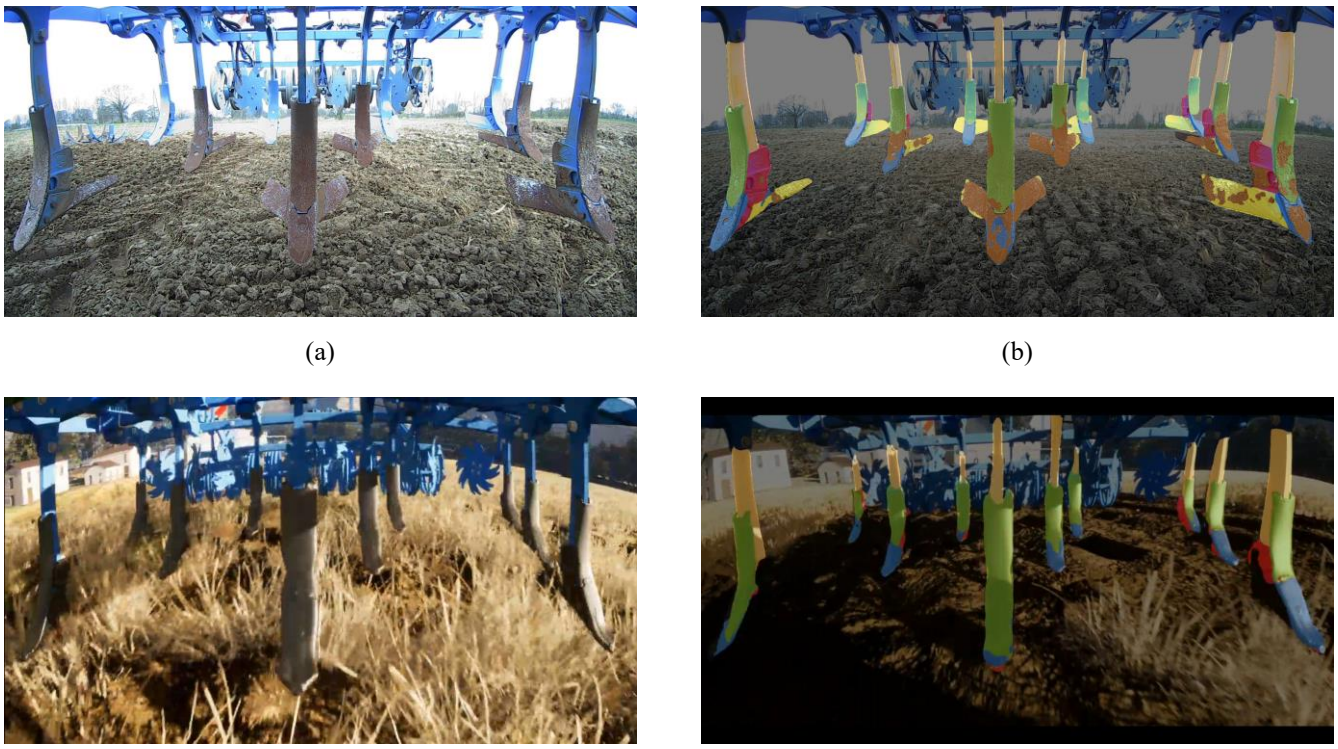

(a) (b)

(c) (d)

Figure 2: (a) real camera image, (b) annotation based on real camera image, (c) virtual camera image, (d) annotation based on virtual camera image

References

[1] Kooperationsprojekt Maschinenfabrik Bernard Krone GmbH & Co. KG & LEMKEN GmbH & Co. KG. (n.d.). *Combined Powers.* Retrieved September 22, 2022, from https://combined-powers.com/

[2] S. Röttgermann, G. Podann, J. IJsselmuiden, F. Tamminga, N. van de Westeringh, K. Jayaraj, D. Albrecht, “Disturbance Input Detection and Performance Monitoring for Smart Agricultural Implements”, in *AgEng-LAND.TECHNIK 2022 - International Conference on Agricultural Engineering - VDI Berichte*, Berlin: VDI Verlag GmbH, 2022.

[3] S. Röttgermann and H. Hecheltjen and S. Haverkamp, “System Architecture for the Combination of Smart Agricultural Implements with Highly Automated Towing Vehicles, from the Implement Manufacturer's Point of View”, in *2023 ASABE Annual International Meeting*. American Society of Agricultural and Biological Engineers, St. Joseph, Michigan, 2023

[4] J. Bracke, „Entwicklung eines sensorgestützten Verfahrens für die Bestimmung der Bodenebenheit als Parameter der Bearbeitungsqualität während der landwirtschaftlichen Bodenbearbeitung“, Ruhr Universität Bochum, 2020.

Optimal Input Shaper Tuning Using Constrained Bayesian Optimization in Industrial Robot Systems

Mingkun Wu, Burkhard Corves

[1]Institute of Mechanism Theory, Machine Dynamics and Robotics, RWTH Aachen University, Eilfschornsteinstraße 18, 52062 Aachen, Germany, {{wu, corves}@igmr.rwth-aachen.de}

ABSTRACT

1 Introduction

In this article, we propose a data-driven parameter tuning method for industrial robot systems with input shapers. The demand for high-speed and high-acceleration in pick-and-place (PaP) tasks, has made residual vibrations increasingly severe, negatively affecting the working accuracy of industrial robots. The input shaping technique, as an active vibration suppression technology, can effectively mitigate residual vibrations without altering existing control systems or requiring additional materials, making it particularly suitable for commercial industrial robots with unchangeable controllers.

Although input shapers have been proven effective for residual vibration suppression, their performance heavily depends on the dynamic characteristics of robot systems, i.e., natural frequencies and damping ratios. However, accurately determining these dynamic characteristics is nearly impossible, whether through numerical modelling or experiments. Furthermore, the natural frequencies of robot systems are functions of configurations of robots [1], which indicates that simply using the natural frequency of a specific configuration to design an input shaper cannot guarantee optimal performance across motions. While input shapers can reduce residual vibrations, they also lead to trajectory deformation. Although trajectory shape is less critical than positioning accuracy in PaP tasks, trajectory deformation may cause robots to encounter singularities or exceed their workspace limits, especially when the trajectory traverses some sensitive positions [2]. Therefore, designing an optimal input shaper that can not only attenuate residual vibration but also adhere to constraints on trajectory deformation is of significant practical importance.

Compared to designing input shapers by theoretical metrics, data-based metrics provide a more effective and accurate reflection of the real-world performance and conditions of robot systems. These metrics also imply that the optimization objectives are unknown, leading to a black-box optimization problem. Bayesian optimization (BO) is a data-driven, model-free approach that efficiently identifies the globally optimal design variables within relatively few experiments, where the unknown optimization objectives are represented by a surrogate model usually Gaussian process regression (GPR) [3]. BO has been applied in various fields, including controller tuning, hyperparameter optimization, parameter optimization of robots, etc. [4] proposed a sample-efficient joint tuning algorithm for a contour control system using BO, which can enable a trade-off between tracking accuracy, vibration and traversal time. [5] presented a model-free, data-driven parameter tuning method for a PID cascade controller by constrained Bayesian optimization (CBO), where a barrier-like term was introduced into the objective to guarantee safety requirements. BO leverages an acquisition function to determine the next evaluation point, where the acquisition function enables a trade-off between exploitation and exploration [6].

We propose a data-driven parameter tuning approach for input shapers in industrial robot systems performing PaP tasks, aiming to attenuate residual vibrations and improve positioning accuracy. This approach leverages a data-based metric to reflect the actual residual vibrations in the systems. We introduce a constraint to restrict the trajectory deformation. We use GPR to model both the metric and the constraint. We conduct a series of high-fidelity simulations to prove the performance of the proposed auto-tuning method.

2 Main Results

The residual vibration suppression performance of input shapers depends on the design parameters $\theta := [f_n, \xi, k_t]^T \in \Theta \subset \mathbb{R}^3$, where Θ is the feasible set to be predefined,. f_n and ξ denote the natural frequency and damping ratio, respectively. k_t is a parameter related to the time lag of the impulse sequence. These parameters also determine the degree of trajectory deformation. Therefore, we encode an optimization problem with constraints to achieve a trade-off between the residual vibration suppression and trajectory deformation as follows: $\min_{\theta\in\Theta} f(\theta)$ and s.t. $g(\theta) \leq q_m$,, where $f(\theta)$ represents the optimization objective that reflects the residual vibration, while $g(\theta)$ is the constraint function that reflects trajectory deformation. q_m is the maximum trajectory deformation defined by users. Data measured by sensors usually contains noise, hence, we assume that the real metric is defined as $f(\theta) = \bar{f}(\theta) + \varepsilon$, where $\varepsilon \sim N(0, \sigma_\varepsilon^2)$ is the measurement noise with zero mean and variance σ_ε^2.

The simulation is conducted by Simscape. The Delta robot is required to operate a PaP trajectory, where the total time of the reference trajectory is 0.8s and the total time of the simulation is set to be 1.2 s. The sampling time is chosen as $dt = 0.001$s. The performance metric is defined as follows $\bar{f}(\theta) = \sqrt{\frac{1}{m}\sum_{i=1}^{m} ||a_{rv,i}||^2}$, where $a_{rv,i} \in \mathbb{R}^3$, $i = 1, 2, \cdots, m$ denotes the acceleration vector of residual vibrations at sampling time $t = idt$ after the trajectory is finished. The standard deviation is selected as $\sigma_\varepsilon = 0.001$. m is set to be 100 in this article. The constraint is defined as the difference between the reference trajectory and the trajectory after the input shaper, i.e., $g(\theta) = \sqrt{\frac{1}{\varpi}\sum_{i=1}^{\varpi} ||q_{s,i} - q_{r,i}||^2}$, where ϖ denotes the total number of sampling points. $q_{r,i}$ and $q_{s,i}$ are the original reference trajectory and the trajectory after input shapers at ith sampling point, respectively.

©2024 The authors. All rights reserved.
DOI: 10.17185/duepublico/82614

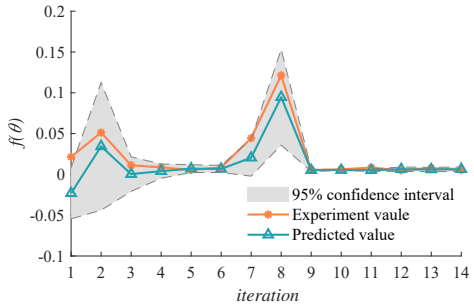

Figure 1: The predicted mean and experimental values over iterations.

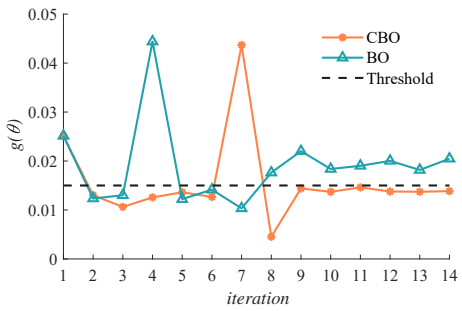

Figure 2: Constraints over iterations for two methods.

We use the constrained *Expected Improvement* (EI) acquisition function to determine the next point to be evaluated [4]. In order to stop the iteration timely, a stopping criterion is necessary during the real experiment. In addition to setting a fixed number of iterations, motivated by [5], we introduce the following criterion $a_{CEI,i} \leq \eta \max_{i \leq \kappa-1} a_{CEI,i} \quad i = \kappa, \kappa+1, \kappa+2$, where $\kappa \geq 2$ denotes κth iteration, and η is a positive threshold. The above inequality implies that once consecutive three expected improvements cannot improve the performance metric effectively compared to all previous iterations, we terminate the optimization process timely. We use consecutive three iterations instead of one to prevent premature termination before finding the optimal value due to a single error. Here, we select η as $\eta = 0.02$.

Fig. 1 illustrates the convergence of the CBO algorithm and the variance of the constrained EI maximum at each iteration. In this case, we set the initial data set to contain 5 experiments. The variance is relatively large at the beginning, because GPR lacks sufficient information for accurate predictions with high confidence. This also explains why the initial prediction is less than zero, which is obviously unreasonable. As the tuning process converges, the predicted mean closely aligns with the experiment value, which demonstrates the accuracy and effectiveness of the GPR model after accumulating enough information. The experiment value increases and decreases twice during the entire optimization process, and then converges to the optimum from 9th iteration. The optimal parameters that can minimize the performance metric and not violate the constraints are found at 12th iteration. At the same time, starting from 12th iteration, the following three consecutive constrained EIs meet the stopping criterion. Although the constrained EI also satisfies the threshold at 10th iteration as well, the optimization process continues thanks to the stopping criterion. The experiment value at 8th iteration deviates from the optimum to a large degree, likely because the constrained EI adopts a set of parameters with more exploration information.

The change in constraints $g(\theta)$ throughout the tuning process is illustrated in Fig. 2, where the results of normal BO with EI are introduced for comparison. It can be found that although we use the constrained EI as acquisition function, the constraint is not always satisfied during the tuning process. Note that the principle of constrained EI is to increase the expected improvement in regions where the constraint has a high probability of being satisfied, and reduce the expected improvement in the other regions, which means it is affected by performance of the GPR model for constraints. As the tuning process converges, the results of CBO are close to the boundary of the constraint without exceeding it. On the contrary, standard BO with EI fails to meet the constraint requirements.

Acknowledgments

This work was supported by China Scholarship Council under Grant 202106250025.

References

[1] Y. Zhao, J. Mei, and W. Niu, "Vibration error-based trajectory planning of a 5-dof hybrid machine tool," *Robot Comput. Integr. Manuf.*, vol. 69, p. 102095, 2021.

[2] Y. Liu, B. Feng, T. Cheng, Y. Chen, X. Liu, J. Zhang, S. Qu, and W. Yang, "Singularity analysis and solutions for the origami transmission mechanism of fast-moving untethered insect-scale robot," *IEEE Trans. Robot.*, 2023.

[3] M. Khosravi, V. Behrunani, R. S. Smith, A. Rupenyan, and J. Lygeros, "Cascade control: Data-driven tuning approach based on bayesian optimization," *IFAC-PapersOnLine*, vol. 53, no. 2, pp. 382–387, 2020.

[4] A. Rupenyan, M. Khosravi, and J. Lygeros, "Performance-based trajectory optimization for path following control using bayesian optimization," in *2021 60th IEEE Conference on Decision and Control (CDC)*. IEEE, 2021, pp. 2116–2121.

[5] M. Khosravi, C. König, M. Maier, R. S. Smith, J. Lygeros, and A. Rupenyan, "Safety-aware cascade controller tuning using constrained bayesian optimization," *IEEE Trans. Ind. Electron.*, vol. 70, no. 2, pp. 2128–2138, 2022.

[6] Q. Lu, K. D. Polyzos, B. Li, and G. B. Giannakis, "Surrogate modeling for bayesian optimization beyond a single gaussian process," *IEEE Trans. Pattern Anal. Machine Intell.*, vol. 45, no. 9, pp. 11 283–11 296, 2023.

On methods to motivate students to self-organized learning and to enable them to acquire "future skills".

Thorsten Bartel[1]

[1]Institute for Mechanics, Technical University Dortmund, Leonhard-Euler-Str. 5, 44227 Dortmund, Germany, {thorsten.bartel@tu-dortmund.de}

ABSTRACT

The growing discrepancy between the rapidly changing requirements for competencies in engineering and the rigid structures at universities is causing ever-increasing frustration, longer study times, high dropout rates and, last but not least, dwindling enrollment figures. The challenges of overcoming these discrepancies seem insurmountable. In this lecture, we would like to explain measures, methods and concepts that are taking the first essential steps towards solving this problem.

1 Introduction

The ability to obtain knowledge or, more generally, information from external sources and to use it effectively and efficiently for one's own work has developed rapidly in recent years. In particular, the use of AI-based tools is revolutionizing modern professional and everyday life. These developments, which will have lasting effects, bring with them completely new demands for urgently required competencies. On this basis, so-called "future skills" have been defined, for example in [1]. In contrast to this, the content and learning objectives of the courses in current engineering degree programs rarely integrate even the use of computers. Furthermore, the learning objectives often include relatively low taxonomy levels, cf. [2, 3], and do not go beyond pure application and, even worse, remain at the level of rote learning. More specifically, the future skills mentioned above are usually not addressed at all. This growing discrepancy between urgently required competencies and those that can actually only be achieved in the course of study generally leads to great demotivation among students. This in turn leads to inadequate examination results, longer study times and ultimately, in the long term, dwindling enrollment figures. The challenges for overcoming these discrepancies are numerous and seemingly insurmountable. On the one hand, they stem from the learners, who are becoming increasingly heterogeneous. On the other hand, the teachers and university structures are so inflexible that, for example, already in [4] the conclusion is drawn that engineering education is resistant to demands for change. In this presentation, we would like to explain elementary concepts and good practice examples that particularly promote the design of motivational teaching — the elementary basis for acquiring "future skills" and, among other things, reducing the average duration of studies.

2 Motivational teaching

Many lecturers assume that students are highly motivated, or should be, since the purpose of their studies is to prepare for their future careers. However, this is where a fundamental problem of current university teaching comes into play: due to a lack of reference to reality and a lack of competence orientation, students cannot recognize at all what the subject matter has to do with their desired profession. Without sufficient motivation, students are often not interested in the subject matter. This is where the role of teachers in modern education according to learning theories based on constructivism becomes apparent: It is our responsibility to motivate students through appropriate concepts and to design a setting that is conductive to learning. This fundamentally includes a high degree of empathy and sufficient positive individual evaluation of learning activities. In this contribution, we present essential building blocks of motivational teaching.

3 Constructive Alignment

One of the biggest problems in the design and implementation of conventional courses, especially in engineering degree programs, is that mainly and sometimes exclusively the topics to be covered, i.e., the curriculum, is defined. However, the learning objectives cannot be derived from the subject matter alone, cf. the examples provided in [5]. The clear definition of learning objectives, including the associated teaching and learning activities, is of fundamental importance because the achievement of these learning objectives is observable for both learners and teachers. In short, learning objectives state what students should be capable of at the end of a course. Constructive Alignment according to [6] in addition states that, in a nutshell, learning objectives, teaching and learning activities, and the type of examination must be optimally aligned with each other. If this is clearly recognizable to students, it also significantly increases their motivation.

4 Good Practice Examples

On June 10 and 11, 2020, the workshop "New Ways in Teaching: From teaching to learning events" organized by the expert committee "Modern Teaching and Didactics in Mathematics and Mechanics" of the German Society for Applied Mathematics and Mechanics, GAMM for short, took place. The workshop was led by several lecturers who already use modern methods of didactics in higher education and have extensive experience with them. One of the aims of the exchange with the participants was to explain

©2024 The author. This work may be used under a Creative Commons Attribution - ShareAlike 4.0 License (CC BY-SA 4.0)

DOI: 10.17185/duepublico/82628

which specific measures have which effects. In a subsequent evaluation and analysis of the discussion contributions, it became clear that the various best-practice examples have one positive effect above all: a significant increase in student motivation. The underlying concepts are briefly introduced below and explained in detail in our presentation, along with the specific good practice examples.

Activation of students

In many cases, courses are still similar to medieval lectures in which the lecturer delivers a 90-minute monologue. In terms of motivation, this is the worst possible form of teaching. And we shouldn't just blame everything on the YouTube or TikTok generation, but rather ask ourselves how long we can concentrate on a lecture that is not didactically optimal at professional conferences. Activating students, e.g. by involving them through audience response systems or other direct forms of participation, significantly contributes to boosting their motivation. Above all, student activation methods also offer significantly better learning progress monitoring for both students and teachers.

Alternative examination formats

The prospect of having to reproduce the knowledge acquired on a specific day, and in most cases within a very short period of time, causes frustration, demotivation and, not least, stress and panic for many students. Alternative and, in particular, formative examination formats offer the advantage of not having to base the assessment on a single "measurement". Students benefit from continuous activity and early and ongoing feedback, which ultimately also helps to increase motivation. In addition, formative examination formats considerably facilitate the possibility of achieving higher levels of competence.

Gamification

Lecturers usually base their choice of lecture format on what they themselves experienced as students and found to be good. However, there are two fundamental problems with this: 1. university lecturers are usually not representative of the average student, 2. the more time passes, the less representative are one's own preferences compared to those of the current younger generation.. Gamification transfers elements of (computer) games into teaching and ensures, among other things, that the younger generation of students are more motivated to engage in learning activities at all. In addition, gamification is perfectly suited to formative examination formats and also provides the opportunity to experience learning with multiple senses.

Practical examples

The question from learners as to why they should do what they are told to do is an absolutely understandable and legitimate one. Statements along the lines of "because it says so in the curriculum" are the worst possible responses. Even the prospect that certain aspects will be needed later in the course of study is far too abstract to serve as motivation for most students. However, to show students that they can now develop solutions to problems that may have even prompted them to study in the first place, leads to a significant increase in motivation.

References

[1] J. Kirchherr, J. Klier, C. Lehmann-Brauns and M. Winde. *Future Skills: Welche Kompetenzen in Deutschland fehlen* [online]. Essen: Stifterverband für die Deutsche Wissenschaft e.V. https://www.stifterverband.org/medien/future-skills-welche-kompetenzen-in-deutschland-fehlen, 2018

[2] B.S. Bloom (Ed.), *Taxonomy of Educational Objectives: The Classification of Educational Goals. Handbook I: Cognitive Domain.* Longmans, Green & Co, 1956.

[3] L.W. Anderson, D.R. Kratwohl, *A Taxonomy for Learning, Teaching, and Assessing: A Revision of Bloom's Taxonomy of Educational Objectives*. Longman, 2001.

[4] F.S. Becker, *Der Europäische Hochschulraum: Bekommen wir die Ingenieure, die wir brauchen?* In: J. Grünberg, I.G. Wenke (eds.), Arbeitsmarkt Elektrotechnik Informationstechnik 12, Berlin: VDE Verlag, 43–54, 2004

[5] T. Bartel, T. Haertel. *A guide to defining learning objectives* [online]. GAMM expert committee "Modern Teaching and Didactics in Mathematics and Mechanics", https://im.mb.tu-dortmund.de/storages/im-mb/r/Praesentationen/GAMM-FA_Didaktik/Bericht_Lernziele_ENG.pdf, 2023

[6] J. Biggs, "Enhancing teaching through constructive alignment". *High Educ*, vol. 32, pp. 347–364, 1996.

Computational and Experimental Analysis of Crutch-Assisted Gait: Findings from a Case Study

Mariana Rodrigues da Silva[1,2], Filipe Marques[1,2], Sérgio B. Gonçalves[3], Miguel Tavares da Silva[3], Paulo Flores[1,2]

[1]CMEMS-UMinho, Departamento de Engenharia Mecânica, Universidade do Minho, Campus de Azurém, Guimarães 4804-533, Portugal, {m.silva@dem.uminho.pt; fmarques@dem.uminho.pt; pflores@dem.uminho.pt}
[2]LABBELS – Associate Laboratory, Braga/Guimarães, Portugal
[3]IDMEC, Instituto Superior Técnico, Universidade de Lisboa, Av. Rovisco Pais, 1, Lisboa 1049-001, Portugal
{sergio.goncalves@tecnico.ulisboa.pt; miguelsilva@tecnico.ulisboa.pt}

ABSTRACT

1 Introduction

The 2022 global report on assistive technology of the World Health Organization and the United Nations Children's Fund (UNICEF) estimates that more than 2.5 billion people globally require the use of one or more assistive devices, and this number is expected to rise to 3.5 billion in 2050 [1]. The use of assistive devices presents crucial functional benefits for subjects with permanent or temporary disability, as they not only improve independence, but also enable and enhance the participation in social activities and reduce the need for hospitalization [2].

An option for patients with mobility disabilities is to use crutches to restore the mobility lost due to the disability and regain some degree of independence [3]. Crutches are utilized as an aid to locomotion by patients with a variety of pathologies, providing them with a good level of mobility and flexibility. They are utilized to increase the patients' balance and base of support, and to partially or fully unload the lower limbs by transferring the body weight to the upper extremities [4].

Despite the existing investigation, the study of crutch-assisted locomotion has not become an established routine yet, and difficulties still exist in understanding how it may impact clinical interventions. Hence, this work aims to develop an advanced biomechanical model of the human movement within the framework of multibody system methodologies in order to study crutch-assisted locomotion with focus on the interaction that occurs between the model and the device. The knowledge on this topic may help provide promising options for the development of mobility assistive devices tailored to the needs of each subject.

2 Biomechanical multibody model

A three-dimensional biomechanical multibody model of the human body (see Figure 1) was developed in MATLAB using an in-house code named MUBODYNA. The model is composed of 18 rigid bodies, which are kinematically connected to each other using 17 geometrically ideal joints. Table 1 presents a complete description of the bodies and joints of the considered biomechanical model. As inferred from the observation of Table 1, the model has a total of 39 degrees of freedom (DoF), which are guided using experimental data of one adult female subject acquired at the Lisbon Biomechanics Laboratory of Instituto Superior Técnico. A kinematic consistency procedure is applied to obtain kinematically consistent positions and velocities, avoiding constraint violation.

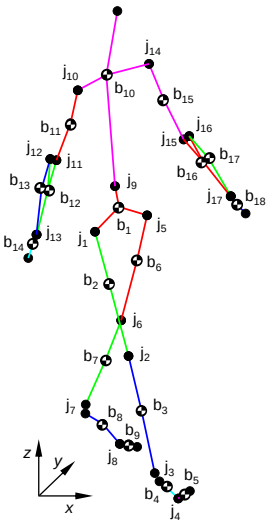

Figure 1: Multibody model

Table 1: Bodies and joints of the considered biomechanical multibody model

Body (nr.)	Joint (nr.)	Joint type	DoF	Connected bodies
Lower Trunk (1)	Hip (1, 5)	Spherical	3	Lower Trunk – Thigh
Thigh (2, 6)	Knee (2, 6)	Revolute	1	Thigh – Leg
Leg (3, 7)	Ankle joint complex (3, 7)	Modified universal [5]	2	Leg – Main Foot
Main Foot (4, 8)	Metatarsophalangeal (4, 8)	Revolute	1	Main Foot – Toes
Toes (5, 9)	Back (9)	Spherical	3	Lower Trunk – Upper Trunk
Upper Trunk (10)	Glenohumeral (10, 14)	Spherical	3	Upper Trunk – Humerus
Humerus (11, 15)	Humeroulnar (11, 15)	Classical universal	2	Humerus – Ulna
Ulna (12, 16)	Radioulnar (12, 16)	Body-follower	0	Ulna – Radius
Radius (13, 17)	Radiocarpal (13, 17)	Spherical	3	Radius – Hand
Hand (14, 18)				

DoF – degrees of freedom

© 2024 The authors. This work may be used under a Creative Commons Attribution - NonCommercial 4.0 License (CC BY-NC 4.0)
DOI: 10.17185/duepublico/82584

3 Crutch-model interaction

The crutches are introduced into the model using two approaches. First, a fixed joint is considered between the hand and the crutch to prevent the relative motion between these bodies, removing six DoF. The kinematic constraint equations are expressed as

$$\mathbf{\Phi}^{(\mathrm{f},6)} = \begin{cases} \mathbf{r}_j^P - \mathbf{r}_i^P = \mathbf{r}_j + \mathbf{s}_j^P - \mathbf{r}_i - \mathbf{s}_i^P = \mathbf{0} \\ \mathbf{a}_i^{\mathrm{T}}\mathbf{b}_j - \mathbf{a}_{i,0}^{\mathrm{T}}\mathbf{b}_{j,0} = 0 \\ \mathbf{c}_i^{\mathrm{T}}\mathbf{d}_j - \mathbf{c}_{i,0}^{\mathrm{T}}\mathbf{d}_{j,0} = 0 \\ \mathbf{e}_i^{\mathrm{T}}\mathbf{f}_j - \mathbf{e}_{i,0}^{\mathrm{T}}\mathbf{f}_{j,0} = 0 \end{cases} \tag{1}$$

where $\mathbf{r}_k^P$ is the global position vector of point P located on body k, $\mathbf{r}_k$ is the global position vector of the center of mass of body k, $\mathbf{s}_k^P$ is the global position vector of point P located on body k with respect to the body's local coordinate system. The last three constraint equations of Eq. (1) are considered in order to establish a constant orientation between vectors $\mathbf{a}_i$, $\mathbf{b}_j$, $\mathbf{c}_i$, $\mathbf{d}_j$, $\mathbf{e}_i$ and $\mathbf{f}_j$ and their coordinates in the initial configuration ($\mathbf{a}_{i,0}$, $\mathbf{b}_{j,0}$, $\mathbf{c}_{i,0}$, $\mathbf{d}_{j,0}$, $\mathbf{e}_{i,0}$ and $\mathbf{f}_{j,0}$). $\mathbf{\Phi}^{(\mathrm{f},6)}$ refers to a fixed (f) joint constraint with six (6) equations. The contribution of the joint to the Jacobian matrix and right-hand side of the acceleration equations is, respectively, as

$$\mathbf{D}^{(\mathrm{f},6)} = \begin{bmatrix} -\mathbf{I} & \tilde{\mathbf{s}}_i^P & \mathbf{I} & -\tilde{\mathbf{s}}_j^P \\ \mathbf{0} & -\mathbf{b}_j^{\mathrm{T}}\tilde{\mathbf{a}}_i & \mathbf{0} & -\mathbf{a}_i^{\mathrm{T}}\tilde{\mathbf{b}}_j \\ \mathbf{0} & -\mathbf{d}_j^{\mathrm{T}}\tilde{\mathbf{c}}_i & \mathbf{0} & -\mathbf{c}_i^{\mathrm{T}}\tilde{\mathbf{d}}_j \\ \mathbf{0} & -\mathbf{f}_j^{\mathrm{T}}\tilde{\mathbf{e}}_i & \mathbf{0} & -\mathbf{e}_i^{\mathrm{T}}\tilde{\mathbf{e}}_j \end{bmatrix} \tag{2}$$

$$\boldsymbol{\gamma}^{(\mathrm{f},6)} = \begin{Bmatrix} -\tilde{\boldsymbol{\omega}}_j\dot{\mathbf{s}}_j^P + \tilde{\boldsymbol{\omega}}_i\dot{\mathbf{s}}_i^P \\ -\mathbf{b}_j^{\mathrm{T}}\tilde{\boldsymbol{\omega}}_i\dot{\mathbf{a}}_i - \mathbf{a}_i^{\mathrm{T}}\tilde{\boldsymbol{\omega}}_j\dot{\mathbf{b}}_j - 2\dot{\mathbf{a}}_i^{\mathrm{T}}\dot{\mathbf{b}}_j \\ -\mathbf{d}_j^{\mathrm{T}}\tilde{\boldsymbol{\omega}}_i\dot{\mathbf{c}}_i - \mathbf{c}_i^{\mathrm{T}}\tilde{\boldsymbol{\omega}}_j\dot{\mathbf{d}}_j - 2\dot{\mathbf{c}}_i^{\mathrm{T}}\dot{\mathbf{d}}_j \\ -\mathbf{f}_j^{\mathrm{T}}\tilde{\boldsymbol{\omega}}_i\dot{\mathbf{e}}_i - \mathbf{e}_i^{\mathrm{T}}\tilde{\boldsymbol{\omega}}_j\dot{\mathbf{f}}_j - 2\dot{\mathbf{e}}_i^{\mathrm{T}}\dot{\mathbf{f}}_j \end{Bmatrix} \tag{3}$$

where $\mathbf{I}$ is the identity matrix, (~) is the skew symmetric matrix, (.) is the derivative with respect to time, $\boldsymbol{\omega}$ is the angular velocity vector. It is assumed that (*i*) point P on the hand is located on its center of mass, (*ii*) point P on the crutch is located on its handle, and (*iii*) the orientation of the hand relative to the crutch is constant during the analysis and equal to the orientation in the first time instant.

The second approach utilized in this work to deal with the crutch-model interaction is to use a spherical joint between the crutch and the hand. To formulate this joint, the first row of Eqs. (1)-(3) is utilized. In this situation, since relative motion between the two bodies is allowed, the number of DoF is adjusted, yielding a biomechanical multibody model with a total of 45 DoF.

4 Results and discussion

Figure 2 depicts the *z*-coordinate of the center of mass of the right crutch, hand and radius. There are no significant differences in the crutch and hand plots, but some differences are visible in the radius. Since there is no relative motion between the hand and the crutch in the fixed approach, in reality, these two segments act as a unique body of the biomechanical model. In this situation, the crutch can be considered an extension of the hand. In the spherical case, three rotational degrees-of-freedom exist between the hand and the crutch and, thus, relative movement between these bodies is allowed. The results for the left side are identical.

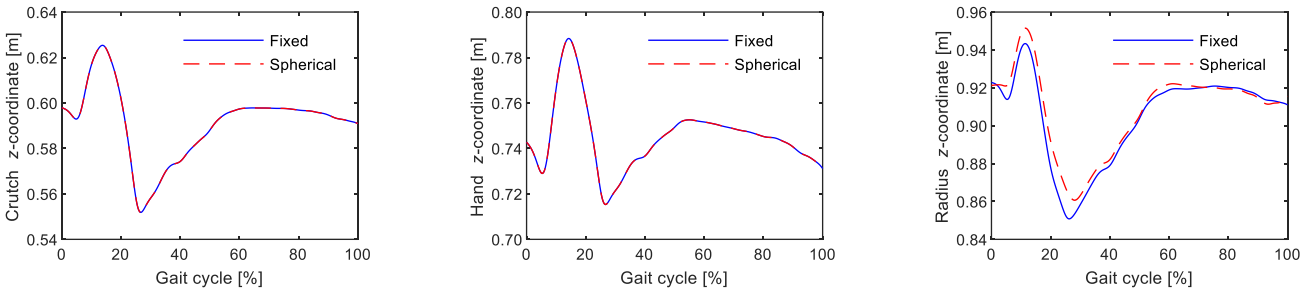

Figure 2: Evolution of the *z*-coordinate of the right (a) crutch, (b) hand and (c) radius throughout the gait cycle.

Acknowledgments

This work has been supported by the Portuguese Foundation for Science and Technology, under the national support to R&D units grant, with the reference project UIDB/04436/2020 and UIDP/04436/2020, as well as through IDMEC, via the projects LAETA Base Funding (DOI: 10.54499/UIDB/50022/2020) and LAETA Programmatic Funding (DOI: 10.54499/UIDP/50022/2020). The first author expresses her gratitude to the Portuguese Foundation for Science and Technology through the PhD grant (DOI: 10.54499/2021.04840.BD).

References

[1] World Health Organization & United Nations Children's Fund - UNICEF, Geneva: Global Report on Assistive Technology. Geneva, 2022.
[2] World Health Organization., Prevalence of coverage of assistive technology in the European Region: a scoping review, World Health Organization. Regional Office for Europe, Copenhagen, 2021.
[3] J. Carver, A. Ganus, J.M. Ivey, T. Plummer, A. Eubank, The impact of mobility assistive technology devices on participation for individuals with disabilities, Disabil Rehabil Assist Technol 11 (2016) 468–477.
[4] C. Johansson, S.A. Chinworth, Mobility in Context: Principles of Patient Care Skills, Second Ed., Spiral Bound, 2018.
[5] M.R. Silva, F. Marques, M.T. Silva, P. Flores, A new skeletal model for the ankle joint complex, Multibody Syst Dyn 60 (2024) 27–63.

Performance comparisons of different numerical methods for obtaining out-of-plane deflections of a resonant AFM micro-cantilever under acoustic emissions

Cagri Yilmaz[1]

[1]Vocational School of Technical Sciences, Akdeniz University, Konyaaltı Kampüs, 07070 Antalya, Türkiye, {cagriyilmaz@akdeniz.edu.tr}

ABSTRACT

1 Introduction

Numerical and analytical methods are widely used to reflect the vibrational dynamics of the resonant micro-cantilevers under external forces for diverse Micro-Electro-Mechanical-System (MEMS) applications. Variations in free oscillation observables such as amplitude, phase shift, and frequency shift responses strongly depend on the patterns of external forces. The micro-cantilevers can be resonated periodically with the driving forces in the absence of other external forces, thereby oscillating with the free amplitudes. Tip-sample interaction force such as Casimir force [1] determines the oscillation characteristics of the Atomic Force Microscopy (AFM) micro-cantilevers in single- and multi-frequency excitations. Dynamic [2] and static acoustic forces [3] can act on the one-side surface of the periodically actuated micro-cantilever in various operating environments. The effects of acoustic forces on the responses of the micro- and nano-systems are to be considered for different technological applications in biophysics and microrheology fields [4]. Thus, sensitivity to target external forces can be explored by isolating the acoustic force effects on the behaviors of micro-structures. In the present work, three AFM micro-cantilevers are driven using single- and bimodal-frequency excitation schemes [5] to improve sensitivity to acoustic forces. The Laplace transformation approach is utilized to obtain analytical expressions of the out-of-plane deflections for the first flexural eigenmode. The fourth-order Runge-Kutta method, the modified Rosenbrock formula, Adams-Bashforth-Moulton formula, and the numerical differentiation formula are applied to the second-order linear differential equations to obtain periodic oscillations. Therefore, the performances of different numerical methods for calculating micro-cantilever deflections are demonstrated considering the analytical results in the current work.

2 Dynamic model

The dynamic model is constructed based on a point mass model, which is introduced as follows:

$$m_e\ddot{z}_i(t) + c_i\dot{z}_i(t) + k_i z_i(t) = \delta(t)\, F(t) \tag{1}$$

Where $\ddot{z}_i(t)$, $\dot{z}_i(t)$, and $z_i(t)$ represent the acceleration, the velocity, and the displacement of the micro-cantilever for the eigenmode i respectively. m_e, c_i, and k_i denote the effective mass, the damping factor, and the spring constant for the eigenmode i respectively. The external force F(t) is applied over a short period of time by using the unit impulse function $\delta(t)$. In single-frequency excitations, the micro-cantilever is actuated at a resonance frequency at the fundamental or higher flexural eigenmode. The micro-cantilever is resonated at multiple resonance frequencies simultaneously in multi-frequency operations [6]. Dynamic acoustic forces act on the one-side surface of the periodically resonated micro-cantilever. The out of plane displacements at the first eigenmode of the micro-cantilever under acoustic and excitation forces are obtained for single- and bimodal-frequency operations, as illustrated in Figure 1.

Analytical expressions of the out-of-plane displacements are determined using the Laplace transformation method. Open loop transfer functions are obtained for single- and bimodal-frequency excitations. The numerical methods which are the fourth-order Runge-Kutta method, the modified Rosenbrock formula, Adams-Bashforth-Moulton formula, and the numerical differentiation method are utilized to obtain the micro-cantilever deflections for different excitation schemes. Initial displacement and velocity are taken as zero and the time step is set to 10^{-6} s for the numerical methods. All the analytical and numerical computations are performed in MATLAB environment.

3 Results and discussions

The analytical and numerical results are compared and evaluated considering especially forced amplitudes of the out-of-plane deflections. The results suggest that the performances of numerical methods strongly depend on applied excitation schemes, acoustic force frequencies, and mechanical properties of the AFM micro-cantilevers. For instance, a higher closeness to analytical results is achieved using the numerical differentiation formula for the time domain of 19.14 – 19.18 ms (Figure 2). For this case, the Brucker: MPP - 3310 micro-cantilever [7] is exposed to the acoustic force at the frequency of 250 kHz in monomodal operations. Additionally, there does not exist any remarkable difference in the frequencies of the forced deflections among the numerical methods. Phase shifts are almost the same for the numerical methods when considering the forced deflections obtained

©2024 The author. All rights reserved. DOI: 10.17185/duepublico/82605

using the analytical expressions. On the other hand, the forced amplitudes significantly change for different numerical methods. Sensitivity to initial conditions, discretization, and rounding errors in numerical methods are the main factors leading to notable differences among the obtained results. As mentioned before, different numerical results are acquired for different AFM micro-cantilevers under diverse acoustic forces in single- and multi-frequency operations. Changes in oscillation observables for different time domains are also to be considered while evaluating the effectiveness of the numerical methods. Additionally, the time steps considerably affect the forced amplitudes at the first eigenmode. For instance, the amplitudes of the forced vibrations under acoustic emissions vary between 800 and 1200 pm as the time step changes in the range of 0.1-0.0001 ms, as introduced in [8]. It is also worth mentioning that the maximum amplitude sensitivity is observed when the acoustic force sensitivity becomes closer to the first eigenmode frequency. To illustrate, the maximum forced amplitude of around 2.8 nm is obtained in measurement of acoustic forces at the frequency of around 49.4 kHz [2].

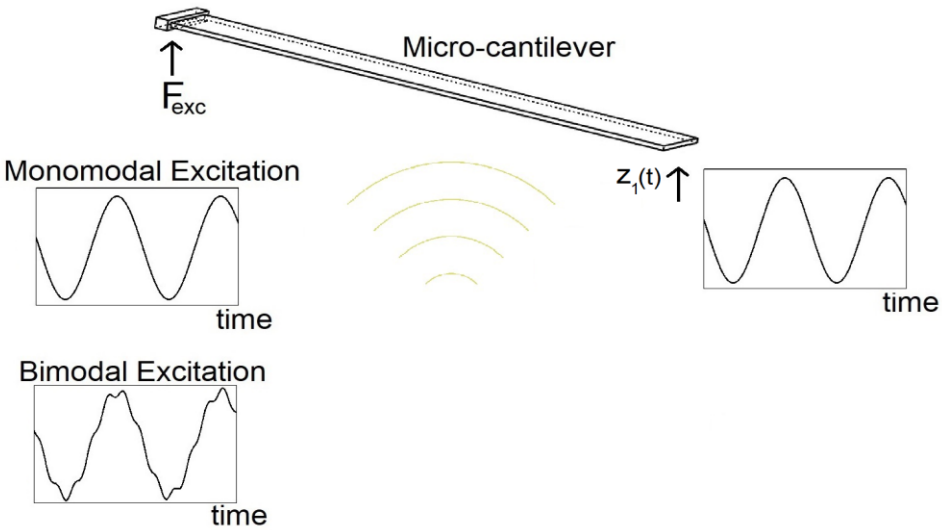

Figure 1: A schematic representation for dynamic interaction of an AFM micro-cantilever with acoustic emissions in single- and bimodal-frequency operations.

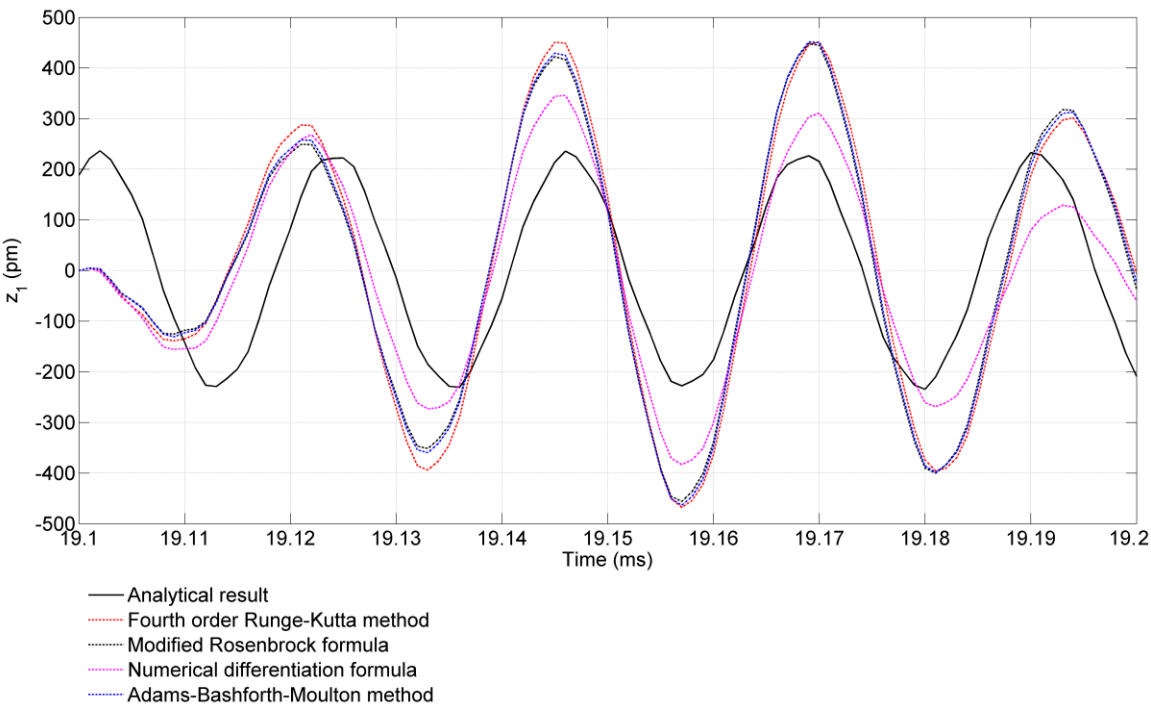

Figure 2: Analytical and numerical results of deflections of the resonantly driven micro-cantilever under acoustic force at the frequency of 250 kHz with the force strength of 1138.5 pN in single-frequency excitations.

4 Conclusions

The behaviors of AFM micro-cantilevers under external forces can be predicted using numerical methods. Analytical expressions describing forced oscillatory motions can be used to evaluate the performances of the numerical results. In the present work, the Laplace transformation method as a novel method is applied to obtain analytical expressions of the resonant micro-cantilever deflections under dynamic acoustic forces. It should be mentioned that various factors such as excitation schemes, mechanical properties of AFM micro-cantilevers, and characteristics of target external forces should be considered while exploring oscillation observable sensitivity. Moreover, the numerical results vary depending on the selected time domains. The variations in the forced amplitudes are to be analyzed with the consideration of the effects of numerical simulation parameters. Therefore, the dynamics of micro-cantilevers under driving and acoustic forces can be assessed using the analytical and numerical results for different MEMS applications.

References

[1] C. Yilmaz, "Utilizing a forced Van der Pol-Rayleigh-Helmholtz oscillator under heptamodal-frequency operations in Casimir force measurement", *Indian Journal of Physics*, vol. 2024, pp. 1-13, 2024.
[2] C. Yilmaz, R. Sahin, and E. S. Topal, "Theoretical study on the sensitivity of dynamic acoustic force measurement through monomodal and bimodal excitations of rectangular micro-cantilever", *Engineering Research Express*, vol. 3, 045035, 2021.
[3] C. Yilmaz, R. Sahin, and E. S. Topal, "Exploring the static acoustic force sensitivity using AFM micro-cantilever under single- and bimodal-frequency excitation", *Measurement Science and Technology*, vol. 32, 115001, 2021.
[4] C. Yilmaz, "Theoretical and experimental approaches for fluidic AFM operations and rheological measurements using micro-cantilevers", *Journal of the Brazilian Society of Mechanical Sciences and Engineering*, vol. 46, 398, 2024.
[5] S. Solares and G. Chawla, "Frequency response of higher cantilever eigenmodes in bimodal and trimodal tapping mode atomic force microscopy", *Measurement Science and Technology*, vol. 21, 125502, 2010.
[6] J. R. Lozano and R. Garcia, "Theory of multifrequency atomic force microscopy", *Physical Review Letters*, vol. 100, 076102, 2008.
[7] M. Ehsanipour, M. Damircheli and B. Eslami, "Effect of cantilevers' dimensions on phase contrast in multi-frequency atomic force microscopy", *Microscopy Research and Technique*, vol. 82, pp. 1438–1447, 2019.
[8] C. Yilmaz, "A Numerical Analysis of Single-Frequency Responses of the Resonant Micro-Cantilever to Dynamic Acoustic Forces Based on the Forced Van der Pol-Rayleigh-Mathieu Oscillator", *Acoustical Engineering - The Intricate World of Sound Technology [Working Title]*. IntechOpen, Jul. 19, 2024.

Mobile Robotic Platform Architecture Adaptable to Several Agricultural Applications

Pau Català[1], David Caballero[2], Carles Domenech-Mestres[2], Alba Perez Gracia[3]

[1]IDepartment of Mechanical Engineering, Universitat Politècnica de Catalunya (UPC), EPSEM, Av. de les Bases de Manresa 61-73,08242 Manresa, Spain, {pau.catala@upc.edu}
[2]Centre de Disseny d'Equips Industrials (CDEI), Universitat Politècnica de Catalunya (UPC), Llorenç Artigues 4, 08028, Barcelona, Spain, {david.caballero.flores@upc.edu, carles.domenech@upc.edu}
[3]Department of Mechanical Engineering, Universitat Politècnica de Catalunya (UPC), ETSEIB, Av. Diagonal 647,08028 Barcelona, Spain, {alba.perez.gracia@upc.edu}

ABSTRACT

This study presents the adaptability to several agricultural applications of an ongoing developed architecture of an autonomous mobile robotic platform, three-wheeled, with omnidirectional maneuverability.

1 Introduction

Humanity is facing a continuous rise in food demand in parallel with the negative consequences of the global warming. These two challenges are included within big initiatives such as the Sustainable Development Goals (SDG), more specifically SDG 2 (zero hunger), SDG 8 (decent work and economic growth) and SDG 12 (responsible consumption and production). Being aware that the major part of the global food production and agricultural industries are settled in the developed countries, the implementation of Key Enabling Technologies (KET) defined within the paradigm of Industry 4.0 in agricultural applications seem a good solution to achieve SDG. The agricultural industries from developed countries still have a long way to go in implementing these KETs and reach what is so-called Agriculture 4.0 paradigm. One of these KET is autonomous mobile robotics, also referred as Unmanned Ground Vehicles (UGV).

Rondelli et al. [1] have presented an overview of available UGV developed by universities and research groups specifically designed for agricultural tasks; cost reduction is identified as one of the most critical aspects for farmers. Yépez-Ponce et al. [2] have reviewed the recent state of mobile robotics implemented in agricultural applications and have concluded that it is necessary to provide solutions with lower cost and more scalable capability. Oliveira et al. [3], in their review in agriculture robotics, have identified the locomotion systems as one of the four major areas that need future research work.

The main locomotion systems for UGV are: wheels, tracks, or legs. Most of the UGV are prototypes and use as a locomotion system a four-wheels architecture (4W), despite knowing that 4W robots are strongly affected by soil characteristics. Legged robots are an interesting alternative to deal better with unstructured environments, but then cost and complexity increase. An interesting alternative between legged robots and 4W robots, is the three-wheels architecture (3W), which are little reported [3], and offers a trade-off between cost and performance in unstructured agricultural environments. One of the scarce 3W architecture of UGV for agriculture is Fendt Xaver provided by AGCO/Fendt, which is a ready-to-market solution. A different 3W architecture for agricultural applications, is the one presented in this study, named AGROMOBY.

2 Methodology and results

AGROMOBY is based in a patented solution developed by one of the authors [4], which is an already commercial solution deployed for industrial logistic applications. Figure 1 shows the CAD and the schematization for AGROMOBY. Table 1 summarized its main characteristics.

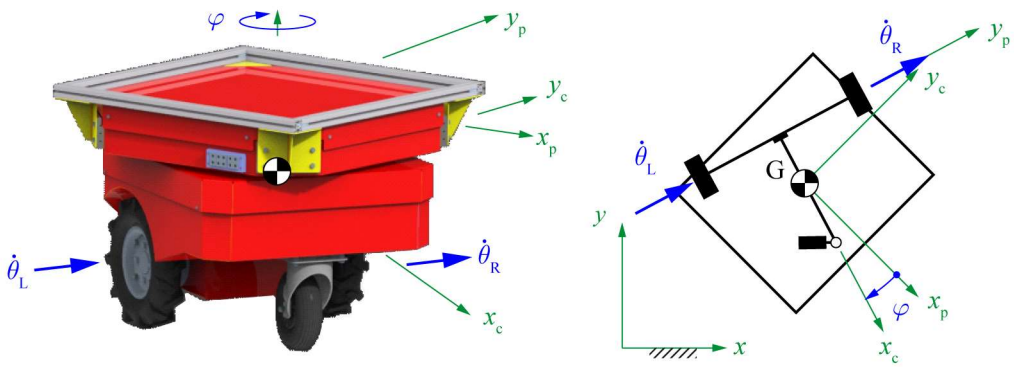

Figure 1: AGROMOBY CAD and schematization

©2024 The authors. This work may be used under a Creative Commons Attribution - NonCommercial - NoDerivatives 4.0 License (CC BY-NC-ND 4.0)

DOI: 10.17185/duepublico/82604

Table 1: AGROMOBY main characteristics

Dimensions	925x960x672 mm	*Caster wheel radius*	130 mm
Approximate weight	300 kg	*Navigation*	Autonomous-GPS, Lidar, RGB-D, IMU
Maximum load	400 kg	*Communication*	Ethernet, Wifi, 4G
Maximum speed	10 km/h	*Battery*	48 V, 50 A
Drive wheels radius	210 mm	*Autonomy*	8 h

AGROMOBY is divided mainly in two main systems, the mobile base or chassis and the rotating platform, which together provide the omnidirectional maneuverability. The mobile base with two degree-of-freedom (2 DOF) is governed with two brushless DC servomotors actuating in two offset differential drive standard wheels (θ_R, θ_L); a passive caster wheel is added for stability reasons. The rotating platform with a 1 DOF (φ), also governed with a DC servomotor, can rotate relative the platform from the mobile base or chassis. The behavior is explained further in [5].

Figure 2a shows the design as a harvester helper (carry the load on the field and deliver it to a storage place). Figure 2b and Figure 2c show two customizations of the rotating platform for carrying different sensors, such as a ground penetrating radar (GRP) for subsoil water detection, and sensors for monitoring crops and PhotoVoltaic (PV) panels from below in an Agri-PV environment.

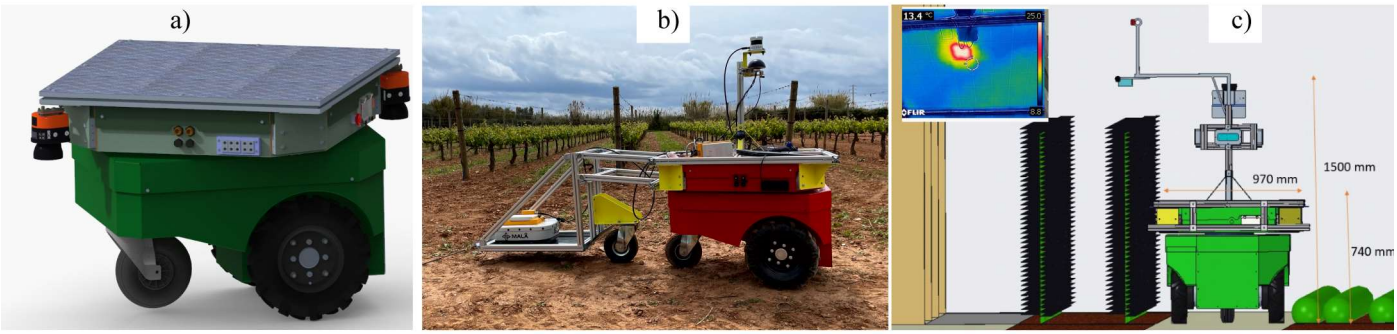

Figure 2: Several AGROMOBY customizations for agricultural applications

3 Conclusions

AGROMOBY is being developed to showcase the benefits of implementing robotics (UGV) in agricultural applications with a clear will to be cost-affordable and with a high grade of customization and flexibility of use.

Acknowledgments

This work was partially sponsored by the following projects: GROPERBOT and AGROMOBY (operation 01.02.01 of the Rural Development Program of Catalonia 2014-2022, Grant 5630141 2021); AI4WATER (Grant TED2021-131877B-I00); SYMBIOSYST (European Union's Horizon Europe Research and Innovation Programme, Grant Agreement N° 101096352).

References

[1] V. Rondelli, B. Franceschetti and D. Mengoli, "A Review of Current and Historical Research Contributions to the Development of Ground Autonomous Vehicles for Agriculture," *Sustain.*, vol. 14, no. 15, 2022, https://doi.org/10.3390/su14159221.

[2] D. F. Yépez-Ponce, J. V. Salcedo, P. D. Rosero-Montalvo and J. Sanchis, "Mobile robotics in smart farming: current trends and applications," *Front. Artif. Intell.*, vol. 6, no. 2018, 2023, https://doi.org/10.3389/frai.2023.1213330.

[3] L. F. P. Oliveira, A. P. Moreira and M. F. Silva, "Advances in agriculture robotics: A state-of-the-art review and challenges ahead," *Robotics*, vol. 10, no. 2, pp. 1–31, 2021, https://doi.org/10.3390/robotics10020052.

[4] J. J. Canuto and C. Domènech-Mestres, "Omnidirectional Platform and Omnidirectional Conveyor," WO2019020861A2, 2019.

[5] J. Badia, A. Perez and C. Domènech-Mestres, "Driving Strategies for Omnidirectional Mobile Robots with Offset Differential Wheels," *Robotics*, vol. 13, no. 1, p. 19, 2024, https://doi.org/10.3390/robotics13010019.

Optimizing Energy Consumption of a Parallel Robot with Elastic Elements via Equilibrium Position Adjustment

Juan Pablo Mora[1,2], Carlos F. Rodríguez[1], Burkhard Corves[2]

[1]Department of Mechanical Engineering, Universidad de los Andes, Cra. 1 Este Nº 19A - 40, 111711 Bogotá, Colombia, {jp.mora807@uniandes.edu.co, crodrigu@uniandes.edu.co}
[2]Institute of Mechanism Theory, Machine Dynamics and Robotics, RWTH Aachen University, Eilfschornsteinstraße 18, 52062 Aachen, Germany, {mora-garota@igmr.rwth-aachen.de, corves@igmr.rwth-aachen.de}

ABSTRACT

1 Introduction

Industrial robots are essential for modern industries due to their efficiency in performing repetitive and dangerous tasks better than humans. Studying their energy consumption has become crucial for increasing profits and reducing carbon footprints. Natural motion exploitation appears as a strategy that combines hardware and software enhancements to reduce the energy consumption of mechatronic systems during cyclic tasks [1]. Natural motion is defined as the system's response due to the conversion of potential energy into kinetic energy, and several works implementing this strategy are reviewed and classified in [2]. The objective is to add springs to the system so that their design parameters and the trajectory of the actuators align with the task.

The springs' parameters are calculated along with a trajectory increasing the energy efficiency of a Delta robot in [3]. As the method is applied to scenarios where the pick-and-place positions are previously fixed, a major deviation from these positions could cause a rise in energy consumption because the springs' design is linked with the task specification. This is addressed in [4] by simultaneously updating the springs' equilibrium position and the manipulator's trajectory. However, the designed trajectories do not fully meet smoothness requirements for dwell times because the zero jerk condition is not specified at the pick-and-place positions. Moreover, updating the parameters of the multi-point trajectory and the equilibrium position of the springs requires an optimization problem with several decision variables. This contribution brings together the mentioned publications and deals with two principal challenges. First, a set of necessary border conditions to incorporate dwell times in the task, namely zero velocity, acceleration, and jerk in the stop positions, is implemented in the trajectory planning. Second, point-to-point trajectories are implemented in motion planning along with adjusting the equilibrium positions of the elastic elements to reduce energy consumption while maintaining a simple optimization problem with fewer decision variables.

2 Method, Results, and Discussion

The parallel robot studied is a planar five-bar linkage actuated by two rotational servomotors at the frame joints. Natural motion is exploited by incorporating two torsional springs parallel assembled in these joints. Additionally, the trajectories are defined in joint space as point-to-point polynomial trajectories (P2P), meaning they do not include intermediate control positions, or multi-point piecewise polynomial trajectories that consist of time-equidistant intermediate control positions. The trajectory definition makes the system kinematically determined by providing a driving function for each degree of freedom. This allows the equations of motion to be solved numerically to obtain the actuation torques. The energy consumption can be estimated following [4].

A typical packing industrial scenario is studied, where the pick position is fixed, and a place square grid is considered as shown in Fig. 1a). The spring parameters are calculated based on a nominal task, defined by the mentioned fixed pick position and the centroid of the squared grid as the placement position. Additionally, a nominal P2P trajectory can be defined between those positions as shown in Fig. 1a). The point-to-point trajectories are calculated with seventh-order polynomials considering the required zero velocity, acceleration, and jerk border conditions at the pick-and-place positions. The minimum energy multi-point trajectories (ME) are also calculated using seventh-order polynomials that include the mentioned required border conditions and five control positions as shown in Fig. 1a). Moreover, P2P trajectories are implemented when adjusting the equilibrium positions of the springs. Both minimum energy trajectory and equilibrium position updates can be formulated as optimization problems. In this formulation, the cost function is the energy consumption while the decision variable χ corresponds to the control intermediate positions for calculating a minimum energy multi-point trajectory, and a 2-element vector for adjusting the equilibrium position of the springs.

Fig. 1 presents the results for the two types of trajectories implemented, namely P2P and ME. In the case of the P2P trajectories, the motion was simulated for the manipulator extended with springs (wS) and without them (woS). The trajectory named P2P wS θ_0 corresponds to an update of the equilibrium position of the springs. As shown in Fig. 1b), when there are no springs the energy consumptions of the P2P trajectories are always above the energy consumptions obtained using the ME trajectories. On the other hand, when the nominal springs are incorporated and P2P trajectories are implemented, energy consumption is reduced in certain regions. In other regions, the energy consumption increases above the ME trajectories without springs as presented in Fig. 1c). In

©2024 The authors. This work may be used under a Creative Commons Attribution - ShareAlike 4.0 License (CC BY-SA 4.0)
DOI: 10.17185/duepublico/82626

this case, it will be more beneficial to remove the springs; however, the presented method manages to further reduce energy consumption by updating the equilibrium position of the springs through the optimization problem solution. As shown in Fig. 1d), when a P2P trajectory is implemented with the adjusted equilibrium positions, the energy consumptions are always below the trajectories with the fixed nominal equilibrium positions. These observations are also obtained by analyzing Fig. 1e-f), which are sections of the surface for constant values of the y position $y = 0.4$ and $y = 0.5$, respectively. The importance of performing this adjustment becomes evident due to the varying order of the four energy curves.

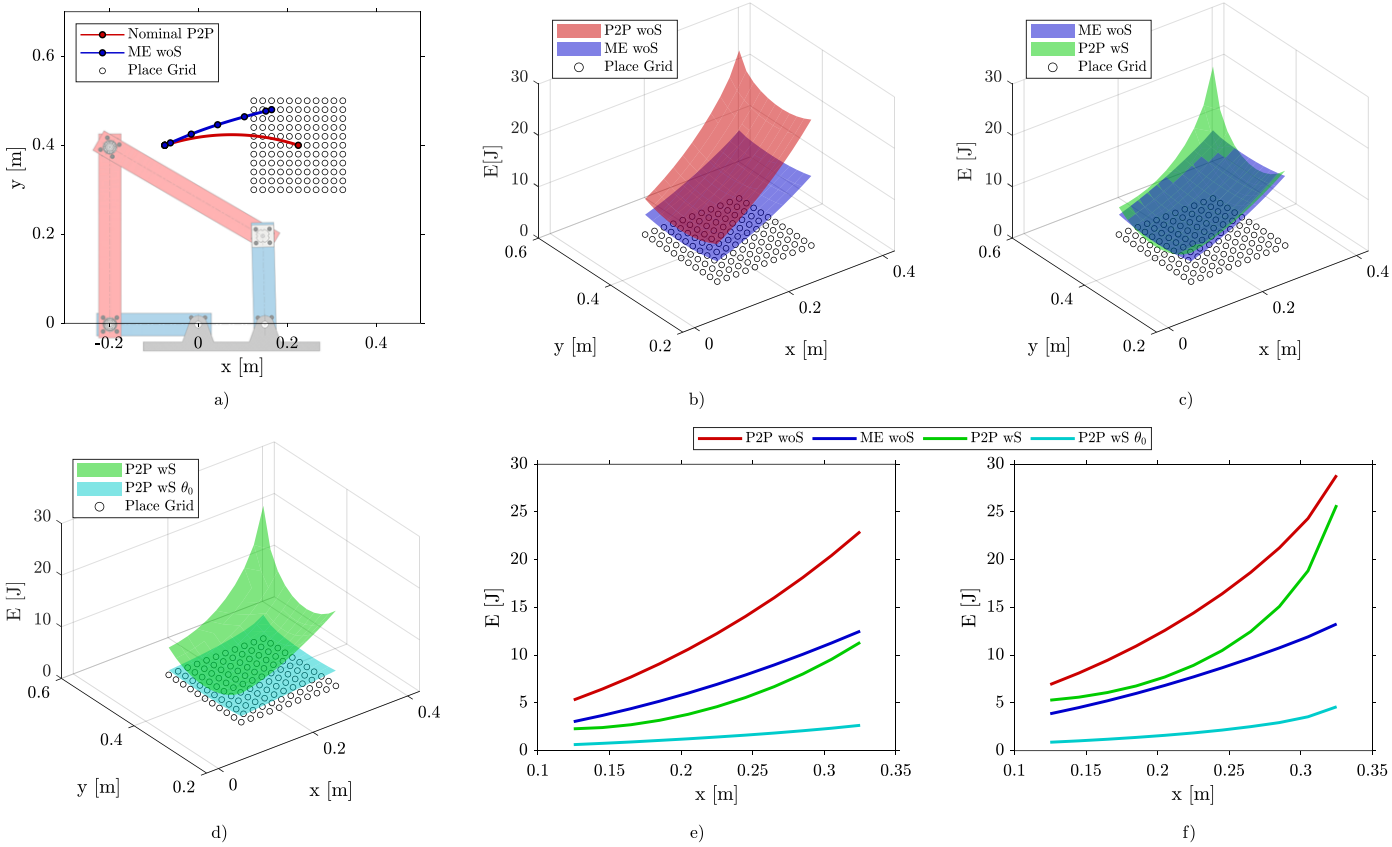

Figure 1: a) Task specification, b-d) Energy surfaces related to the place grid, e-f) Section analysis for a constant value of y.

3 Conclusion and Future Work

P2P and ME trajectories including necessary border conditions for dwell times are evaluated for a manipulator with and without springs, demonstrating that using springs and exploiting natural motion reduce energy consumption for pick-and-place tasks. The solution of a minimum-energy optimization problem allowed multi-point trajectories to outperform P2P trajectories if no springs were used. However, if nominal springs are assembled and used with P2P trajectories, energy consumption is reduced around the nominal task region compared to the ME trajectories without springs. Moreover, further energy reductions are achieved within a wider region by adjusting the equilibrium position while maintaining fewer decision variables than the ME optimization formulation. Although the method was implemented for a planar five-bar linkage it can be applied to other robots extended with elastic elements. Special attention will be paid to the selection of the nominal task and the cycle time in future work.

References

[1] G. Carabin, E. Wehrle, and R. Vidoni, “A Review on Energy-Saving Optimization Methods for Robotic and Automatic Systems,” Robotics, vol. 6, no. 4, 2017, doi: https://doi.org/10.3390/robotics6040039.

[2] L. Scalera, I. Palomba, E. Wehrle, A. Gasparetto, and R. Vidoni, “Natural Motion for Energy Saving in Robotic and Mechatronic Systems,” Applied Sciences, vol. 9, no. 17, 2019, doi: https://doi.org/10.3390/app9173516.

[3] J. P. Barreto and B. Corves, “Resonant Delta Robot for Pick-and-Place Operations,” in Advances in Mechanism and Machine Science, T. Uhl, Ed., Cham: Springer International Publishing, 2019, pp. 2309–2318. doi: https://doi.org/10.1007/978-3-030-20131-9_228.

[4] J. P. Mora, J. P. Barreto, and C. F. Rodriguez, “Energy Optimization of a Parallel Robot in Pick and Place Tasks,” in Multibody Mechatronic Systems, M. Pucheta, A. Cardona, S. Preidikman, and R. Hecker, Eds., Cham: Springer International Publishing, 2022, pp. 191–200. doi: https://doi.org/10.1007/978-3-030-88751-3_20.

Towards the development of a simulation framework to assess and enhance crutch-assisted gait

Benet Fité Abril [1], Carlos Pagès Sanchis[1], Míriam Febrer-Nafría[1]

[1]Biomechanical Engineering Lab, Universitat Politècnica de Catalunya, Diagonal 647, 08028 Barcelona, Spain
{bfiteabr7@alumnes.ub.edu, carles.joan.pages@upc.edu, miriam.febrer@upc.edu}

ABSTRACT

1 Introduction

Crutches are widely used to assist gait in individuals with lower limb impairment. Walking with crutches alters both upper and lower body loading, potentially leading to discomfort and injury [1]. As such, it is important to study how crutch-walking affects upper and lower extremity movement patterns under different conditions, e.g., altered crutch lengths or gait pattern. Improper crutch length fitting may result in upper limb pain and injury. Computer modelling and simulation can help predict how varying parameters in a gait aid may affect patient outcomes, without the need to expose patients to tiring gait lab experiments.

We recently developed an optimal control prediction framework to predict crutch-assisted gait patterns with a three-dimensional ideal-torque driven model [2]. The framework successfully predicted different gait patterns (four-point, two-point and swing-through), and the effect of changing axillary crutch length on upper limb kinematics during swing through gait generally matched experimental observations [3]. Yet joint kinematics, especially at the ankle, were not well predicted, mainly because ideal torques were not able to represent physiological joint torques. In order to include muscle forces in the model, without adding excessive complexity, it has been proposed to use physiological muscle torque actuators (MTGs) to represent the resultant torques being generated by muscle forces [4].

The main goal of this study was to enhance our crutch-assisted walking prediction framework to improve the realism of the predicted gait patterns. Specifically, our aims were: (1) to predict three-point crutch walking, (2) to add physiological muscle torque generators to actuate the model, and (3) to evaluate if the model was capable of predicting realistic crutch walking patterns under different conditions (e.g., different speeds and stride lengths).

2 Methods

A musculoskeletal model comprising 21 degrees of freedom was employed for the simulations. The foot-ground contact model (CM) consisted of a viscoelastic contact model for the normal force and a simple continuous friction model addressing tangential forces. In contrast, the crutch-ground CM was simplified to a viscoelastic contact model along the crutch's axis. The hand-crutch contact was modelled as a welded joint, directly transferring forces from the crutch-ground CM. The gait of this model was predicted on GPOPS-II, using the direct collocation method in a single-phase optimal control problem and an implicit formulation of the musculoskeletal dynamics. The cost function consisted of a combination of mechanical power, residual forces and muscle activation and joint jerk (derivative of acceleration) minimization. Regarding the boundary conditions on the state variables, they were taken from experimental unassisted gait measurements of different subjects.

To implement the new gait pattern, the maximum force output of one foot was limited, and the crutches were virtually coupled with it, forcing the model to distribute the weight across all three contact points. Then, muscle torque generator functions, including angle-dependent, angular velocity dependent and passive torque production at each joint, were calibrated using experimental data from a young healthy male collected with a BIODEX dynamometer equipment [5]. Finally, to study the effects of spatiotemporal parameters on the crutch-assisted gait pattern, we performed several simulations, for a variety of mean walking speeds (between 0.6 and 1 m/s), and for a variety of stride lengths (between 0.8 and 1.2).

3 Results and discussion

The desired improvements were successfully implemented to the simulation framework, at a cost of nearly doubling the simulation time. When comparing the MTG and torque-driven approach, the ground reaction forces predicted by the model appeared physiological, with the model distributing the weight similarly between the two crutches and the injured feet. Regarding shoulder and lumbar joint torque prediction, the MTG-driven model performed similarly than the more ideal-torque-driven model (Fig. 1 left, top), with an average difference of 2.0 and 13.3 Nm and maximum difference of 19.3 and 32.6 Nm, respectively. Nevertheless, the MTG-driven model better predicted the initial shoulder torque, which is commonly hard to simulate, yielding a torque that was 22% smaller compared to the predicted by the ideal-torque-driven model. Regarding joint coordinates (Fig. 1 left, bottom), the model driven by MTGs was capable of predicting a more upright position, in general for all simulations. In summary, adding MTGs to the model resulted in a slightly improvement of the predicted gait pattern. More research is needed to compare more in depth both modelling approaches. In future work we will use MTGs to personalise muscle group weakness for specific subjects, which may not be possible using ideal torques.

©2024 The authors. This work may be used under a Creative Commons Attribution 4.0 License (CC BY 4.0)
DOI: 10.17185/duepublico/82613

The simulation outputs showed that the framework was also capable to predict gait under different conditions, to get detailed insights about the joint loading. For this proof of concept study, where we varied speed and stride length (Fig. 1, right), we could observe that higher speed usually lead to higher torques in the lumbar load, and that for a fixed speed, it peaked out at around 1 m/s. Regarding the shoulder load, it could be seen that at higher speeds, an increase in stride length yielded a reduction in joint loading, as a higher stride translated to a reduction in cadence.

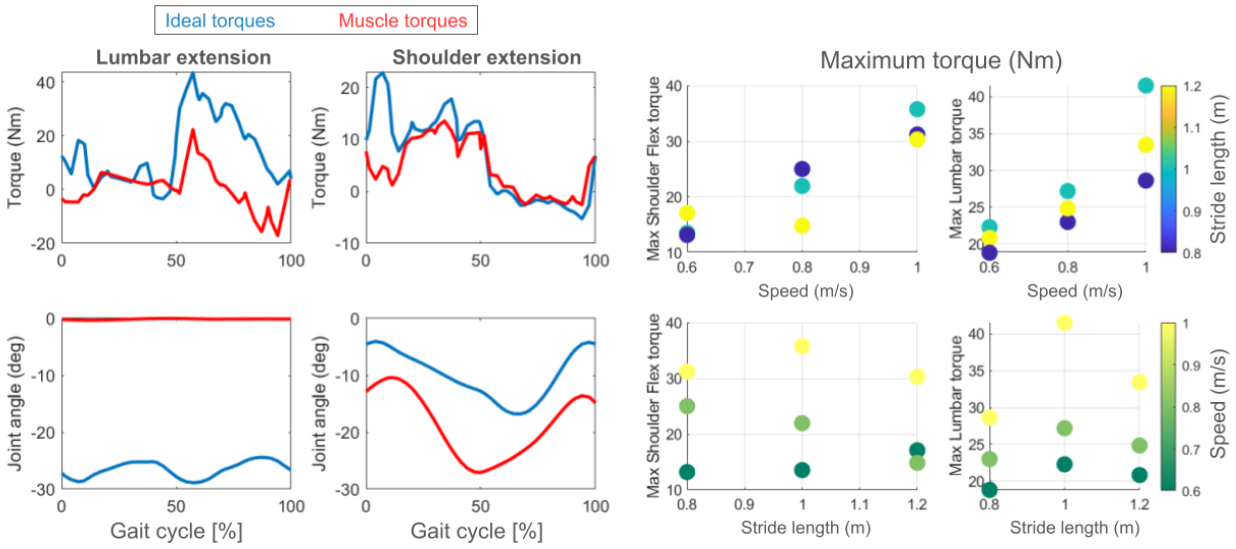

(a) (b)

Figure 1: (a) Comparison of shoulder and lumbar torque and angle between ideal-torque-driven (blue) and MTG-driven (red) simulation. (b) Shoulder and lumbar torques under different speed and stride length combinations.

4 Conclusion

This study shows how this simulation framework can successfully accept new gait patterns and more complex muscle actuators, while keeping a high degree of realism. Furthermore, with the shown predictions we can observe how interconnected parameters like speed and stride length are and how much they can impact joint loading. On the long term, the availability of an algorithm that allows the prediction of crutch walking patterns could be useful to study the impact of different conditions on crutch walking (such as type of crutch, walking pattern and different spatiotemporal parameters). This algorithm, together with neuromusculoskeletal models personalised to specific patients with mobility impairments (such as spinal cord injury subjects), could be used in the future to define rehabilitation treatments aimed at maximising recovery of walking function.

Acknowledgments

This research study has been supported by the project PID2021-123657OB-C33 funded by MCIN/AEI/10.13039 /501100011033 and by ERDF “A way of making Europe” (C.P.S.); and by the project Ajut ALECTORS-2023 (M.F.N.).

References

[1] Manocha RHK, MacGillivray MK, Eshraghi M, Sawatzky BJ. “Injuries associated with crutch use: a narrative review”. PM&R, 13(10), 1176-1192, 2021.

[2] Febrer-Nafría, M., Pallarès-López, R., Fregly, B.J. “Prediction of three-dimensional crutch walking patterns using a torque-driven model”. Multibody System Dynamics, 51(1), 1-19, 2021.

[3] Kuntze G, Russell M, Jivan S, Ronsky JL, Manocha RHK. “The effect of axillary crutch length on upper limb kinematics during swing-through gait”. PM&R, 2023.

[4] Inkol, K.A., Brown, C., McNally, W., Jansen, C., McPhee, J. “Muscle torque generators in multibody dynamic simulations of optimal sports performance”. Multibody Syst. Dyn. 50(4), 435–452, 2020.

[5] Pagès Sanchis, C. “ Development of personalized physiological torque-actuated musculoskeletal models to predict gait for clinical application”. Master thesis report, Universitat Politècnica de Catalunya, 2024.

Contact modeling between torus surfaces and plane using compliant force models

Filipe Marques[1,2], Mariana Rodrigues da Silva[1,2]

[1]CMEMS-UMinho, Departamento de Engenharia Mecânica, Universidade do Minho, Campus de Azurém, Guimarães 4804-533, Portugal, {fmarques@dem.uminho.pt, m.silva@dem.uminho.pt}
[2] LABBELS – Associate Laboratory, Braga/Guimarães, Portugal

ABSTRACT

1 Introduction

In mechanical systems involving complex geometries, accurately modeling the interaction between surfaces is a crucial aspect of predicting their dynamic behavior, especially in systems where contact phenomena play a role. One class of geometric surfaces that frequently arises in practical applications are toroidal surfaces, which can be used to represent elements such as tires, seals, and various types of rings. The torus, with its continuous circular symmetry, presents a unique challenge in contact mechanics due to its nontrivial geometry, which often results in complex contact interactions when dealing with planar surfaces or other curved bodies.

The use of compliant force models is a widely adopted approach to model contact forces with multibody dynamics framework [1]. These methods are preferred for their simplicity and efficiency in imposing contact constraints by penalizing interpenetration between bodies, thus generating contact forces proportional to the extent of the overlap. They have been extensively applied to various geometric forms, such as spheres, ellipsoids, and superellipsoids [2, 3], but its application to toroidal geometries has received relatively less attention. Both the contact detection and contact forces evaluation phases present significant challenges in terms of computational efficiency and accuracy due to this distinctive geometry. The accurate contact modeling is essential for predicting wear, friction, and overall system behavior.

This work explores the contact dynamics between a torus and a plane using a penalty method, focusing on the evaluation of normal and tangential forces. In contrast to simpler geometric shapes, the contact region in a torus-plane system can vary significantly depending on the orientation and deformation of the bodies, making the development of efficient numerical models critical.

2 Description of Toroidal Geometry

The torus is a surface of revolution generated by rotating a circle in three-dimensional space around an axis coplanar with the circle but not intersecting it. Mathematically, the torus is characterized by two radii: the major radius R, which represents the distance from the center of the circle to the axis of rotation, and the minor radius r, which corresponds to the radius of the rotating circle. The torus surface can be defined in two ways (i) using an implicit equation defined in a local reference system (ξ_T, η_T, ζ_T), represented in Figure 1, or (ii) considering a parametric surface, whose position and orientation can be defined in the three-dimensional space as a function of the location of the torus center point and the unit vector along the axis of revolution, $\mathbf{v}_i$.

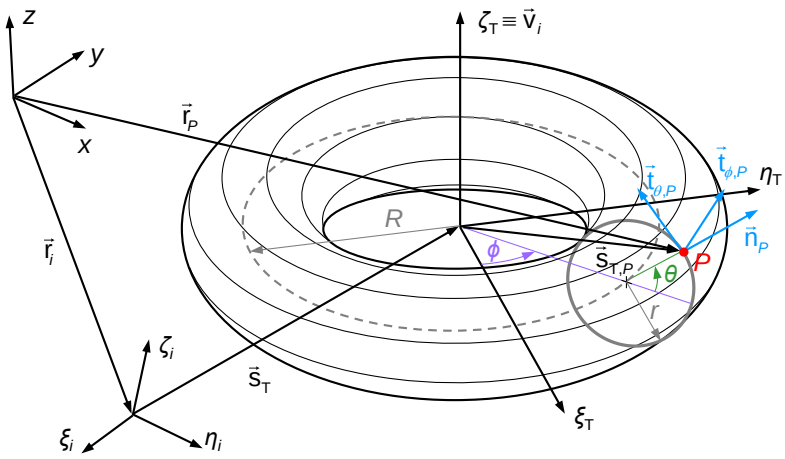

Figure 1: Schematic representation of torus surface parametrization

The use of the implicit form of torus equation is not convenient for the contact detection methodology adopted in this work. Thus, the torus surface can be treated as a parametrized surface, in which any point P located at that surface can be fully described by a set of two angular parameters, θ define the angle along the circular cross-section and ϕ denotes the rotation around the axis of the torus. Based on these parameters the location of the point P in torus local coordinate system can be defined as

©2024 The authors. This work may be used under a Creative Commons Attribution - NonCommercial - NoDerivatives 4.0 License (CC BY-NC-ND 4.0)
DOI: 10.17185/duepublico/82625

$$\mathbf{s}'_{\mathrm{T},P}\left(\phi_P,\theta_P\right)=\left\{\left(R+r\cos\theta_P\right)\cos\phi_P \quad \left(R+r\cos\theta_P\right)\sin\phi_P \quad r\sin\theta_P\right\}^{\mathrm{T}} \tag{1}$$

Having this in mind, and following the representation of figure 1, the location of point P on the torus surface that belong to body i, can be established in global coordinates as

$$\mathbf{r}_P=\mathbf{r}_i+\mathbf{s}_{\mathrm{T}}+\mathbf{s}_{\mathrm{T},P} \quad \text{in which} \quad \mathbf{s}_{\mathrm{T},P}=\mathbf{A}_i\mathbf{A}_{\mathrm{T}}\mathbf{s}'_{\mathrm{T},P} \tag{2}$$

in which $\mathbf{r}_i$ is location of the center of mass of body i in global coordinates, $\mathbf{s}_{\mathrm{T}}$ denotes the distance vector between the center of the torus and the center of mass, and $\mathbf{s}_{\mathrm{T},P}$ represents the location of point P with respect to the torus center in global coordinates and can be obtained through the rotation of the vector obtained in Eq.(1) with $\mathbf{A}_i$ being the body i transformation matrix and $\mathbf{A}_{\mathrm{T}}$ expressing the torus transformation matrix with respect to the body coordinate system, which can be defined as $\mathbf{A}_{\mathrm{T}} = [\mathbf{m}_i\ \mathbf{n}_i\ \mathbf{v}_i]$ where $\mathbf{m}_i$, $\mathbf{n}_i$ and $\mathbf{v}_i$ denote three unit vectors along the ξ_{T}, η_{T} and ζ_{T} axes in the body local coordinates.

3 Torus-Plane Interaction

To model the contact between the torus surface and a general plane, the torus is divided into N_s equal sized slices, and the contact is searched between each slice and the plane. It must be noted that the plane is generally described by a normal unit vector $\mathbf{n}_{\mathrm{P}}$ and any point Q belonging to its surface. The contact properties at a given slice j are obtained through the evaluation of the penetration of its middle section and the plane. If penetration exists, the contact points are identified in both surfaces, the contact stiffness is estimated based on the local material and geometrical properties and considering that the contact is close to cylindrical, and, finally, the contact forces are evaluated. The approximation of each slice to a cylinder can be done if the number of slices adopted is high enough. For the normal force, a Hunt and Crossley's based model [4] is considered, while, for the tangential forces, a regularized static friction model is applied [5].

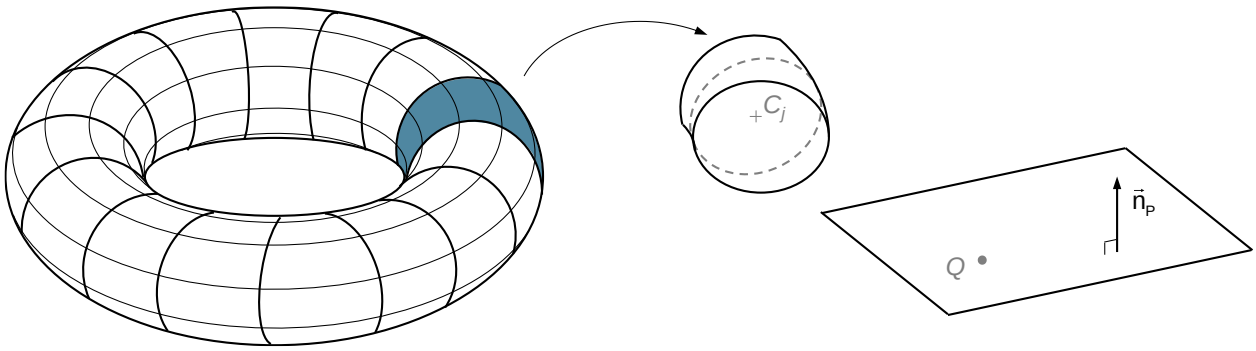

Figure 2: Representation of the division of torus geometry into slices to handle the contact with a plane surface.

This methodology is applied in several different dynamic cases in which a torus-shaped body contacts the ground, i.e., a fixed plane. The results demonstrate that the dynamic response of the system is highly sensitive to the contact properties (e.g., stiffness and damping), as well as to the number of slices adopted to discretize the torus. Although the proposed model to deal with the contact between a torus and a plane was successfully implemented, further validation is needed.

Acknowledgments

This work has been supported by the Portuguese Foundation for Science and Technology, under the national support to R&D units grant, with the reference project UIDB/04436/2020 and UIDP/04436/2020. The second author expresses her gratitude to the Portuguese Foundation for Science and Technology through the PhD grant (DOI: 10.54499/2021.04840.BD).

References

[1] P. Flores, “Contact mechanics for dynamical systems: a comprehensive review”, *Multibody System Dynamics*, vol. 54(2), pp. 127–177, 2022.

[2] J. Ambrósio, “A general formulation for the contact between superellipsoid surfaces and nodal points”, *Multibody System Dynamics*, vol. 50(4), pp. 415–434, 2020.

[3] E. Corral, R.G. Moreno, J. Meneses, M.J.G. García and C. Castejón, “Spatial algorithms for geometric contact detection in multibody system dynamics”, *Mathematics*, vol. 9(12), art. no. 1359, 2021.

[4] M. Rodrigues da Silva, F. Marques, M. Tavares da Silva and P. Flores, “A compendium of contact force models inspired by Hunt and Crossley's cornerstone work”, *Mechanism and Machine Theory*, vol. 167, art. no. 104501, 2022.

[5] F. Marques, P. Flores, J.C. Pimenta Claro and H.M. Lankarani, “A survey and comparison of several friction force models for dynamic analysis of multibody mechanical systems”, *Nonlinear Dynamics*, vol. 86(3), pp. 1407–1443, 2016.

Mobile robot for agriculture support in uneven terrain – design and simulation

Michal Olinski[1]

[1]Department of Fundamentals of Machine Design and Mechatronic Systems K61W10D07, Faculty of Mechanical Engineering, Wrocław University of Science and Technology (WUST), Łukasiewicza St. 7/9, 50-371 Wroclaw, Poland, {michal.olinski@pwr.edu.pl}

ABSTRACT

1 Introduction

Robotics and mobile platforms are becoming essential in agriculture automation [1, 2], as they support human labor in challenging tasks, with large equipment and potentially harmful substances, while also boosting productivity. In this work, the goal is to develop a robot that can assist with agricultural tasks such as harvesting premium tomatoes. The intention is to design a mobile platform, with a mounted manipulator, that will have great mobility and adaptability in irregular ground conditions (off-road).

2 Materials and methods

The predicted operating circumstances (Fig. 1a), which were then utilized to determine the kinematics and dimensions of the robot, were acquired thanks to the literature review and anticipated work environment for tomato picking. Therefore, the selected manipulator has a spatial linear structure with mobility of 6 and solely rotational joints.

In addition, the robot must be able to maneuver in unstructured areas, such as off-road terrain. For this purpose, reliable stability and mobility may be achieved with wheels, when paired with suitable control systems and suspension. Particularly, in order to achieve a light and compact design, an independent double wishbone suspension system with mobility of two is used. This mechanism allows for both the vertical wheel movement and the realization of wheel track changes. All these aspects will improve the vehicle's balance and implementation flexibility, enabling it to overcome ordinary obstacles and to evade big/vast obstructions. Moreover, to reduce the possible excessive vertical motions and vibrations of the platform, a semi-active suspension [3], with magnetorheological (MR) dampers, which can in real time adjust the level of damping force, is considered.

The manipulator and platform's (Fig. 1b) 3D dynamic numerical models are constructed in Adams software based on the selected kinematics and dimensions, likewise on their planned characteristics, anticipated operating circumstances and intended usage. Under predetermined scenarios and planned experimental modes, a selection of couple simulations is carried out. Several trajectories and objectives are defined for the manipulator to demonstrate its capabilities, particularly in terms of workspace (max. vertical/horizontal reach of 1.1 m/1.25 m), pose adaptability, and potential to make up for base orientation/position inaccuracies. Two different barriers (step, sinusoidal) and scenarios with fixed or variable damping coefficients are taken into account for the platform's simulations.

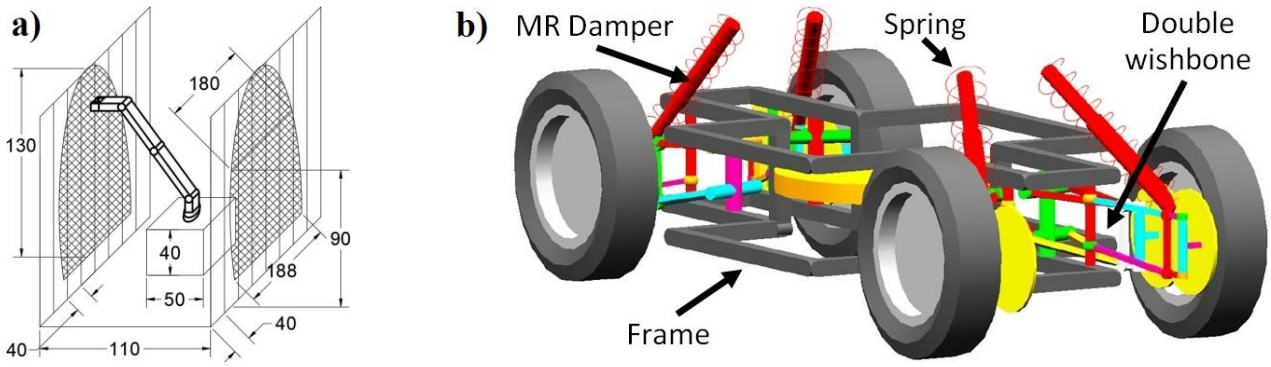

Figure 1: a) Expected operating environment for gathering tomatoes (values in cm) and crosshatched - "primary operating plane" of the manipulator [4], b) Platform's 3D numerical model constructed in Adams with key components designated by arrows [5]

3 Results

Some of the simulation findings are shown in the following figures. For instance, for the manipulator's maximum horizontal reach experiment, Fig. 2a shows that the motor at the bottom of the manipulator must deliver the maximum torque of 58.1 Nm in order to move almost the entire device. For the platform, generally, when the damping coefficient was adjusted, the degree of uncontrollably occurring vertical motions decreased. The maximum acceleration value decreased by 0.1 m/s^2 to 9.7 m/s^2 and its RMS value decreased by 0.04 m/s^2 to 1.77 m/s^2 for experiment with three step obstacles (height of 50 mm and length of 300 mm). Furthermore,

© 2024 The author. This work may be used under a Creative Commons Attribution - NonCommercial 4.0 License (CC BY-NC 4.0)

DOI: 10.17185/duepublico/82638

the average wheel torque was around 3.75 Nm and the vertical acceleration was less than 0.4 m/s^2 in terrain with sinusoidal barriers (Fig. 2b). Additionally, the vertical ground reaction forces and the amount of time that the wheels were off the ground were measured.

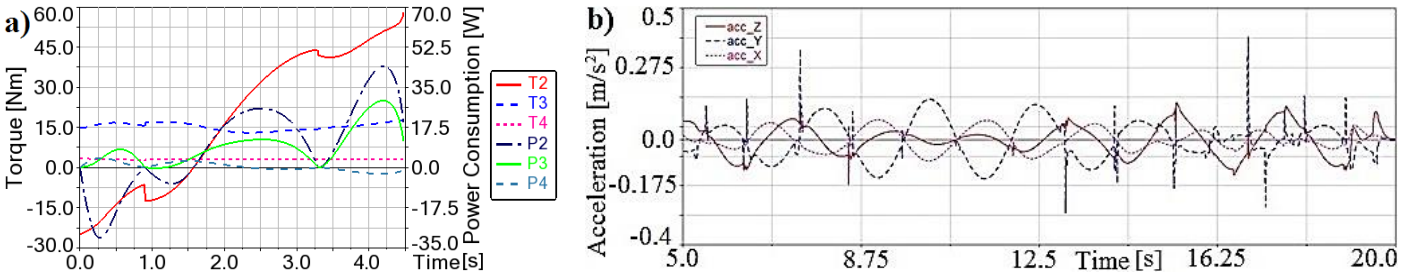

Figure 2: a) Torques and power consumption of manipulator's motors in simulation of max. horizontal reach [4], b) Accelerations of vehicle's chassis centre of mass, while riding on a road with sinusoidal obstacles, with variable damping coefficient [6]

Finally, using standardized parts and chosen motors, conceptual 3D CAD models are created in Inventor – the manipulator with gripper (Fig. 3a) and the platform (Fig. 3b). These models serve as a solid foundation for future fabrication of a research prototype.

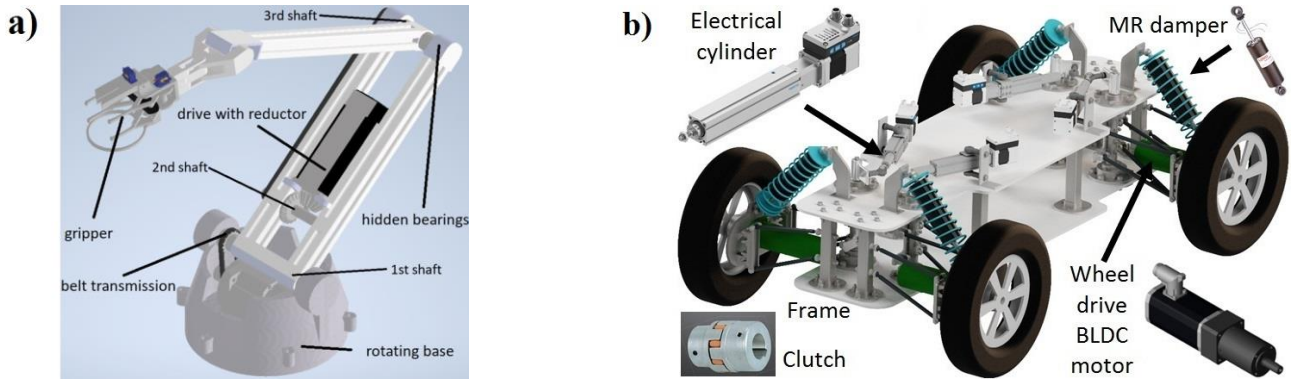

Figure 3: Designed 3D models created in Inventor (CAD software): a) manipulator with indicated main parts [4], b) mobile platform with suspension system and some of the selected items, motors, MR damper etc. [6]

4 Summary and conclusions

The goal of the project was to design a wheeled mobile robot that could negotiate rough terrain and assist with agricultural tasks, such as gathering tomatoes. The ultimate objective is to apply autonomous machinery to reach precise and smart farming.

In summary, the conducted simulation trials have validated the practical attributes of the manipulator's design, such as its broad applicability owing to its vast workspace and its exceptional flexibility (mobility of 6), which is significant in agriculture (convenient amid branches and creepers). Likewise, further findings demonstrated the viability of the platform and the ability of the semi-active suspension system, which included MR dampers, to reduce the unwanted vertical movement and acceleration of the vehicle's body. This, together with the possibility of changing the track of wheels, could potentially increase the vehicle's maneuverability and adaptability to different types of terrain, agricultural settings and specific situations in unstructured and uneven areas.

References

[1] Roldan et al., "Robots in agriculture: State of art and practical experiences", *Service Robots*, 2018. 10.5772/intechopen.69874

[2] Q. Feng, et al., "Design and test of robotic harvesting system for cherry tomato", *International Journal of Agricultural and Biological Engineering*, vol. 11, pp. 96-100, 2018.

[3] D. Fischer and R. Isermann, "Mechatronics semi-active and active vehicle suspensions", *Control Engineering Practice*, vol 12(11), pp. 1353-1367, 2004. https://doi.org/10.1016/j.conengprac.2003.08.003

[4] M. Olinski, et al., "Design of a Manipulator for Agriculture", in *Advances in Mechanism and Machine Science: proceedings of the 16th IFToMM World Congress on Mechanism and Machine Science*, Tokyo, 2023. doi: 10.1007/978-3-031-45770-8_65.

[5] M. Olinski and K. Cholewa, "Design and simulation of a mobile platform with a semi-active suspension for uneven terrain", *Journal of Theoretical and Applied Mechanics*, vol. 62(2), pp. 279-292, 2024. doi: 10.15632/jtam-pl/184231.

[6] K. Cholewa, "Design of a mobile platform for agricultural purposes" (in Polish), Master Thesis, Faculty of Mechanical Engineering, Wroclaw University of Science and Technology, Wroclaw, Poland, 07.2023.

Dynamics of Towing for Trailer Path Tracking

Ünal Dana[1,2], Levent Çetin[2]

[1]Graduate School of Natural and Applied Sciences, Department of Robotics Engineering, İzmir Kâtip Çelebi University, Çiğli, 35620, İzmir, Turkey, {unal.dana@ikcu.edu.tr}
[2]Department of Mechatronics Engineering, İzmir Kâtip Çelebi University, Çiğli, 35620, İzmir, Turkey, {levent.cetin@ikcu.edu.tr}

ABSTRACT

1 Introduction

The demand for production efficiency has contributed to the increase of automation within the industry. In the past decade, the human labor started to be inefficent , leading to the promotion of Industry 3.0, which encourages the implementation of robotic systems for automation. Advancements in technology related to indoor robotics, along with a growing confidence in automation, have facilitated the integration of mobile robots in industrial facilities. These robots are mostly utilized for transportation (logistics) and assembly tasks [1] [2] . Common method of transport is usualy placing cargo directly on the robot's surface [3]. While mobile robots aim to optimize energy consumption through efficient path generation and tracking, the existing transportation methods tend to be simple and inefficent [4] [5] [6]. This research proposes a method of transportation with existing trailers to be towed by mobile robots to address these transportation inefficiencies. This study focuses on analyzing, controlling, and testing the dynamics of the trailer under external towing forces.

2 Problem Describtion

The focus of study presented in this research is to control a trailer path by applying external forces therefore dynamic analysis, path generation and path tracking are carried out . The test environment and mechanical system for this problem has some constraints and assumptions those are; the trailer has 3 degrees of freedom,trailer wheels are non holonomic,there is no slip between wheel and the ground ,the center of mass is between middle of the 2 wheels of trailer shown on the figure 1 (b) .Figure 1 (a) presents an established trailer.

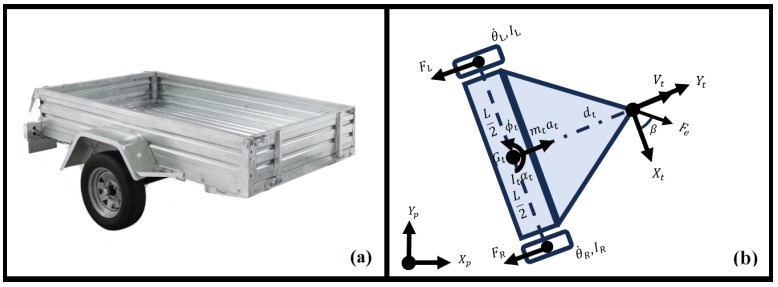

Figure 1: (a) Simple trailer , (b) forces acting on trailer

The relationship between external force and trailer velocities is analyzed in order to calculate corresponding external forces needed to control trailer velocities and path. The equation 1 is the inverse kinematic analysis and equation 2 is the dynamical analysis of towed trailer. This equations calculate output external forces acting on the connection joint of trailer to attain desired velocities.

$$\begin{bmatrix} \dot{\theta}_L \\ \dot{\theta}_R \end{bmatrix} = \frac{1}{2r_t} \begin{bmatrix} 2 & -L \\ 2 & L \end{bmatrix} \begin{bmatrix} V_t \\ \dot{\phi}_t \end{bmatrix} \tag{1}$$

$$\begin{bmatrix} F_{ex} \\ F_{ey} \end{bmatrix} = \begin{bmatrix} \frac{I_L L}{2d_t r_t} + \frac{I_t r_t}{d_t L} & \frac{I_R L}{2d_t r_t} + \frac{I_t r_t}{d_t L} \\ \frac{I_L}{r_t} + \frac{m_t r_t}{2} & \frac{I_R}{r_t} + \frac{m_t r_t}{2} \end{bmatrix} \begin{bmatrix} \ddot{\theta}_L \\ \ddot{\theta}_R \end{bmatrix} \tag{2}$$

3 Path Planning and Tracking

In an ideal environment with no obstacles the easiest method to achieve desired pose is to move in the shortest linear path but this linear path is not feasable and inefficent because it causes rotations around center of mass of trailer therefore a path generation with a cubic Bezier curve (n=3) function is used for path planning.Equation 3 and 4 [4] defines the Bezier curve for any number of control points (n).

$$f(t) = \sum_{i=0}^{n} b_i B_i^n(t), \quad 0 \le t \le 1 \tag{3}$$

©2024 The authors. This work may be used under a Creative Commons Attribution - NonCommercial - NoDerivatives 4.0 License (CC BY-NC-ND 4.0)
DOI: 10.17185/duepublico/82592

$$B_i(t) = \binom{n}{i} t^i (1-t)^{n-i}, \quad i = 0, \ldots, n \tag{4}$$

Path tracking is achieved by applying pure pursuit function [5] outputs as inputs to the dynamical equations (4).Pure pursuit function takes position errors to the next waypoint and outputs velocities.

4 Results and Discussion

Path generation with cubic Bezier curves and path tracking algorithm works as intended. The simulation results show .The final position is reached within the range of ± 0.01 m.The desired final angle is reached without rotations around center of mass. Simulation path is almost identical to the desired path with RMS error of 0.0297 m .The desired path is % 0.62 longer than the simulated path.The simulated linear velocity settles to desired simulation velocity in 12 seconds.Desired angular velocity changes rapidly therefore the simulated angular velocity doesn't have time to settle or make smooth transitions.

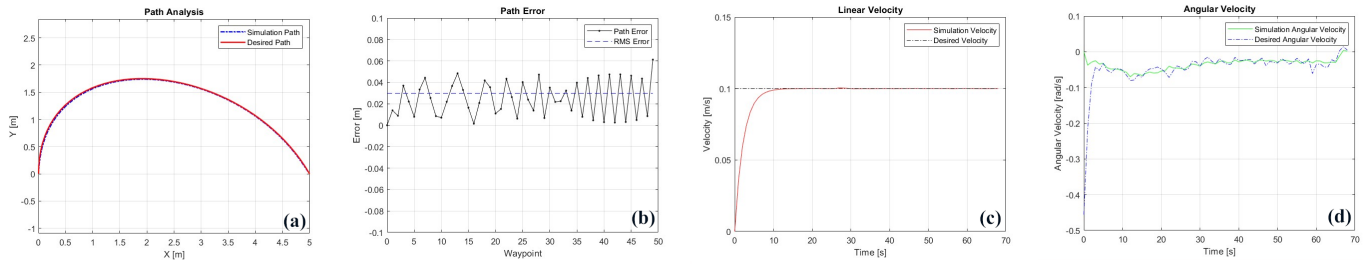

Figure 2: Simscape simulation results:(a) Path analysis, (b) path error, (c) linear velocity, (d) angular velocity.

The simulation result on figure 2 shows the trailer controlled by external forces on the joint tracking the generated path. Results in figure 2 (c) shows that the control of trailers linear velocity is successfull and can be achieved using mobile robot connected to the trailer. The angular velocity changes would be hard to achieve using mobile robot connected to the trailer, therefore a smoother curve in desired angular velocity in figure 2 (d) is essential. Overall system works however improvements on the settling time of linear velocity and smoother transitioning angular velocity should be done in the future.

Acknowledgments

This work has been financially supported by İzmir Kâtip Çelebi University (project no: 2024-TYL-FEBE-0008).

References

[1] R. Raj and A. Kos, "A Comprehensive Study of Mobile Robot: History, Developments, Applications, and Future Research Perspectives," Jul. 01, 2022, MDPI. doi: 10.3390/app12146951.

[2] J. Sinnemann, M. Boshoff, R. Dyrska, S. Leonow, M. Mönnigmann, and B. Kuhlenkötter, "Systematic literature review of applications and usage potentials for the combination of unmanned aerial vehicles and mobile robot manipulators in production systems," *Production Engineering*, vol. 16, no. 5, pp. 579–596, Oct. 2022, doi: 10.1007/s11740-022-01109-y.

[3] A. Yudiansyah, D. S. Ayu, and Y. Keke, "CAN THE MOBILE ROBOT BE A FUTURE ORDER-PICKING SOLUTION?: A CASE STUDY AT AMAZON FULFILLMENT CENTER."

[4] G. Tian, F. Zhou, and B. Song, "Bézier curve based smooth path planning for mobile robot," 2011. [Online]. Available: http://www.joics.com.

[5] C. Coulter, "Implementation of the Pure Pursuit Path Tracking Algorithm," 1992.

[6] M. Abdelwahab, V. Parque, A. M. R. Fath Elbab, A. A. Abouelsoud, and S. Sugano, "Trajectory tracking of wheeled mobile robots using Z-Number based fuzzy logic," *IEEE Access*, vol. 8, pp. 18426–18441, 2020, doi: 10.1109/ACCESS.2020.2968421.

Development of a Graphical User Interface for Personalized Transfemoral Prosthesis Design

Mertcan Koçak, Erkin Gezgin

Department of Mechatronics Engineering, İzmir Katip Çelebi University, Çiğli, 35620 İzmir, Turkey,
{mertcan.kocak@ikcu.edu.tr, erkin.gezgin@ikcu.edu.tr}

ABSTRACT

1 Introduction

Multiple factors can lead individuals to undergo surgical operations that result in amputation, defined as the removal of an extremity or part of it [1]. Given the personalized nature of surgeries involving extremities, along with variations in individuals' anatomical structures and desired post-surgical activity levels, customized prosthetic solutions are often required. Focusing specifically on transfemoral (above-knee) amputations, one of the most critical parameters to address is stability during the stance phase, which ensures user safety. Additionally, ease of flexion during the swing phase is vital for enhancing usability. Ongoing research and development in this field, along with efforts toward commercialization, are driven by the demand for high-quality, accessible and personalized prosthetic solutions that enable easy adaptation.

Stance phase of the gait cycle demands stability while the foot is on the ground, achieved in polycentric prosthetics through an increased instantaneous center of rotation (ICR) in the sagittal plane, providing a natural locking mechanism. Conversely, during the swing phase, ICR should align with the knee's natural center to ensure smooth flexion. Radcliffe's studies [2, 3] evaluated performance criteria for stance stability across various prosthetics, which have since been adopted in other works [4, 5] for assessing and comparing the stability of different kinematic designs.

Authors aim to contribute to the field by developing a novel transfemoral prosthesis using an analytical kinematic synthesis procedure for a single-degree-of-freedom polycentric mechanism, personalized to individual needs for both stance and swing phases [6]. Two modular designs are proposed for each phase, synthesized using kinematic principles with the objective of integrating them. Design method allows for various ICR trajectories through analytical approaches, but parameters like the polycentric mechanism's center and precision points on the ICR are challenging to define without appropriate tools or interfaces. Thus, this work advances by implementing a user-friendly graphical user interface (GUI) developed in MATLAB App Designer, designed to automate the process of optimizing parameters and defining individual ICR trajectories or precision points as specified by the user, due to the fact that it is thought the personalized solutions would be one of the future perspectives in such designs. Inclusion of stance stability models provides objective performance metrics for comparison. Additionally, the GUI's visualization capabilities enhance the personalization of prosthetic designs, enabling clearer insights into their customization and suitability for individual needs.

2 Development of graphical user interface

In previous work [6], kinematic synthesis methodology was implemented through MATLAB scripting, allowing manual input of precision points and optimization parameters. To maintain software consistency, a graphical user interface (GUI) is developed in MATLAB App Designer, enabling users to easily customize their ICR trajectories and precision points. It is important to note that multiple sets of precision points can yield different mechanisms, so GUI incorporates constraints and requirements to ensure that the generated designs adhere to predefined criteria. This ensures that users can explore various configurations and limitations while maintaining design accuracy.

To enable motion visualization in relation to human anatomy, it is necessary to integrate a visual model of the human body. Given the individual variability in anatomy, anthropometric data are generally used in the design process [7]. In developed GUI, visualization relies on such data, but users can customize specific parameters, including buttock depth and lateral femoral epicondyle height, allowing for a more personalized representation of the anatomical structure during prosthetic design.

Figure 1 illustrates GUI for visualizing the human lower extremity in the sagittal plane, featuring versatile user input options and the capability to upload pre-generated ICR trajectories with detailed data points and corresponding flexion angles. This interface enables users to view, add, delete and modify trajectory points as needed. By comparing figures 1a and 1b, users can also observe modifications to body dimensions, specifically adjustments to buttock depth values as an example. A slider and text input control are provided to adjust the flexion angle, offering real-time updates to the lower extremity movement visualization. Additionally, different stance trajectories, based on real prosthetic models, are available for visualization in the sagittal plane. Users can select each data point, along with associated flexion angle, for further modification or deletion. Figure 1c highlights the interface's capacity to customize trajectories by adding specified points, which appear both on the human visual and in the trajectory list. GUI allows users to save modified trajectories and precision points to a local ".mat" file and supports uploading and adjusting natural swing phase trajectories for the second part of the design.

©2024 The authors. This work may be used under a Creative Commons Attribution - NonCommercial - ShareAlike 4.0 License (CC BY-NC-SA 4.0)
DOI: 10.17185/duepublico/82619

3 Conclusion and future works

A graphical user interface has been developed using MATLAB App Designer to facilitate the input of specified ICR trajectory and optimization parameters, enabling kinematic synthesis procedures aimed at creating an innovative transfemoral prosthesis. This interface provides visualization that aids in kinematic simulations, allowing for comparisons of different mechanisms based on Radcliffe's performance criteria. Future developments will incorporate dynamic simulations to determine the required torques for these mechanisms. This approach presents a significant opportunity to automate the design process for personalized transfemoral prosthetics.

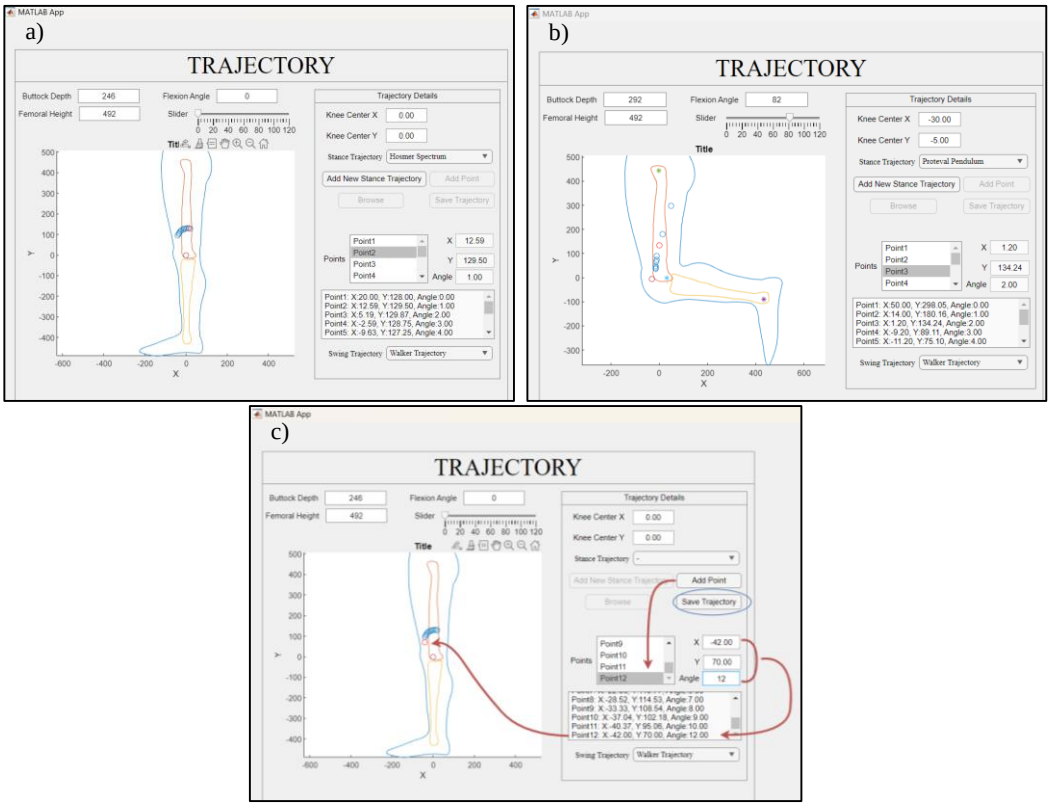

Figure 1: (a) ICR trajectory with zero flexion angle and default antropometric data. (b) ICR trajectory with non-zero flexion angle and increased buttock depth in visual. (c) Customized ICR trajectory with features.

Acknowledgments

This work has been financially supported by İzmir Kâtip Çelebi University (project no: 2023-TDR-MÜMF-0019).

References

[1] J. F. Soriano, J. E. Rodríguez and L. A. Valencia, "Performance comparison and design of an optimal polycentric knee mechanism", *Journal of the Brazilian Society of Mechanical Sciences and Engineering*, vol. 42, pp. 1–13, 2020.

[2] C. W. Radcliffe, "Four-bar linkage prosthetic knee mechanisms: kinematics, alignment and prescription criteria", *Prosthetics and Orthotics International,* vol. 18(3), pp. 159–173, 1994.

[3] C.W. Radcliffe, M. E. Deg, "Biomechanics of knee stability control with four-bar prosthetic knees", in *ISPO Australia Annual Meeting* (vol. 11, pp. 1-25) Melbourne, 2003.

[4] W. Liang, et al. "Mechanisms and component design of prosthetic knees: A review from a biomechanical function perspective" *Frontiers in Bioengineering and Biotechnology,* vol. 10, 950110, 2022.

[5] T. S. Anand, and S. Sujatha, "A method for performance comparison of polycentric knees and its application to the design of a knee for developing countries", *Prosthetics and Orthotics International,* vol. 41(4), pp. 402–411, 2017.

[6] M. Koçak, E. Gezgin, "Utilization of Kinematic Synthesis Methodology on a Novel Polycentric Mechanism for Transfemoral Knee Prosthesis", in Lovasz, EC., Ceccarelli, M., Ciupe, V. (eds) *Mechanism Design for Robotics. MEDER* 2024.

[7] C. C. Gordon, et al. "2012 anthropometric survey of us army personnel: Methods and summary statistics", *Army Natick Soldier Research Development and Engineering Center MA, Tech. Rep,* 2014.

Intent Detection Method and Assistive Device Development for Supporting Sit-to-Stand

Jian ZHENG [1], Qizhi MENG [2], Ming JIANG [3]

[1] Department of Mechanical Engineering, Institute of Science Tokyo, 1528550, Ookayama 2-12-1, Tokyo, Japan {zheng.j.ab@m.titech.ac.jp, qizhi.meng@foxmail.com, jiang.m.ad@m.titech.ac.jp }

ABSTRACT

1 Introduction

The study of assistance in sit-to-stand (STS) activity becomes increasingly important in the aging society. The lower extremity strength of the elderly is reported approximately half as strong as that of younger individuals [1]. This poses a significant challenge to the daily lives of the elderly. To address this, various assistive devices have been developed [2]. We proposed a novel method to detect STS intent using mechanical stimulus on the toes and monitoring reaction forces at the toes and heel. This method is implemented in a chair-type assistive device [3], which we have developed. This extended abstract provides a brief introduction to the STS assistance system.

2 Method

2.1 Detecting STS Intent

Figure 1 shows the experimental device for detecting the STS intent. A pedal-shaped device is located under the user's foot. The toe pedal, rotated by a motor, lifts the user's toes and provides the mechanical stimulus. The stimulus is provided when a potential STS intent from the user is detected. We hypothesize that after this stimulus, which tends to impede the STS motion, is applied, there will be a more obvious change in the reaction force at the foot. Two force sensors are placed at the toes and heel to measure the reaction forces during STS. In addition, a load cell is fixed to the seat to monitor the instant when the buttocks leave the seat. When the reaction force on the seat decreases to 0, it is considered that the user has left the seat.

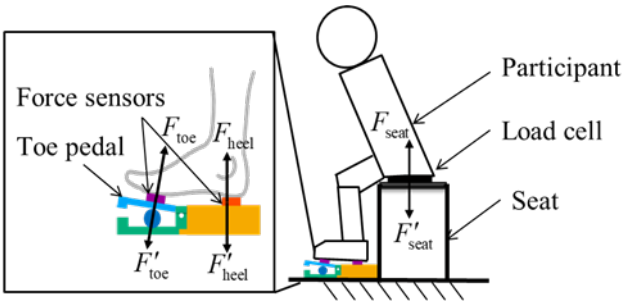

Figure 1: Intent detection system [3]

We conducted two types of experiments. Initially, we performed offline experiments to establish thresholds for STS intent, focusing on the heel and toe reaction forces and their rate of change. If all four values (F_{heel}, F_{toe}, and their change rates) simultaneously exceed the predetermined thresholds, we conclude that the user intends to stand up. Then, online experiments were executed to verify that the STS intent could be effectively detected with the decided thresholds. Our previous study has proven the concept to accurately detect STS intent and distinguish it from other interfering motions [4].

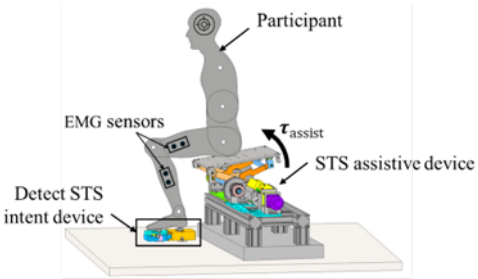

Figure 2: Integrated STS assistance system

©2024 The authors. This work may be used under a Creative Commons Attribution - NonCommercial - NoDerivatives 4.0 License (CC BY-NC-ND 4.0)

DOI: 10.17185/duepublico/82601

2.2 STS Assistive Device

To apply the proposed intent detection method in STS assistance and investigate the assistance effect at different assistance-provided timing, we developed a 1-DOF chair-type assistive device equipped with a Redundant Hybrid Actuator (RHA) [3], as shown in Figure 2. This device alleviates the burden of users on knee and hip joints during STS by lifting the seat. Additionally, the RHA can switch between small and large torque assistance modes automatically to adapt to the users' physical with a mechanical stopper and help users to complete the STS motion.

3 Evaluation

We integrated our STS detection method into the assistive device, as illustrated in Figure 2. The assistance effects of the chair-type device are compared under conditions with and without considering the user's STS intent. The assistance effect is evaluated using electromyography (EMG) sensors attached to the vastus lateralis, rectus femoris, tibialis anterior, and vastus medialis. These muscles are selected for measurement because they exhibit peak activity during the STS movement, playing a critical role in the mechanics of standing.

Acknowledgement

This paper has been partly presented in MISW (15th Multidisciplinary International Student Workshop 2024). This study is partly supported by Hirose Foundation, Mikiya Foundation and JSPS KAKENHI Grant Number JP 24K21156.

References

[1] Gross, M. M., Stevenson, P. J., Charette, S. L., Pyka, G., & Marcus, R. (1998). Effect of muscle strength and movement speed on the biomechanics of rising from a chair in healthy elderly and young women. Gait & posture, 8(3), 175-185.

[2] Tsukahara, A., Kawanishi, R., Hasegawa, Y., and Sankai, Y., `` Sit-to-stand and stand-to-sit transfer support for complete paraplegic patients with robot suit HAL.", Advanced robotics, Vol.24, No.11(2010), pp.1615-1638

[3] Kotaro Muramatsu, Jian Zheng, Takamaru Saito, Ming Jiang, Yusuke Sugahara, Jun Nango, Yukio Takeda. "Development of a Sit-to-Stand Assist Device Driven by Redundant Hybrid Actuator for Assist-As-Needed Control," presented at the JSME MDT2024, Japan, 2024.

[4] Ming Jiang, Jian Zheng, Qizhi Meng, Yusuke Sugahara, Yukio Takeda. Detecting the Intention of Sit-to-Stand by Analyzing Reaction Forces on the Foot with Pareto Optimum, Proceedings of 46th Annual International Conference of the IEEE Engineering in Medicine and Biology.(In press)

Nonlinear-Stiffness Mechanism Inspired in Nature for Wave Energy Conversion: A Quick Performance Evaluation of its Linear-Stiffness Zone

Claudio Villegas[1], Diego Carrasco[1], Fabián Pierart[1]

[1]Department of Mechanical Engineering, Universidad del Bio-Bio, Collao 1202, Concepcion, Chile, {cvillegas@ubiobio.cl}

ABSTRACT

1 Introduction

The world seeks now to consume fewer fossil fuels and more renewable energy. The most used types of renewable energy are nowadays solar and wind energy. They are plentiful on our planet, but they are also intermittent, as they depend on daylight and wind conditions, respectively. A more stable energy source can be harvested from sea waves [1]. It has great brute power, estimated to be about 2 TW [2], and most of it is located on the southern and northern coasts of the world [3]. To harvest wave energy, wave energy converters (WECs) are required. WECs have not yet reached a standardized form [4], and its power is highly dependent on the location they are installed at [5]. Particularly, a WEC located in Chile would have to deal with waves with long periods, about 10 s to 12 s [6]. On the other hand, the best configuration of a WEC for optimal Power Take-Off (PTO) control is when the system is in a resonant state. Hence, the WEC would have to match very low frequencies. This is a problem for the typical point absorber WECs because their shape gives them eigenfrequencies above the wave frequency, making it difficult for them to reach a resonant state. Some research has been carried out to tackle this problem using Negative Spring Mechanisms (NSMs). For example, in [7], a compressed spring is used in an arm-type WEC to create a nonlinearity in the stiffness and generate a negative-stiffness zone, which produced a resonant state in the system, increasing the converted power. This model was tested both analytically and experimentally in regular and irregular waves. Furthermore, a point absorber WEC was modified to include a snap-through configuration of springs and was studied numerically [8]. This point absorber increased its average converted power for regular waves. In this direction, we have found an interesting bio-inspired NSM that can produce fairly constant negative stiffness and have not been tested for wave energy conversion [9]. Therefore, the aim of this contribution is to find dimensions for the NSM that gives a sought negative stiffness and model a laboratory point absorber as a 1-DoF WEC with this negative spring attached to the system in parallel. Then, its converted power is calculated and compared to that of the WEC without NSM.

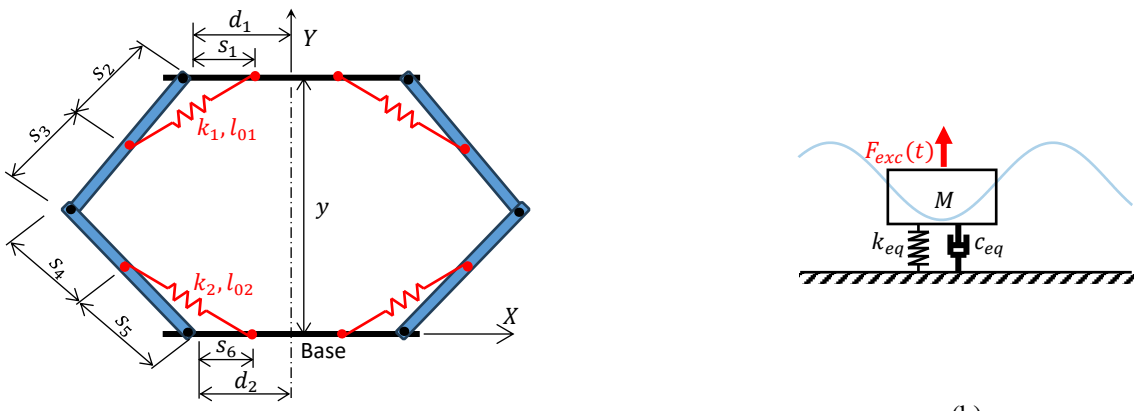

(a) (b)

Figure 1: (a) Diagram of the negative-stiffness device [9]; (b) Simplified mass-spring-damper system of the WEC

2 Methodology

The NSM presented in [9], which moves vertically varying its distance from the base y, can be seen in Figure 1(a). This device shows a quasilinear negative-stiffness zone, depending on its constructive parameters. Thus, the dimensional parameters s_i, d_j and l_{0j}, as well as the stiffness k_j ($i = 1$ to $6, j = 1,2$), are adjusted in this work to produce a negative stiffness zone that drives the WEC of our laboratory into resonance when attached to it. This analysis was done analytically, under the assumption of linear behavior, solving the 1-DoF equation of motion set with NEWTON's method (eq. 1) and neglecting the mass of the NSM. See Figure 1(b). Wave parameters as added mass μ_{add}, radiation damping coefficient c_{eq} and Froude-Krylov excitation force F_{exc} are obtained with ANSYS AQWA™ using Boundary Elements Methods. The excitation force is considered harmonic as a regular wave. The WEC dimensions and mass M are measured on site. The resulting converted power is compared with that of the WEC of our laboratory without using NSM, which is calculated analytically and validated experimentally.

$$(M + \mu_{add})\ddot{y} + c_{eq}\dot{y} + k_{eq}y = F_{exc}(t). \quad (1)$$

©2024 The authors. This work may be used under a Creative Commons Attribution 4.0 License (CC BY 4.0)

DOI: 10.17185/duepublico/82701

3 Results and discussion

The analysis of the WEC conditions gave a required stiffness of -130 N/m to reach resonance. Adjusting the NSM parameters s_i, d_j, l_{0j} and k_j, a stiffness of -125 N/m was reached for a mechanism that is completely symmetrical with each $s_i = 40$ mm, $d_j = 60$ mm, $l_{0j} = 64$ mm and $k_j = 2500$ N/m (set 2). See its stiffness function in Figure 2 and other sets used as example results. The RMS (Root Mean Square) power of the WEC without springs reached 449.7 mW, and the RMS power of the WEC with NSM set 2 was 2564 mW. This shows an increase of 4.7 times in the power generated.

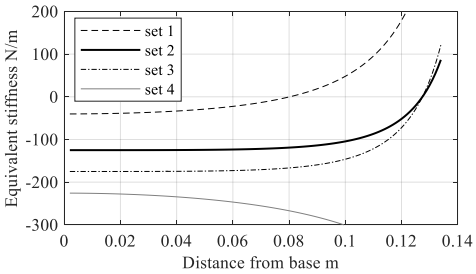

Parameter	Set 1	Set 2	Set 3	Set 4	Unit
s_1 and s_6	40	40	40	40	mm
s_2 and s_5	30	40	40	50	mm
s_3 and s_4	50	40	40	30	mm
l_{0j}	64	64	64	64	mm
k_j	2500	2500	3500	2500	N/m

Figure 2: Resulting stiffness of the negative-stiffness device vs the distance of the superior plate from the base y and example sets shown at the right-hand side of the figure

4 Conclusions

This work gives a quick evaluation of the potential that a bio-inspired mechanism for negative stiffness can have for wave energy conversion. Theoretically, the converted power was augmented almost 5 times. This result must be taken cautiously. There are still things to be tuned. A list of future work to be done are setting a correct precharge for the system so it can maintain its position; an experimental validation in laboratory; measuring the real power generated with NSM; create a correct design that fits a determined WEC shape and correction of potential energy loses in the functioning of the NSM.

Acknowledgments

Funded by project IN2360424 of Universidad del Bio-Bio

References

[1] H. Hu, W. Xue, P. Jiang, and Y. Li, “Bibliometric analysis for ocean renewable energy: An comprehensive review for hotspots, frontiers, and emerging trends,” Renewable and Sustainable Energy Reviews, vol. 167, p. 112739, Oct. 2022, doi: 10.1016/j.rser.2022.112739.

[2] K. Gunn and C. Stock-Williams, “Quantifying the global wave power resource,” Renew Energy, vol. 44, pp. 296–304, Aug. 2012, doi: 10.1016/J.RENENE.2012.01.101.

[3] M. Shadman et al., “A Review of Offshore Renewable Energy in South America: Current Status and Future Perspectives,” Sustainability, vol. 15, no. 2, p. 1740, Jan. 2023, doi: 10.3390/su15021740.

[4] H. Hu, W. Xue, P. Jiang, and Y. Li, “Bibliometric analysis for ocean renewable energy: An comprehensive review for hotspots, frontiers, and emerging trends,” Renewable and Sustainable Energy Reviews, vol. 167, p. 112739, Oct. 2022, doi: 10.1016/j.rser.2022.112739.

[5] R. Ahamed, K. McKee, and I. Howard, “Advancements of wave energy converters based on power take off (PTO) systems: A review,” Ocean Engineering, vol. 204, p. 107248, May 2020, doi: 10.1016/J.OCEANENG.2020.107248.

[6] F. G. Pierart, C. Villegas, C. Basoalto, M. Hüsing, and B. Corves, “Model and Control Analysis for a Point Absorber Wave Energy Converter in Lebu, Chile,” 2023, pp. 19–26. doi: 10.1007/978-3-031-32439-0_3.

[7] A. Têtu, F. Ferri, M. B. Kramer, and J. H. Todalshaug, “Physical and Mathematical Modeling of a Wave Energy Converter Equipped with a Negative Spring Mechanism for Phase Control,” Energies (Basel), vol. 11, no. 9, p. 2362, Sep. 2018, doi: 10.3390/en11092362.

[8] X. Zhang, J. Yang, and L. Xiao, “An oscillating wave energy converter with nonlinear snap-through Power-Take-Off systems in regular waves,” China Ocean Engineering, vol. 30, no. 4, pp. 565–580, Jul. 2016, doi: 10.1007/s13344-016-0035-5.

[9] H. Pu et al., “Bio-inspired quasi-zero stiffness vibration isolator with quasilinear negative stiffness in full stroke,” J Sound Vib, vol. 574, p. 118240, Mar. 2024, doi: 10.1016/j.jsv.2024.118240.

An Optimization Approach for Array Geometry in Hall Effect Sensor Based Microrobot Tracking

Tuğrul Uslu[1], Erkin Gezgin[2],

[1]Department of Mechanical Engineering, İzmir Katip Çelebi University, İzmir, Çiğli, Turkey, {tugrul.uslu@ikcu.edu.tr}
[2]Department of Mechatronics Engineering, İzmir Katip Çelebi University, İzmir, Çiğli, Turkey, {erkin.gezgin@ikcu.edu.tr}

ABSTRACT

1 Introduction

A surgical navigation system capable of tracking a microrobot in a black box environment where contents cannot be observed through optical measurements non-intrusively, should also employ other means of performing tracking. In this study, a sensor board containing multiple hall effect sensors to perform magnetic tracking is utilized for real world data collection, and a simulation environment is constructed to be utilized in calculating workspace and tracking error based on the real world data. Utilized sensor board consists of, 8 hall effect sensors (UGN3503) for measuring magnetic field created by a microrobot, a multiplexer chip (CD4051), and a microcontroller board (Raspberry Pi Pico) for data acquisition and serial communication.

2 Methodology

In a previous study [1], a microrobot is controlled through a mockup cochlear canal model utilizing 2 permanent magnets manipulated by a macro-micro robot. Position feedback of the microrobot is supplied by optical means. By integrating hall effect sensors in microrobot position tracking, dependency of optical tracking can be reduced and allow the microrobot to be tracked through opaque materials. In light of this [2], around 21000 position values of a microrobot are collected by hand from the optical tracking system together with corresponding hall effect sensor array data from the sensor board. Utilizing the Scikit-learn [3] toolkit, an artificial neural network (ANN) is constructed. With the ANN, relation found between hall effect sensor data and the microrobot position is improved compared to linear regression approaches, given the coefficient of determination (r^2) value of 0.940 showing significant relationship between real and predicted microrobot positions. The ANN also showed sub-millimeter accuracy with RMS values of 0.945 mm and 0.719 mm for test data and all data respectively.

To further study the relation between microrobot and hall effect sensors, a simulation environment, together with test cases is constructed. Python based MagPyLib [4] library is utilized for numerical solutions of magnetic flux from in the virtual environment. The virtual microrobot is modeled as a 10 mm cube N35 permanent magnet with a magnetic polarization value of 5274 Gauss. Utilized UGN3503 hall effect sensors are also modeled as virtual sensors in the virtual environment. For simulated optical tracking of the microrobot, position of the virtual microrobot in the virtual environment is also collected.

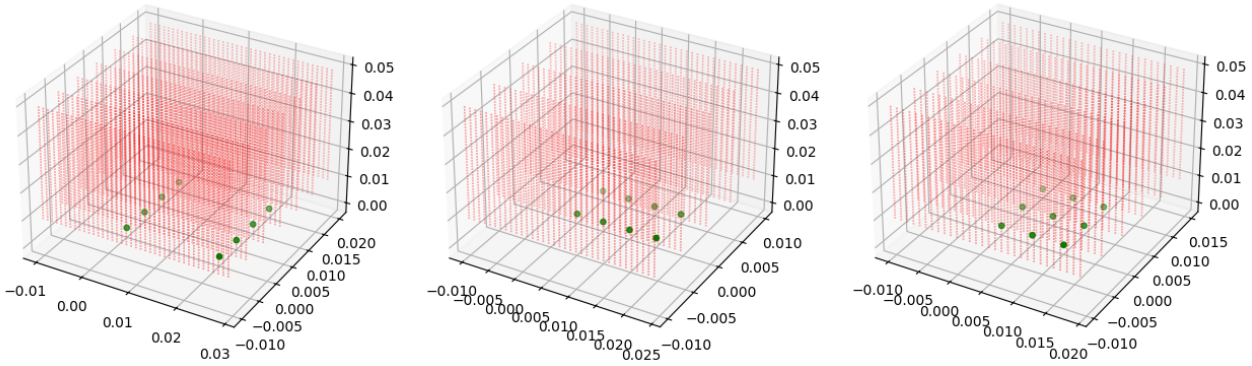

Figure 1: Scan volume of case 1 (left), case 2 (center), case 3 (right)

3 Results

For the first case, the virtual environment is set up to be similar to previously tested physical environment. Distances between virtual sensors are set to be 20 mm between rows and 5 mm between columns. Virtual microrobot is set to scan 56000 mm^3 volume. For every case, desired volumes are scanned with 1 mm distances between data collection points and with fixed microrobot orientations. Running the simulation, usable workspace volume of this hall effect sensor arrangement is found to be 7368 mm^3. The workspace volume is approximated numerically by finding each valid point that causes at least 10% of sensor saturation value as feedback on

©2024 The authors. This work may be used under a Creative Commons Attribution 4.0 License (CC BY 4.0)
DOI: 10.17185/duepublico/82623

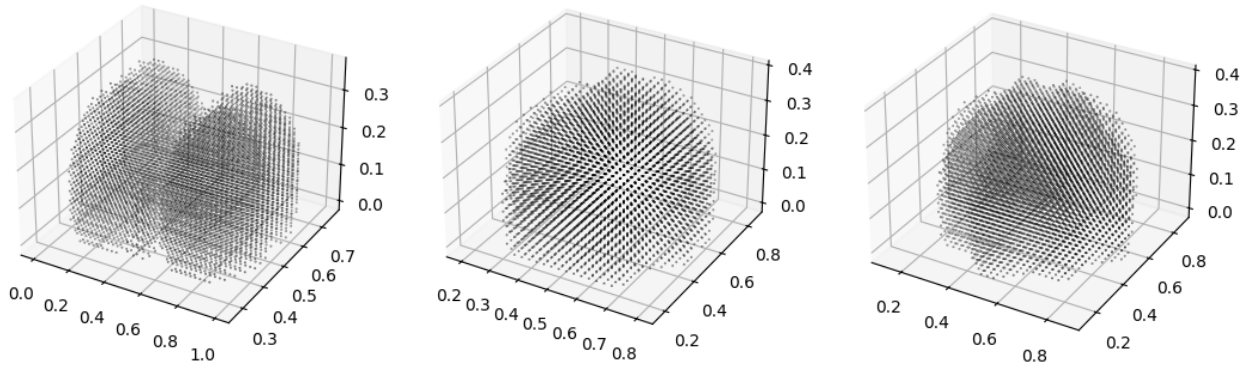

Figure 2: Workspace volume of case 1 (left), case 2 (center), case 3 (right)

3 virtual sensors. Similar to previous study [2], each valid position data together with corresponding hall effect sensor data in the workspace is utilized in linear regression and artificial neural network (ANN) approaches. Virtual environment showed better fitting values compared to the physical case. In the second case, simulation is run with reducing distance between sensor rows from 20 mm to 5 mm compared to previous case and a volume of 35000 mm^3 is scanned. Workspace volume of case 2 found to be 7024 mm^3. Reducing the distances between hall effect sensors also caused workspace to reduce. Case 3 utilized 9 sensor in a 3x3 arrangement. A volume of 36000 mm^3 is scanned and the workspace volume of case 3 is calculated to be 7523 mm^3. Figures for scanned volumes and found workspace volumes of cases are given in figure 1 and 2.

4 Conclusion

r^2 and RMS values for linear regression and ANN approaches are given in table 1. Both ANN and linear regression fit values seem to be saturated with further improvement proving unfeasible. Although a limited number of cases, linear regression fit has shown to be unstable in cases where hall effect sensors are closer together. Further tuning of the virtual environment simulation may allow the optimization of parameters for final revision of the sensor board.

Table 1: r^2 and RMSE (mm) values of predicted positions of the microrobot by methodology

#	Rows (row distance)	Columns (col distance)	Scanned Volume (mm^3)	Workspace volume (mm^3)	Linear Reg. r^2	RMS(mm)	ANN r^2	RMS(mm)
Real Case	2 (20 mm)	4 (5 mm)	-	-	0.78	1.95	0.94	0.95
Case 1	2 (20 mm)	4 (5 mm)	56000	7368	0.98	1.04	0.99	0.76
Case 2	2 (5 mm)	4 (5 mm)	35000	7024	0.92	1.34	0.99	0.19
Case 3	3 (5 mm)	3 (5 mm)	36000	7523	0.89	1.67	0.99	0.13

References

[1] E. Gezgin *et al*, “On the design of a macro-micro parallel manipulator for cochlear microrobot operations“ *The International Journal of Medical Robotics and Computer Assisted Surgery*, vol 20(4), 2024.

[2] T. Uslu and E. Gezgin, “A Preliminary Study on 3D Tracking“, *Mechanism Design for Robotics*, pp 108-114. 2024.

[3] F. Pedregosa *et al*, “Scikit-learn: Machine Learning in Python“, *Journal of Machine Learning Research*, vol. 12, pp 2825-2830. 2011.

[4] M. Ortner and L. G. C. Bandeira, “Magpylib: A free Python package for magnetic field computation“ *SoftwareX*, vol 11, 2020.

Collaborative Learning Environments for Research-based Teaching of Mechanical Engineering

Joaquim Minguella-Canela[1], Jordi Romeu Garbí[2]

[1]Grup de Recerca en Tecnologies de Fabricació (TECNOFAB), Departament D'Enginyeria Mecànica (DEM), Escola Tècnica Superior D'Enginyeria Industrial de Barcelona (ETSEIB), Centre CIM, DigiFACT- Agrupació de Centres per a la Factoria Digital Avançada, Universitat Politècnica de Catalunya (UPC), Campus Sud, Edif. PF, Av. Diagonal 647, 08028 Barcelona, Spain, {joaquim.minguella@upc.edu}
[2]Laboratori d'Enginyeria Acústica i Mecànica (LEAM), Departament D'Enginyeria Mecànica (DEM), Escola Superior d'Enginyeries Industrial, Aeroespacial i Audiovisual de Terrassa (ESEIAAT), Universitat Politècnica de Catalunya (UPC), Campus Terrassa, Edif. TR45, C/ Colom 11, 08222 Terrassa, Spain, {jordi.romeu@upc.edu}

ABSTRACT

1 Introduction

The skills and capacities required to Mechanical Engineering Master graduates to work in industrial environments have evolved towards interdisciplinary assets (such as Digital literacy; Creative problem solving; inter-cultural, -disciplinary, Inclusive mindset; Efficient handling of increasing complexity) [1] that require new teaching methods with a holistic approach. This trend has also been seen in the context of Industry 4.0 [2] and Industry 5.0 topics [3] yielding a value-driven initiative with an important emphasis on human centricity [4, 5].

In the standing point, technical leading universities may act as independent teaching silos. This is not optimal from the expertise (technical specialisation) point of level, nor for teaching experience (research-based). Indeed, technical universities convey research-based master studies on Mech. Eng. [6]. Research-based learning is seen as a relevant approach for acquiring and developing the skills and mindset required in Industry and can also motivate people and forge STEAM vocations when at early ages.

Still, individual teaching centres they can leverage their joint potential when taking part in Networks and Alliances of universities [7] and industry [8]. Integrating the different teaching insights and expertise niches from different technical sites across different countries can bring diversity and position the student at the centre of research-based learning, as a notable evolution of Project-based learning [9]. In the master's degrees offered by the different technical universities, there is a big opportunity to leverage Research Assignments that are currently undertaken only locally to widen the scope and to internationalise the content. Digital campus facilities [10] are nowadays in a plateau of development that can enhance seamless collaborative environments.

2 Collaborative Research-based Learning (multi-topic and multi-site)

With this context, different research teams from Mech. Eng. and related depts. in different universities have a strong synergic potential body of collaboration regarding industrial technologies, in particular in areas related to Mechanisms and Machines. Taking as a Case study a 2-degrees of freedom mechanism that can serve as a commanding joystick [11], collaborative research assignments can be offered in areas regarding different Mech. Eng. topics such as design, simulation, fabrication, and testing (See Fig. 1).

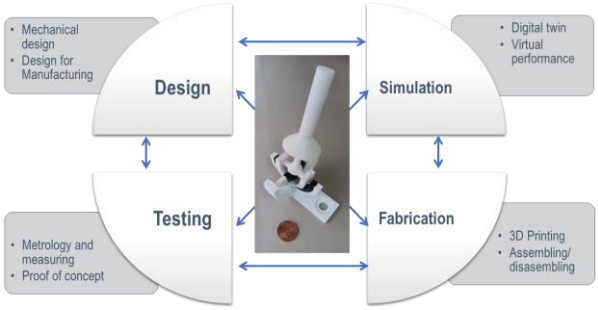

Figure 1: Research-based Case study in the field of Mechanisms (2-dof multi-material 3D printed Joystick)

To be able to convey such collaboration, each participating entity should have at least a running official Master, in which the students could undertake a research assignment in a certain moment of the year (e.g.: spring), that would bear between 12 and 30 ECTS at the institution of origin. If that were to be the case, then it would be possible to establish student exchanges that allow them to study at another university that can be specialized in a complementary field than that of the university of origin. Those exchanges can be framed within a common course with hybrid-on-distance material, for the entire group of students regardless of its home and host university. The course should be taught in collaboration by the teachers involved of every university, each one with his/her expertise.

During the course each student should receive a research-based assignment, which will perform partly at the original institution, and partly at the host institution, teaming up with other students. These assignments should bridge different ends in the field, for example "design + fabrication", "design + simulation" or "fabrication + physical testing"; thus, leveraging collaboration and going beyond silo expertise's. The deployment if such research-based assignments is the one including a short mobility stay (min. 2 months), that could be in-presence or virtual depending on the case. The stays should be laboratory-based, so the students can have a good research insight. The ambition in this kind of experiences would be to have a balanced participation between universities, meaning that (on average) each university sends and hosts approximately the same number of students. From a more operational point of view, students and teachers undertaking physical travelling could benefit from the Erasmus + mobility schemes when

©2024 The authors. This work may be used under a Creative Commons Attribution - NonCommercial - NoDerivatives 4.0 License (CC BY-NC-ND 4.0)
DOI: 10.17185/duepublico/82606

applicable. Also, for the easiness of communication it is advised to stablish English to be used as lingua franca.

3 Digital Facilities and Evaluation in a shared context (digital courses and collaborative teaching)

Concerning the set-up of the Collaboration Environments a Virtual Campus would be the central learning management platform for all members, and to use it for the trainings, workshops, teaching and lectures. This would be central to the development of innovative teaching and learning formats (e.g.: COIL, VECP, etc.), and for the intercultural or international learning environments for co-creation. Concerning to the coordination of the collaboration, most meetings could be held on-line, so to be the most cost effective. Before the start of the course, specific synergic preparatory work should be completed to define the research assignments. At this stage, many interactions and discussions should be envisaged (both virtual and live). Apart from the teaching, monthly on-line meetings should be scheduled to follow-up during all the teaching duration. The assignments should have to be evaluated following the home institution regulations (specific rubrics), and the effectiveness of collaborations overall with a global framework (general rubric) [12-13]. Teacher's travelling in person would in some cases be also necessary to produce some evaluations.

Regarding outreach, the blend of physical and virtual could easily generate dissemination assets for the universities and alliances, that could be used in promotion to attract potential new students, and even more interestingly, to foster the engineering motivation and, in a broader sense, more STEAM vocations. The framework of collaborative learning environments for research-based teaching is to foster collaboration among universities via a continued research sustainable activity in Mechanical Engineering and could be further extended to other fields of interest (sustainability, energy, entrepreneurship) and for new partners as well.

4 Expected results and main conclusions

Several expected benefits from the deployment of Collaborative Teaching and Learning Environments, that can be expanded further from Mechanical Engineering topics to others in fields such as Sustainability, Energy o Entrepreneurship are the following: (1) Preparation of a framework for Research-based Teaching and Learning, (2) Strengthening the collaboration not only in teaching but also in research activities between the participating universities, (3) Completion of joint research assignments, combining the expertise of each university and centre, and (4) Attraction and motivation of young potential candidates to research careers.

Acknowledgments

The author Joaquim Minguella-Canela is a Serra Húnter fellow professor (lecturer). Unite! Seed Fund "Teaching & Learning in the Unite! Focus Areas (Summer 2024)".

References

[1] WMF 2019, World Manufacturing Foundation, 2019 World Manufacturing Forum Report, Skills for the Future of Manufacturing, **2019**, www.worldmanufacturingforum.org

[2] T. Curià Piñol et al. "Study of the training needs of industrial comp. in the Barcelona Area and prop. of Training Courses and Method. to enhance further competitiveness.", *P. Manuf.*, vol. 13, pp. 1426-1431, **2017**, DOI: 10.1016/j.promfg.2017.09.159.

[3] I4MS, "Towards Industry 5.0: news skills and capabilities working group," I4MS Training Catalogue, **2022**. https://i4ms.eu/towards-industry-5-0-news-skills-and-capabilities-working-group/

[4] X. Xu et al. "Industry 4.0 and Industry 5.0—Inception,conception and perception", Journal of Manufacturing Systems, vol. 61, pp. 530-535, **2021**. DOI: 10.1016/j.jmsy.2021.10.006

[5] J. Crnobrnja et al. (2024). "Digital Transformation Towards Human-Centricity: A Systematic Literature Review", Conference: APMS. IFIP, AICT 731, Part IV, Springer, pp. 89-102, **2024**. DOI: 10.1007/978-3-031-71633-1_7

[6] MUREM: Master Universitari en Recerca en Enginyeria Mecànica. UPC, **2024**. https://eseiaat.upc.edu/ca/estudis/estudis-en-enginyeries-industrials/master-universitari-recerca-enginyeria-mecanica/master-universitari-recerca-enginyeria-mecanica

[7] Unite! University network for Innovation, Technology and Engineering, **2024**. www.unite-university.eu/

[8] UNITECH international alliance, **2024**. www.unitech-international.org/

[9] A.D. Lantada. "Engineering Education 5.0: Strategies for a Successful Transformative Project-Based Learning" in Insights Into Global Engineering Education After the Birth of Industry 5.0. Ed. IntechOpen, pp. 1-17. **2022**. DOI: 10.5772/intechopen.102844

[10] J. Alcober, et al. "The digital platform for the Unite! Alliance: The Metacampus". Ed. UPV, pp. 161-169, **2023**. DOI: 10.4995/HEAd23.2023.16265

[11] J. Minguella-Canela et al. "Sistema resistivo impreso en 3D multi-material para comandar sistemas robóticos". XLV Jornadas de Automática. Robótica, Núm. 45, **2024**. DOI: 10.17979/ja-cea.2024.45.10849

[12] Cornell University: How to evaluate group work. **2024**. Accessible on line: https://teaching.cornell.edu/teaching-resources/active-collaborative-learning/collaborative-learning/how-evaluate-group-work

[13] Q. Wang. "Design and evaluation of a collaborative learning environment" Comp. & Educ., vol 53, Issue 4, pp 1138-1146, 2009, DOI: 10.1016/j.compedu.2009.05.023

Pronosupination Device to assist Pronation and Supination Movements of the Forearm Rehabilitation with Virtual Interface

Ríos-Hincapie J.A[1], Contreras-Calderón MG[1], Porras-Ramirez O[1], Gomez-Nava A[1]

[1]División de Tecnologías de la Automatización e Información, Universidad Tecnológica de Querétaro, Querétaro, México, {ma.gpe.contreras.c@gmail.com}

ABSTRACT

1 Introduction

The development of technological devices for rehabilitation as new alternatives for therapies has brought solutions for assistance in physical rehabilitation. Robotics improve patient outcomes by promoting neuroplasticity, helping the brain rewire and relearn lost motor skills, and accelerating functional recovery in conditions like stroke. Robotic systems also enable continuous tracking progress, allowing for personalized treatment adjustments, which further supports efficient rehabilitation and recovery speed compared to traditional methods [1]. These devices allow repetitive movements with specific trajectories that generate exercises such as flexion-extension, adduction, pronation, and supination, among others, whether passive or active therapies. Also, they provide optimal rehabilitation; stand out reproducibility, programs oriented to specific tasks, and a quantified progression. With the previous benefits, an increase in strength, improved coordination, modifications in muscle tone, motor reeducation, and greater functional independence, among others, are obtained, although some studies show controversial results [2]. The aim of rehabilitation is not therapist substitution; it's a tool to assist so that he can provide optimal rehabilitation to all their patients. In rehabilitation, pronation and supination exercise improve flexibility, strength, and the overall functionality of the forearm and hand, making these movements key focus areas in restoring upper limb mobility and independence for patients [3]. Fifty relevant devices have been reported [4], twenty-four of which are end-effector devices and only six consider pronation and supination exercises. The best known are InMotion Arm [5], Gentles [6], Braccio Di Ferro [7], and Adler [8], all above are of end-effector type. Only the InMotion Arm considers pronosupination, however, this movement is carried out independently of the rehabilitation exercises, while the others are limited to execute movements of flexion-extension, adduction, and abduction. The exercises assisted by these devices can be complemented by pronosupination to perform more complete therapies. In this paper, a pronosupination device design is proposed and implemented. A user interface developed in Unity was implemented that allows the user to interact with the mechanism while playing a game, with trajectories using in rehabilitation.

2 Pronosupinator CAD Design and Prototype

The pronosupinator consists of five main parts: A forearm holder, a cylinder with a circular rack, a pinion, a cd motor, and an optical sensor (see figure 1). The forearm holder has motor support and a hole where the bolt can be placed to fix the position of the cylinder. The union of the end effector and optical sensor has a bearing to allow it to rotate on its axis and adapt the arm to the mechanism's movement. The cylinder has a grab bar with a strain gauge and a circular rack that matches the pinion to form a motion transmission system. The motor is attached to the holder; the pinion is fixed to the motor shaft to make permanent contact with the cylinder circular rack. The cylinder rotates freely inside the holder through two circular guides (cylinder) and two grooves (holder). The mechanism has one degree of freedom, and can slide on the XY plane, in order to provide movements such as abduction, flexion and, extension of the arm.

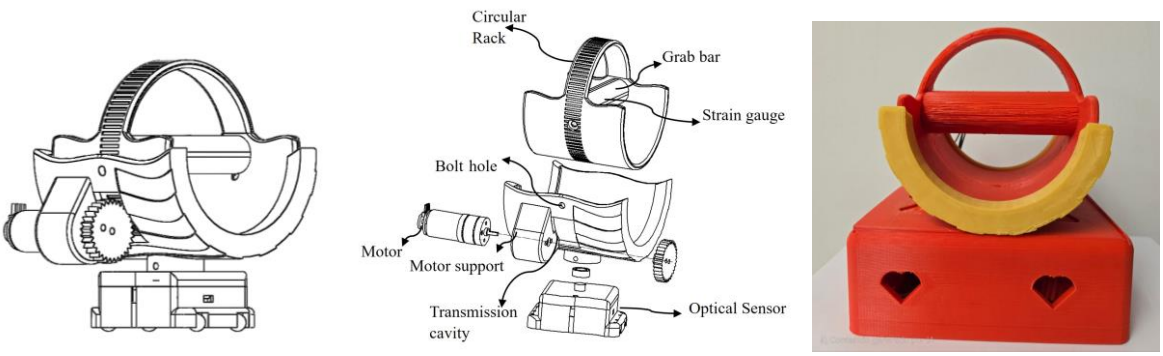

Figure 1. Pronosupinator CAD model and prototype

The strain gauge allows to send of the force detected from the device to the virtual interface, to convert the patient´s force in the movement of the virtual object. The prototype was fabricated with 3D print and PLA material.

©2024 The authors. All rights reserved.
DOI: 10.17185/duepublico/82645

3 Virtual Interface for Arm Rehabilitation

The virtual interface purpose is patient interaction with dynamic games through the pronosupinator. The patient holds the device grab bar and moves virtual object. Thanks to the strain gauge attached to grab bar, which is used to measure the force exert by the patient during the game, the object in the virtual interface jumps depending on the force. A series of games were developed for helping patients to perform rehabilitation therapies actively while playing.

Games are designed so that patients, during the game, perform pronosupination, adduction, and flexion-extension movements in a controlled way, while the mechanism slides in XY plane. The software used for development of the games was Unity with C# language [9]. The features considered for the virtual interface are, patient must be able to follow the therapies trajectories while playing, stimulate strength in the muscles involved in the movements with the gauge, game's purpose is to improve patient precision and motor control, and therapist must be able to select the game level. Interface must display or save the game score to use as a patient's progress.

Games that are included in the interface are, see figure 3, jumping the river and cook pizza. The pizza game movements depend on pronation and supination angles during the device rotation, the pronosupination angle is automatically measured and send to the interface to virtually manipulate the objects (ingredients to cook a pizza). In the jumping the river, the animated character jumps depending on the force exert by the patient and walk side to side depending on the rotation. Figure 2 shows the device used by a volunteer and the board of two games.

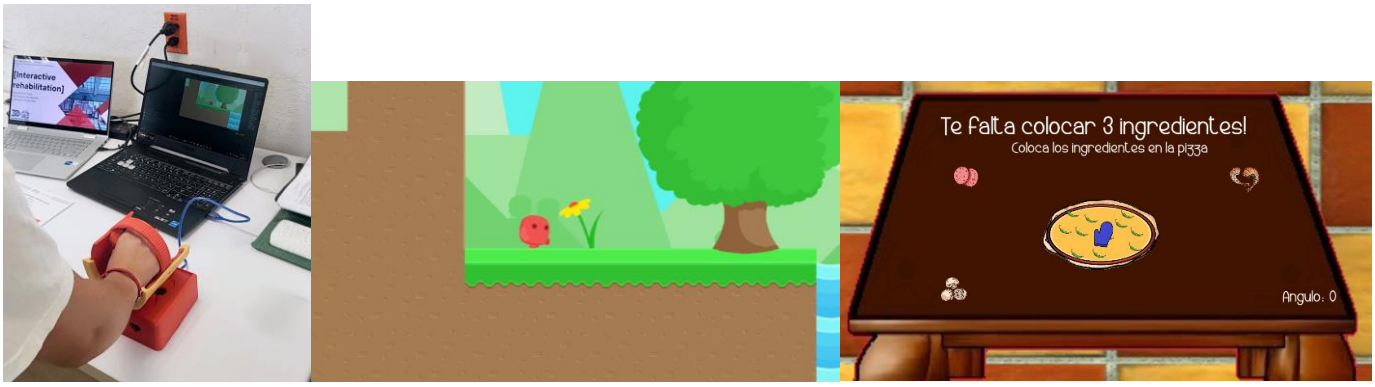

Figure 2. Pronosupinator with games

4 Conclusions

The pronosupination exercise is one of the most important for arm rehabilitation. A pronosupinator device, was developed and tested with some volunteers. The device assists the pronosupination movement and allows the patient arm to rotate according with natural arm movement during the trajectory's execution. Two games were developed to allow a dynamic patient interaction with assisting active rehabilitation therapies. To play the games, the patient must perform movements of pronosupination of the forearm and apply force in the sensor. On the other hand, during the game, the patient feels the need to improve his score and has a tendency to perform wider and precise arm movement. In this way, the game represents an incentive for the patient not to abandon therapies and thus reduce recovery time.

Acknowledgments

This work was financially supported by the program Nuevos Talentos Científicos by CONCYTEQ.

References

[1] A.D. Banyai, C. Brișan, "Robotics in Physical Rehabilitation: Systematic Review", Healthcare, vol. 12, pp. 1720, 2024.
[2] P. Loeza-Magaña, "Introduction to robotic rehabilitation for the treatment of cerebral vascular disease: a review", Revista Mexicana de Medicina Física y Rehabilitación, 27, 2015.
[3] Inner Body, "Forearm Motion: Pronation, Supination & Body Mechanics", Available online: https://www.innerbody.com/image/musc03.html (accessed on 11 Nov 2024)
[4] L. Rodríguez-Prunotto, R. Cano, A. Cuesta-Gómez, I.M. Alguacil-Diego, F. Molina-Rueda, "Terapia robótica para la rehabilitación del miembro superior en patología neurológica", Rehabilitación, vol.48(2), pp. 101-128, 2014.
[5] Interactive Motion Technologies, "InMotionArm", Available online: https://www.bioniklabs.com/products-/inmotion-arm (accessed on 11 Nov 2024).
[6] R. Loureiro, F. Amirabdollahian, M. Topping, B. Driessen, W. Harwin, "Upper Limb Robot Mediated Stroke Therapy-GENTLE/s Approach", Autonomous Robots, vol 15, pp. 35-51, 2000.
[7] F. Vergaro, M. Casadio, V. Squeri, P, Giannoni, P. Morasso, V. Sanguineti, "Selfadaptative training of stroke survivors for

continuous tracking movements", Journal of NeuroEngineering and Rehabilitation, vol. 7, pp. 7-13, 2010.
[8] M, J. Johnson, K.J Winsneski, J. Anderson, D. Nathan, E. Strachota, J. Kosadih, J. Johnston, R.O Smith, "Task-oriented and Purposeful Robot-Assisted Therapy", Rehabilitation Robotics, vol. 221-242, 2007.
[9] UNITY. Available online: https://unity3d.com/es (accessed on 30/09/2024).

Proposed Design of New Drones for Specific Applications in Field Cultural Heritage

Mohammed Khadem[1*], Dmitry Malyshev[1], and Giuseppe Carbone[1]

[1] DIMEG, University of Calabria, Rende,87036, Italy, mohammed.khadem@unical.it /dmitry.malyshev@unical.it /giuseppe.carbone@unical.it

ABSTRACT

1 Introduction

Recently, we have witnessed new challenges in many sectors, including industry, transportation, and other sectors. Therefore, drones have played an important role in confronting these problems and enabling humans to deal with the new challenges with complete comfort [1, 2]. The drones are mainly based on a number of high-performance motors for manoeuvring and moving in several degrees of freedom and task execution. We mention some applications that we found use the drone to deal with it, for example, agriculture [3], construction industry [4], civil protection [5], and underwater applications [6]. Control strategies and algorithms are very important in the internal system of the drone for achieving stabilisation and good performance. There are many different control strategies used in several searches. PID control [7] is very robust strategy. It has provided good performance in many experiments of recent research. Adaptive robust control is also a good strategy that is used in some searches [8]. It used for trajectory tracking, regulating and correcting the trajectories. It should also be noted sliding mode control [9], machine learning [10], and intelligent artificial [11]. These strategies are used in many recent investigations, especially machine learning and intelligent artificial, because they have proven their high efficiency and have received a lot of attention recently. This work aims to present the proposed design for develop new drone for specific application in field cultural heritage. The goal of this drone is conducting exploration and inspection of coastal built cultural heritage sites by termocamera. We define a systematic approach for building drone with good criteria that insure high performance in specific applications.

2 The intended operation scenario

The process of searching and exploring for historical antiquities in rugged areas covered with trees or complex sites that are difficult to reach constitutes a big challenge for archaeologists, which makes the search for historical sites full of risks. So that we suggest novel design of drone for use to exploration and inspection of coastal built cultural heritage sites by use termocamera. An infrared termocamera is a technology that uses opto-electronic devices to detect and measure radiant energy (electromagnetic waves) and creates a process that correlates radiation with surface temperatures without direct contact with the object. The characteristics of our proposed design: medium size, average flight level with a maximum altitude of 200 m. It also has transfemoral legs in order to base it on them, and at the same time it can carry some important things or tools using these transfemoral legs. After completing the construction of this drone, it will be tested in multiple environments several times in order to determine the efficiency of this drone through to sure form full protection from drops of water, sand, gravel, and other physical factors and reveal the possibility of further development or being satisfied with the results obtained. Some commercial drones are highly efficient, but they may not be suitable in our project because these drones are programmed with fixed algorithms and cannot be customised and modified in terms of the internal system. In our project we need to add some modifications and some new features, such as saving the discovered locations, determine its coordinates and other features that require modification to the drone's internal system in order to apply them. The Product Design Specification (PDS) for the drone are presented in Table 1. Required velocity, flight time in a workspace area of 8 km^2 is 30min are an important point in special applications, and these values were determined in order for the drone to be able to carry out the required tasks in record conditions. For example, according to the criteria mentioned in the table, this drone will be able to survey a range of 8 km^2 in only 8 times. If we change these values, the number of tasks will increase, and this process will be slow. Therefore, these requirements are important in our project in order to achieve good, highly efficient work in cultural heritage applications.

3 A proposed design concept

In this section, we present the PDS that were obtained by summarising the important information from previous searches. Table 1 presents the proposal design and the PDS for specific applications in field cultural heritage. The figure in the table presents the proposed design with 6 Dofs. The PDS are very important for good performance in specific applications. Minimum velocity 12m/s is introduced for arriving at the site in a short time, payload 2 kg introduced for a camera with 200 g and auxiliary components. Control range 8 km is required for good workspace covers big city area square. We plan to use a good battery for 30 min flight (suitable value for cultural heritage applications taking into account 12m/s velocity). Shields around the propellers and IP for water and solids are introduced for safety because the drone will be operated near sea and near the mountains.

©2024 The authors. This work may be used under a Creative Commons Attribution 4.0 License (CC BY 4.0)

DOI: 10.17185/duepublico/82582

Table 1: The proposed design and Product Design Specification

▪ *Heritage Drone*	▪ *6 Dofs*	▪ *Requirement*	*Define*
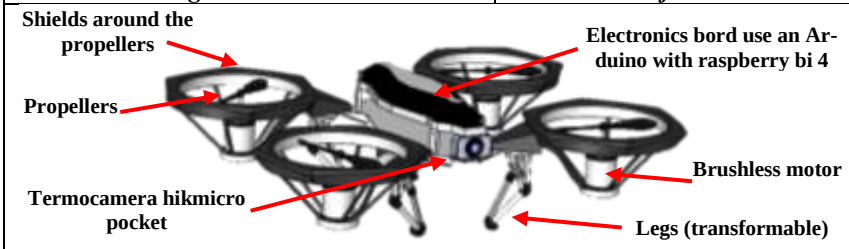		➢ Velocity	12 m/s
		➢ Payload	2 kg
		➢ Control range	8km
		➢ Height	200 m
		➢ Time flight	30 min
		➢ Shields around the propellers	4
		➢ IP for water	>=4
		➢ IP for solid	>= 5

These requirements are needed to achieve a drone with full protection from water drops and sand, gravel and other physical factors. The PDS is the result of a comprehensive search in literature sources in order to analyse characteristics of drones and extract the important requirements for specific applications in the field cultural heritage.

3 Conclusion

The proposed design with criteria required for cultural heritage applications has been presented in this paper. This stage is considered the conclusion of the previous works through analysis a lot of information about the drone from many different projects in different industry sectors. The analysis conducted allowed us to obtain a PDS and develop an innovative drone for application in exploration and inspection of coastal built cultural heritage sites by using a termocamera.

Acknowledgements.

The authors acknowledge the support of the PNRR Project TECH4YOU.

Financial Support. This paper has been partially funded by the PNRR Next Generation EU "T4Y S4G4PP1" – CUP H23C22000370006.

References

[1] Conway HG. Drone Aircraft. The Journal of the Royal Aeronautical Society. 1959;63(579):163-174. https://doi.org/10.1017/S036839310007084X

[2] Bergen PL, Rowland J. World of Drones: The Global Proliferation of Drone Technology. In: Bergen PL, Rothenberg D, eds. Drone Wars: Transforming Conflict, Law, and Policy. Cambridge University Press; 2014:300-342. https://doi.org/10.1017/CBO9781139198325.020

[3] Ahirwar, S., R. Swarnkar, S. Bhukya and Namwade, G. 2019. Application of Drone in Agriculture.Int.J.Curr.Microbiol.App.Sci. 8(1): 2500-2505. doi: https://doi.org/10.20546/ijcmas.2019.801.264

[4] Choi, Hee-Wook, et al. "An overview of drone applications in the construction industry." Drones 7.8 (2023): 515. https://doi.org/10.3390/drones7080515

[5] Avanzato, Roberta, Francesco Beritelli, and Mario Vaccaro. "Identification of mobile terminal with femtocell on drone for civil protection applications." 2019 10th IEEE International Conference on Intelligent Data Acquisition and Advanced Computing Systems: Technology and Applications (IDAACS). Vol. 1. IEEE, 2019. https://doi.org/10.23919/ICACT48636.2020.9061508

[6] Williams SB, Newman P, Rosenblatt J, Dissanayake G, Durrant-Whyte H. Autonomous underwater navigation and control. Robotica. 2001;19(5):481-496. doi:10.1017/S0263574701003423 https://doi.org/10.1017/S0263574701003423

[7] Lopez-Sanchez, Ivan, and Javier Moreno-Valenzuela. "PID control of quadrotor UAVs: A survey." *Annual Reviews in Control* 56 (2023): 100900. https://doi.org/10.1016/j.arcontrol.2023.100900

[8] Elhennawy, Amr M., and Maki K. Habib. "Trajectory tracking of a quadcopter flying vehicle using sliding mode control." *IECON 2017-43rd Annual Conference of the IEEE Industrial Electronics Society*. IEEE, 2017. https://doi.org/10.1109/IECON.2017.8217089

[9] Mercado D, Castillo P, Lozano R. Sliding mode collision-free navigation for quadrotors using monocular vision. *Robotica*. 2018;36(10):1493-1509. https://doi.org/10.1017/S0263574718000516

[10] Giorgiani do Nascimento, Renato, Kajetan Fricke, and Felipe Viana. "Quadcopter control optimization through machine learning." AIAA Scitech 2020 Forum. 2020. https://doi.org/10.2514/6.2020-1148

[11] Altshuler Y, Yanovsky V, Wagner IA, Bruckstein AM. Efficient cooperative search of smart targets using UAV Swarms. *Robotica*. 2008;26(4):551-557. https://doi.org/10.1017/S0263574708004141

Origami inspired engineering: Challenges and opportunities in portable and foldable mechanisms in solar-power generation

Daniel Lavayen-Farfán[1] & Enrique Pujada-Gamarra[1,2]

[1]Applied Mechanics, Machines and Mechanisms Group, Pontificia Universidad Católica del Perú, Universitaria Ave. 1801, 15088 Lima, Perú, {dlavayen@pucp.edu.pe}
[2]Fakultät Maschinenbau, Technische Universität Ilmenau, Ehrenbergstraße 29, 98693 Ilmenau, Germany,

ABSTRACT

Origami can be a source of inspiration for engineers and professionals in R&D, as complex figures can be obtained by folding a flat sheet of paper. Among the various applications of origami-inspired engineering, solar-power generation has emerged as a particularly promising field. Solar-powered systems are typically heavily constrained by the surface area they need to cover to produce electricity. The more power needed, the more surface area that requires to be covered. Foldable panels overcome this difficulty by folding the panels one on top of the other to temporarily reduce their footprint. However, to adequately design these products, several factors need to be accounted for, such as: the dynamics of the movement, the joint design, and the thickness of the panels, which might affect the Origami motion. These factors have a huge impact in the structural integrity, quality and performance of the panels. Thus, these factors also present themselves as challenges that must be overcome in a growing field with more and more applications. In this work, the authors present some of these challenges, as well as opportunities of research and development in this promising field.

1 Introduction

Origami, the ancient japanese art of folding paper, can be a limitless source of inspiration for engineers dedicated to research and development. By folding a flat sheet of paper, complex 3d shapes can be created. The hidden potential in origami lies precisely in these folds: a complex and compact and folded shape can be "unfolded" to occupy a larger footprint. This property has found several uses in different fields, including robotics [1, 2], space exploration [3, 4], solar-power generation [5], among others [6]. However, to fully exploit its potential, further study on the kinematics and design methodologies must be done [7, 8, 9].

2 Thick Origami: challenges and opportunities

One particular and often useful way of analyzing origami, is to consider that it is actually a 3d linkage mechanism. By this analogy, the kinematics of existing and even new Origami patterns can be studied as the kinematics of a 3d linkage. This analogy is also useful to determine the number of degrees of freedom of an Origami pattern, which is extremely useful since this information can be used to build the driver system and structure of the Origami.

Unlike paper Origami, otherwise known as thin Origami, most engineering applications require to account for panel thickness and stiffness. This applications lie in the field known as thick Origami. The inclusion of thickness makes flat foldability almost impossible unless the folds are redesigned using the so-called thickness-accommodation techniques [10]. Some of these techniques have been widely studies, whereas others have been neglected despite their advantages, because of limitations that have yet to be overcome. The challenge is to build a thick origami which can reliably achieve flat foldability, preserve Origami-like motion, with hinges that can be able to withstand continuous and repetitive use without breaking or collapsing.

3 Impact and possible applications

As mentioned, there are several possible applications for Origami-inspired foldable solar-panels. Even though they were initially conceived with space-exploration applications in mind, plenty other ground and maritime applications exist. For instance, foldable solar panels can be installed on naval vessels, with extreme space constraints and limited surface area; therefore increasing the energy efficiency of the vessel and significantly reducing the fuel costs [11]. On the other hand, mining facilities (typically located far away from the main cities or the electric grid) rely heavily on portable diesel generators for electricity for human use; thus, mobile and/or portable solar-power generation systems can not only reduce the fuel costs, but also contribute to a cleaner and greener environment [5].

Moreover, foldable solar panels can enhance agricultural photovoltaic systems (AgriPV), where the ability to adjust panel configurations dynamically can increase land productivity by optimizing energy output for different types of crops. These applications showcase not only the versatility of foldable solar panels but also their capacity to contribute to more sustainable, cost-efficient solutions across multiple sectors. As the technology matures, further innovations in the design and deployment of foldable solar panels promise to expand their impact in different applications.

©2024 The authors. This work may be used under a Creative Commons Attribution 4.0 License (CC BY 4.0)
DOI: 10.17185/duepublico/82639

4 Conclusions

In conclusion, origami inspired engineering presents a large variety of opportunities in the development mechanisms for foldable and portable solar panels. While the challenges of joint design, panel thickness, and kinematics are still significant, they also offer important research lines. As the demand for sustainable and mobile energy solutions grow, advances in origami inspired design could play a major and critical role in solar-power generation.

References

[1] D. Rus and M. T. Tolley, "Design, fabrication and control of origami robots," pp. 101–112, 6 2018.

[2] S. Mintchev, J. Shintake, and D. Floreano, "Bioinspired dual-stiffness origami," *Science Robotics*, vol. 3, p. 275, 7 2018. [Online]. Available: https://www.science.org

[3] E. Landau, "Solar power, origami-style," 8 2014. [Online]. Available: https://www.jpl.nasa.gov/news/solar-power-origami-style

[4] J. Fulton and H. Schaub, "Deployment dynamics analysis of an origami-folded spacecraft structure with elastic hinges," *Journal of Spacecraft and Rockets*, vol. 59, pp. 401–420, 3 2022.

[5] D. Lavayen, E. Pujada, D. Olivera, A. Maguina, M. Choque, and W. Bullon, "Design of a solar powered mobile illumination tower with a solar tracker mechanism for increased efficiency," *Mechanisms and Machine Science*, vol. 71, 2019.

[6] Y. Zhang, M. Li, Y. Chen, R. Peng, and X. Zhang, "Thick-panel origami-based parabolic cylindrical antenna," *Mechanism and Machine Theory*, vol. 182, 4 2023.

[7] Y. Zhu, M. Schenk, and E. T. Filipov, "A review on origami simulations: From kinematics, to mechanics, toward multiphysics," *Applied Mechanics Reviews*, vol. 74, 5 2022.

[8] R. Peng and G. S. Chirikjian, "A methodology for thick-panel origami pattern design," *Mechanism and Machine Theory*, vol. 189, 11 2023.

[9] Z. Xia, C. Tian, L. Li, and D. Zhang, "The novel synthesis of origami-inspired mechanisms based on graph theory," *Mechanism and Machine Theory*, vol. 192, 2 2024.

[10] R. J. Lang, K. A. Tolman, E. B. Crampton, S. P. Magleby, and L. L. Howell, "A review of thickness-accommodation techniques in origami-inspired engineering," *Applied Mechanics Reviews*, vol. 70, 1 2018.

[11] E. Pujada, D. Olivera, D. Lavayen, and J. Rodriguez, "Paneles fotovoltaicos plegables: la innovacion inspirada en origami," *FABRICUM*, vol. 4, 2023.

Nonlinear Robust Control Design for a Planar Robot Arm

Zeki Okan Ilhan[1]

[1]McCoy School of Engineering, Midwestern State University, 3410 Taft Blvd, Wichita Falls, TX, 76308, USA, {zeki.ilhan@msutexas.edu}

ABSTRACT

1 Introduction

This work aims to conduct a comprehensive analysis of the kinematics, dynamics, motion planning, and nonlinear control design for a basic two-link planar robot arm (Fig. 1). As interest in robotics continues to grow, the two-link arm remains fundamental for the development and control of more advanced serial robotic manipulators [1] and humanoid robots [2]. In this study, the system dynamic model is first developed using Lagrange's equations [3] in a non-conservative format. Additionally, an inverse kinematic analysis is conducted to determine the target joint variables for executing circular motion in the task plane. The dynamic model is then integrated with a feedback controller based on the nonlinear, Sliding Mode Control (SMC) strategy [4]. The tracking performance of the proposed controller is tested in closed-loop numerical simulations, in which the target trajectories are set to the joint variables obtained from the inverse kinematic study. Furthermore, the dynamic model is slightly altered in the simulation by adding 5% extra weights to the links in order to assess the controller's robustness against external disturbances.

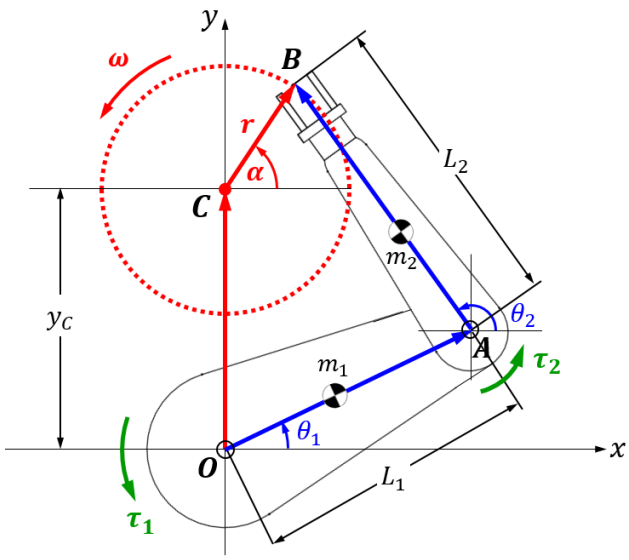

Figure 1: A sketch of the 2-link (RR) planar robot

Table 1: A list of the model parameters

Parameter	Value	Description
L_1, L_2	0.50 m	Lengths of the links
L_{m_1}, L_{m_2}	0.25 m	CoM lengths of the links
m_1, m_2	3.00 kg	Masses of the links
I_1, I_2	0.25 kg·m^2	Moments of inertias of the links
r	0.25 m	Radius of the circular path
ω	100 °/s	End-effector rotational speed
x_C	0.00 m	Abscissa of the center point, C.
y_c	0.50 m	Ordinate of the center point, C.
$\theta_1(t), \theta_2(t)$	–	Angular positions of the links
$\tau_1(t), \tau_2(t)$	–	Torque inputs on the joints

2 Dynamic Model

Lagrange's equations are applied in a non-conservative format to develop the dynamic model for a torque input scenario. As Lagrange modeling relies on energy principles, it was essential to derive the expressions for the total kinetic and potential energy of the robot, along with the total work done by the non-conservative factors such as the torque inputs. By selecting angles θ_1 and θ_2 (Fig. 1) as the independent generalized coordinates, the dynamic model can be written compactly in the following matrix form [3]:

$$\begin{bmatrix} A_{11} & A_{12} \\ A_{21} & A_{22} \end{bmatrix} \begin{bmatrix} \ddot{\theta}_1(t) \\ \ddot{\theta}_2(t) \end{bmatrix} + \begin{bmatrix} 0 & B_{12} \\ B_{21} & 0 \end{bmatrix} \begin{bmatrix} \dot{\theta}_1^2(t) \\ \dot{\theta}_2^2(t) \end{bmatrix} + \begin{bmatrix} c_1 \\ c_2 \end{bmatrix} = \begin{bmatrix} \tau_1(t) \\ \tau_2(t) \end{bmatrix} \tag{1}$$

where, the elements of the matrices A, B, c in (1) are related to the link inertia, geometry and joint variables (Table 1) as follows:

$$A_{11} = I_1 + m_2 L_1^2 \tag{2}$$

$$A_{12} = A_{21} = m_2 L_1 L_{m_2} \cos(\theta_1 - \theta_2) \tag{3}$$

$$A_{22} = m_2 L_{m_2}^2 + I_2 \tag{4}$$

$$B_{12} = -B_{21} = m_2 L_1 L_{m_2} \sin(\theta_1 - \theta_2) \tag{5}$$

$$c_1 = \left(m_1 g L_{m_1} + m_2 g L_1\right) \cos\theta_1 \tag{6}$$

$$c_2 = m_2 g L_{m_2} \cos\theta_2 \tag{7}$$

©2024 The author. This work may be used under a Creative Commons Attribution 4.0 License (CC BY 4.0)

DOI: 10.17185/duepublico/82637

3 Inverse Kinematic Analysis

One possible configuration of the robot for this motion plan is sketched in Fig. 1. Forming a vector chain along the links ($\overrightarrow{OA} + \overrightarrow{AB}$), and a separate vector chain avoiding the links ($\overrightarrow{OC} + \overrightarrow{CB}$), a Loop Closure Equation (LCE) could be obtained. Separation of the horizontal and vertical components of the LCE leads to the following two nonlinear equations for the joint variables (θ_1, θ_2):

$$L_1 \cos\theta_1 + L_2 \cos\theta_2 = r\cos\alpha(t) \tag{8}$$

$$L_1 \sin\theta_1 + L_2 \sin\theta_2 = y_C + r\sin\alpha(t) \tag{9}$$

where, $\alpha(t) = \omega t$ assuming a constant rotational speed, ω while tracing the circle. The time evolution of the angular positions (θ_1, θ_2) of the links are obtained and plotted in Fig. 2 as the "target" trajectories to achieve in the closed-loop control simulations.

4 Sliding-Mode Control Design and Simulation Results

To initiate control design, the Lagrange model (1) is first re-organized in the following explicit form:

$$\ddot{\Theta}(t) = f(\Theta, \dot{\Theta}, t) + u(t) \tag{10}$$

where, $\Theta = [\theta_1 \quad \theta_2]^T$ is the state vector, $f(\Theta, \dot{\Theta}, t) = -A^{-1}B\dot{\Theta}^2 - A^{-1}c$, and $u(t) = A^{-1}\tau(t)$ is the control input. To quantify the tracking performance, a cost function is also defined by combining position tracking error and velocity tracking error as follows:

$$e(t) = \left(\dot{\Theta} - \dot{\Theta}_d\right) + \lambda(\Theta - \Theta_d)\ ,\ \ (\lambda > 0) \tag{11}$$

where, Θ_d refers to the desired (target) trajectories. Note that error-free tracking implies: $e = 0$ (or, $\dot{e} = 0$). Hence, after taking the first derivative of (11), and then substituting the dynamic model (10), the control input $u(t)$ is obtained as follows:

$$u(t) = \ddot{\Theta}_d - f\left(\Theta, \dot{\Theta}, t\right) - \lambda\left(\dot{\Theta} - \dot{\Theta}_d\right) - K\mathrm{sat}[e(t)/\phi] \tag{12}$$

The last term on the right side of (12) is added to provide state feedback action to enable control switching for robustness. The saturation function eliminates input chattering due to repetitive switching action especially when the states are very close to their respective targets [4]. The results of the closed-loop control simulation are provided in Figs. 2-3. Perfect tracking is achieved despite the 5% increase on the link masses, which validates the robustness of the proposed control law against external disturbances.

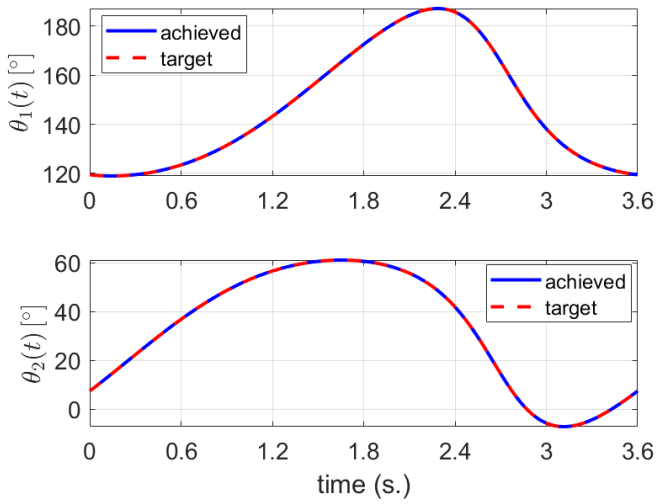

Figure 2: Time evolution of the joint variables

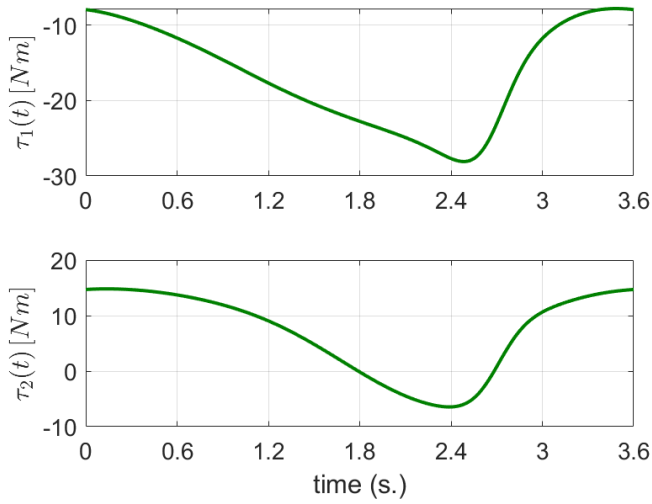

Figure 3: Time evolution of the torque inputs

References

[1] M. K. Ozgoren, *Kinematics of General Mechanical Systems.* Wiley, 2020.

[2] V. De-León-Gómez et al. "A procedure to find equivalences among dynamic models of planar biped robots", *Simulation Modelling Practice and Theory,* vol. 75, pp. 48-66, 2017.

[3] Z. Ilhan, "Benchmarking various nonlinear control design techniques for a two-link planar robot arm", in *Proceedings of the ASME 2022 International Mechanical Engineering Congress and Exposition*. Columbus, OH, USA. 2022.

[4] J-J. E. Slotine and W. Li, *Applied Nonlinear Control*. Prentice Hall, 1991.

DMP-Based Cartesian Trajectory Learning from Multiple Demonstrations

Tao Ma, Burkhard Corves

Institute of Mechanism Theory, Machine Dynamic and Robotics, RWTH University, 52062 Aachen, Germany, {ma, corves@igmr.rwth-aachen.de}

ABSTRACT

Robot learning plays a critical role in the field of robotics, particularly in industrial applications where robots are required to perform complex, repetitive tasks with high precision. Traditional motion planning methods are often time-consuming and struggle with environmental changes, limiting their use in dynamic settings when tackling complex tasks such as assembly, manipulation, and human-robot collaboration. With the increasing demand for robots capable of handling complex tasks, robot learning methods that can autonomously learn from demonstrations and adapt to new scenarios are gaining importance. Learning from Demonstration (LfD) has emerged as a powerful approach in this domain, allowing robots to acquire skills by observing demonstrations. This method enhances the robot's adaptability to complex environments while reducing the time and costs associated with reprogramming[1].

Dynamic Movement Primitives (DMPs) provide a robust LfD method, known for their high adaptability, reliability, and strong performance in encoding complex trajectories. However, DMPs are traditionally limited to learning from a single demonstration. To address this, Prados [2] et al. introduced a DMP-based Gaussian Model Regression (GMR) approach to analyze multiple demonstrations and generate new imitating trajectory. With its strength in handling uncertainties, Fanger [3] et al. proposed integrating DMPs with Gaussian Processes Regression (GPR) to learn from multiple demonstrations. Despite its advantages, GPR complexity remains a challenge, particularly for large datasets. Another limitation of DMPs is their reliance solely on positional data, making it difficult to express trajectories in Cartesian space. Ude [4] et al. improved and extended the classic DMP to represent trajectory orientation, developing DMPs based on rotation matrices and quaternion method respectively.

To enhance the overall capability of trajectory learning, we integrate classic DMP for position with quaternion DMP for orientation, while employing sparse GPR to improve adaptability across multiple demonstrations. This framework enables simultaneous learning of both position and orientation, with GPR predicting non-linear terms from demonstrations. The use of sparse representation reduces computational complexity, making the approach more efficient.

In the proposed framework, the principle of DMP is to transform the simple attractor dynamic system model into a nonlinear dynamic system through the learning of attractor landscapes to generate the desired goal. The DMP model could be consider a damp and spring system which present by the equations (1) and (2). Meanwhile the quaternion DMP can be writen as euqations (3) and (4).

Table 1: Classic and Quaternion DMP

	Classic DMP	*Quaternion DMP*
Main part	$\tau\dot{z} = \alpha_z(\beta_z(g-y)-z)+f(x)$ (1) $\tau\dot{y} = z$ (2)	$\tau\dot{\eta} = \alpha_q(\beta_q \log(q_g \cdot \bar{q}) - \eta) + f_0(x)$ (3) $\tau\dot{q} = \frac{1}{2}\eta \cdot q$ (4)
Non-linear term	$f(x) = \frac{\sum_{i=1}^{N}\varphi_i(x)w_i}{\sum_{i=1}^{N}\varphi_i(x)}(g-y_0)$ (5)	$f_0(x) = \frac{\sum_{i=1}^{N}\varphi_i(x)w_i}{\sum_{i=1}^{N}\varphi_i(x)} \cdot 2\log(-q_g \cdot \bar{q}_0)$ (6)
Gaussian function	$\varphi_i(x) = \exp(-h_i(x-c_i)^2)$ (7)	
Canonical system	$\tau\dot{x} = -\alpha x$ (8)	

In Table 1, the parameters α and β are positive time constants, τ is a temporal scaling factor, g is the attractor point and q_g is the goal quaternion, y and $\dot{y}$ correspond to the position and velocity respectively, f and f_0 are the non-linear term, Equation (7) is Gaussian function and equation (8) is the canonical system.

GPR is a Bayesian non-parametric regression method widely used for modeling complex functional relationships[5]. The advantage of GPR lies in its ability to naturally quantify uncertainty in the predictions without requiring a predefined functional form, making it robust in applications with small sample sizes or noisy data. The probability model of GPR $p(y_* \mid X, y, x_*) \sim \mathcal{N}(\mu^*, \Sigma^*)$ is build by observing the mapping from inputs X and outputs y to predict the values at new input locations x_*, the mean μ^* and covariance Σ^* of the new output y_* are computed as $\mu^* = k(x_*, X)\left[K(X,X)+\sigma_n^2 I\right]^{-1} y$ and $\Sigma^* = k(x_*, x_*) - k(x_*, X)\left[K(X,X)+\sigma_n^2 I\right]^{-1} k(X, x_*)$. Here $k(x_*, x)$ is kernel function, $k(x_*, X)$ is the covariance vector between the test point x_* and the training points X, $K(X,X)$ is the

©2024 The authors. All rights reserved DOI: 10.17185/duepublico/82615

covariance matrix of the training points, σ_n^2 is the noise variance. The time complexity of GRP is $O(n^3)$, n is number of samples. To mitigate this limitation, the K-means clustering algorithm is used to to select the inducing point, thereby enabling the construction of Sparse GPR. This approach reduces the complexity to $O(n^2m)$, m is the inducing number chose by the K-means algorithm.

The proposed approach is evaluated through a simulation experiment where a robot arm grasps a cylindrical object initially positioned horizontally on a lower platform and places it upright on a higher platform as shown in Figure 1, involving the adjustment of the object's orientation from horizontal to vertical. The process begins by constructing a dataset comprising multiple Cartesian trajectories, which are generated with the assistance of human guidance over time. Each trajectory's position and orientation are then analyzed separately using both classic DMP and quaternion DMP to compute the corresponding non-linear term. Sparse GPR is subsequently applied to derive the final non-linear term. Following the learning phase, the robot arm is capable of autonomously executing the pick-and-place task. This ability persists even when the pick-and-place locations or the object's orientation vary. The Figure 2 illustrates the execution of the proposed method. The demonstration trajectory includes three components of position data (x, y, z) and four components of quaternion orientation data (q_w, q_x, q_y, q_z), shown in the upper and lower parts, respectively. Each dimension's force term is computed, with the GPR-based probability distribution indicated by the blue dashed area. The mean output serves as the force term, enabling DMP to compute the generated Cartesian trajectory.

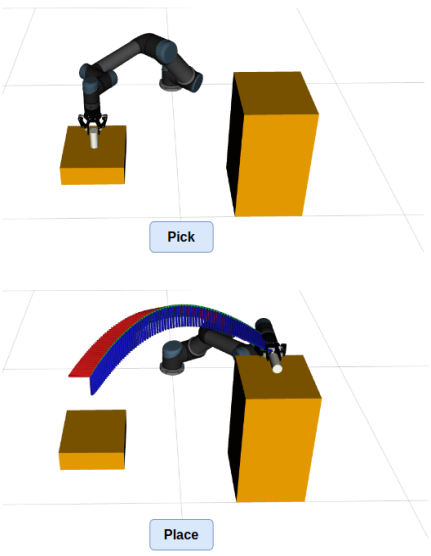

Figure 1: Robot Pick and Place

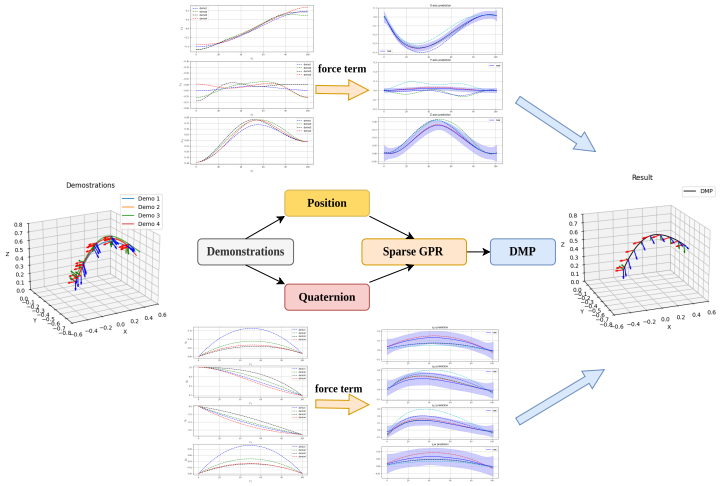

Figure 2: DMP based Cartesian trajectory learning

This abstract presents a trajectory learning process in Cartesian space by combining classic DMP with quaternion DMP. To enhance efficiency, we optimized the approach using sparse GPR, allowing for learning from multiple demonstrations with reduced computational complexity. The proposed method was evaluated through a robotic arm learning pick-and-place task, demonstrating its effectiveness. It provides a robust foundation for robot learning in more complex tasks and environments.

Acknowledgments

This research did not receive any specific funding or financial support.

References

[1] C. Liu, et al., "Robot skill learning system of multi-space fusion based on dynamic movement primitives and adaptive neural network control", *Neurocomputing*, vol. 574, pp. 127248, 2024.

[2] A. Prados, et al., "Learning and generalization of task-parameterized skills through few human demonstrations.", *Engineering Applications of Artificial Intelligence*, vol. 133, pp. 108310, 2024.

[3] Y.Fanger, et al., "Gaussian processes for dynamic movement primitives with application in knowledge-based cooperation.", *2016 IEEE/RSJ International Conference on Intelligent Robots and Systems (IROS)*, pp. 3913–3919, 2016.

[4] A.Ude, et al., "Orientation in cartesian space dynamic movement primitives.", *2014 IEEE International Conference on Robotics and Automation (ICRA)*, pp. 2997–3004, 2014.

[5] M.Wu, et al., "An adaptive learning and control framework based on dynamic movement primitives with application to human–robot handovers", *Robotics and Autonomous Systems* , vol. 148, pp. 103935, 2022.

DuEPublico

Duisburg-Essen Publications online

UNIVERSITÄT DUISBURG ESSEN

Offen im Denken

ub universitäts bibliothek

This text is made available via DuEPublico, the institutional repository of the University of Duisburg-Essen. This version may eventually differ from another version distributed by a commercial publisher.

DOI: 10.17185/duepublico/82370
URN: urn:nbn:de:hbz:465-20241216-143512-1

1st IFToMM Young Faculty Group Symposium on Emerging Fields in Mechanism and Machine Science 2024: 19.11. - 21.11.2024, Online Symposium

© 2024 The Authors. The rights/licenses stated in the individual symposium contributions apply.